Imparting bacteria-triggered self-disinfecting properties to a commercial bioengineered collagen-GAG matrix

by

Sarah Currie

A Thesis submitted to

The Faculty of Graduate Studies of

The University of Manitoba

in partial fulfilment of the requirements

of the degree of

Master of Science

Department of Biosystems Engineering

The University of Manitoba

Winnipeg, Manitoba, Canada

March 2025

Abstract

Infectious complications associated with the use of commercial bioengineered collagen-GAG matrices are of concern due to the high incidence of infection, difficulty of accurately discerning the presence of infection, and high cost and delayed wound healing when it becomes necessary to excise infected areas. We modified the collagen layer of a commercial bioengineered collagen-GAG matrix with a ciprofloxacin-based pro-drug "Pro-Cip" anchored to the matrix by a polydopamine layer in a simple one-pot chemistry. An ad-layer coating strategy enriched the surface with Pro-Cip, and various boosters for lipase activity were added to further enhance the antibacterial potency of the coating. The coated bioengineered collagen-GAG matrix exhibited potent antibacterial activity against MRSA and *P. aeruginosa*, achieving a complete bacterial eradication (no detectable CFU with a detection limit of 33 CFU/mL) within 18 hours at low initial inoculum (~10^4 CFU/mL). When challenged with a higher bacterial burden (10^8 CFU/mL), the coated bioengineered collagen-GAG matrix demonstrated robust antimicrobial efficacy, resulting in 100% (8.0) log reduction in MRSA and *P. aeruginosa* within 5h contact. Zone of inhibition testing yielded clear zones of up to 25 mm diameter, which highlights the ability of the antibiotic to diffuse into the infected wound after bacteria trigger its release from the coated surface. Furthermore, the surface-modified bioengineered collagen-GAG matrix retained excellent cell-adhesion and proliferation, and cell viability remained at 95% after exposure to membrane elutions compared to the unmodified bioengineered collagen-GAG matrix. The self-disinfecting properties of the modified bioengineered collagen-GAG matrix are anticipated to significantly enhance patient outcomes by mitigating the substantial risk of infections, a critical factor in the management of severe wounds such as burns.

Acknowledgements

Firstly, I would like to express my deepest gratitude to my advisor, Dr. Song Liu, for the invaluable guidance, support, and patience throughout this research. I am truly grateful for his mentorship and my experiences in his research group have enriched my life as a researcher and as a person. I am also thankful to my committee members, Dr. Sarvesh Logsetty and Dr. Kangmin Duan, for their constructive feedback and thoughtful discussions which have greatly enriched this thesis.

I am grateful for the financial support from the Natural Sciences and Engineering Research Council of Canada (NSERC) and the University of Manitoba. This project was made possible through the generous support and funding provided by Integra LifeSciences. Their contribution has been instrumental in enabling this research, and I sincerely appreciate their support. Thanks also to the Integra team Steve Bennett, Sunil Saini and Bryan Vayda for the insightful discussions and feedback.

I sincerely appreciate my labmates, past and present, for their camaraderie, insightful discussions, and willingness to lend a hand whenever needed: Farinaz Jonidi Shariatzadeh, Mahamuda Sultana, Changning Yu, and Quin Litke. In particular, I want to thank Dr. Seungil Kim for being my first mentor at the lab and for his patience and kindness in teaching chemistry techniques. I also wish to thank Dr. Hardev Singh for his work in developing the pro-drug upon which this research was based. Thanks to Abigail Harris and Hester Yin who contributed to the preliminary results and lipase assay.

I also greatly appreciate the support provided by the Department of Biosystems Engineering. The wonderful administrative staff (Caitlin Jacques, Heather Innis, Mandy Tanner, and Jen Beaudoin) have provided helpful assistance throughout my time in the program. Thanks to Dennis Joseph for helpful technical support and for coming to the rescue during lab crises (such as the flood). Thanks to Dr. Ravinder Sidhu and Jolly Hipolito from Manitoba Institute for Materials for sharing their expertise in materials characterization techniques.

Finally, thank you to my family and friends for their support. This thesis would not have been possible without all of you.

Table of Contents

List of Tables

List of Figures

List of Schemes

1. Introduction

1.1. Overview & Statement of the Problem

Patients with large burns may not have enough donor sites for immediate grafting with their own skin [1]. Furthermore, for coverage of large burns the donor skin needs to be thinner, more widely meshed, and reharvested more often [2–4]. These obstacles regarding the implementation of skin grafts for treating severe burn wounds result in delayed wound healing and increased scarring [5]. Bioengineered collagen-GAG matrices have been developed to help address these issues and have been used widely as wound healing matrices for burn patients. This thesis is primarily concerned with the antibacterial surface-modification of a commercially available double-layer bioengineered collagen-GAG matrix consisting of an outer siloxane layer which controls the barrier properties of the dressing, with an inner crosslinked collagen/glycosaminoglycan (GAG) matrix layer which contacts the wound bed. The three-dimensional collagen/GAG crosslinked matrix layer functions as a temporary extracellular matrix which guides cell growth and proliferation into the scaffold to enhance wound healing. The collagen is vascularized over two to three weeks, during which time the siloxane helps maintain the integrity of the wound and prevent moisture loss and bacterial contamination from the external environment.

Although bioengineered collagen-GAG matrices address some of the challenges with large burn wounds as mentioned above, the chance of infection is always a concern to physicians. For example, Gonzalez et al. reported infection in 212 out of 1254 Integra® reconstruction sites, an infection rate of 16.9% [6]. Burn wound infection is a major concern due to its contribution to delayed healing, scar formation, bacteremia, and sepsis [7]. Practically all burn wounds become contaminated with bacteria from the surrounding skin microflora, the environment, or mucous

membranes, depending on the wound location [8,9]. The progression from bacteria colonization to infection is typically defined by concentration exceeding 10^5 CFU/g [9]. Since the bioengineered collagen-GAG matrix is designed to cover the wound area until incorporated and cannot be replaced daily, it is at risk for bacterial invasion of the collagen matrix. Furthermore, the siloxane also prevents topically applied antimicrobials from penetrating the collagen matrix. The risk of infection is especially high in the initial stages since at this point, the matrix is not vascularized; therefore, neither white cells nor systemic antibiotics can reach the matrix to target the bacteria. In some cases, infection of the bioengineered collagen-GAG matrix can jeopardize the life of patients (one fatal case has been reported in the literature for Integra® dermal regeneration template) [6].

The current standard is regular (often daily) evaluation of the matrix and to excise the questionable areas. This can be challenging as it is not always easy to distinguish between uninfected and infected areas until there is significant bacterial presence. If a more conservative threshold for removing the suspected infected matrix is used, the burn team risks exposing large areas of the wound and increasing the inflammation, infection, and scarring. Therefore, it is beneficial to incorporate a means of addressing the bacteria infection without having to remove the matrix itself.

1.2. Current State-of-the-Art

Enriching the surface of the commercial bioengineered collagen-GAG matrix with a potent antimicrobial agent would mitigate the risk of infection of the collagen/GAG layer while maintaining the structure and function of the dermal regeneration matrix for wound healing. Some antimicrobial dermal regeneration templates are already on the market, such as an acellular dermal

type III bovine collagen dermal matrix, PriMatrix® Ag Antimicrobial Dermal Repair Scaffold, which is impregnated with ionic silver as an antimicrobial agent. However, ionic silver bears several disadvantages as an antimicrobial for wound care application. The active content of ionic silver may be depleted through leaching from the dermal repair scaffold. Ionic silver leachate may react with chloride anions which are abundant in wound fluid [10,11], or may bind with ECM proteins in skin such as collagen [11,12], which may reduce the potency of the dressing. Furthermore, ionic silver is cytotoxic to keratinocytes and fibroblasts [11,13–17].

Various surface immobilization techniques are available for modification of the matrix with antimicrobials such as self-assembled monolayer, layer-by-layer deposition, plasma treatment or covalent reaction. While non-covalent surface modification techniques offer versatility in incorporating biocidal agents into a wound dressing, the potential leaching of these agents can compromise their availability at the wound site during infection [18,19]. Therefore, physical deposition of the antibacterial agent is a less effective strategy compared to the triggered release of covalently bound antimicrobial agents.

1.3. Proposed Solution

Our group has previously developed a ciprofloxacin-based pro-drug, “Pro-Cip” which contains a labile ester linkage within its structure to allow for cleavage of the pro-drug by bacterial lipase [20]. This avoids indiscriminate release of antibiotics to the wound bed since release of the active drug will only happen when bacteria are present. Lipase serves as a valuable indicator of infection and trigger for drug release since major wound pathogens such as *P. aeruginosa* and MRSA produce lipase, and are the foremost gram-negative and gram-positive pathogens responsible for burn wound infections, respectively [21].

We proposed to covalently anchor the ciprofloxacin-based pro-drug “Pro-Cip” on the wound-contacting collagen/GAG layer of a commercially available bioengineered collagen-GAG matrix without compromising the engineered pore structure and function of the fabricated substrate. This modification can be done using a covalent linker technique inspired by mussel-adhesion using polydopamine (PDA) [22]. In order to achieve this covalent immobilization, the pro-drug was designed with an alkyl chain bearing a terminal primary amine group to allow for facile covalent surface modification of the bioengineered collagen-GAG matrix. By dip coating the collagen layer of the matrix in a solution of dopamine and amine-terminated pro-drug under conditions which lead to the polymerization of dopamine, the polydopamine can act as a covalent linker between the collagen layer and the amine-terminated ciprofloxacin pro-drug. This technique overcomes drawbacks of common surface modification approaches such as layer-by-layer (LbL) deposition, self-assembled monolayer and plasma treatment by leaving the underlying substrates' structure unaltered and not introducing any potentially toxic reagents.

Dopamine undergoes self-polymerization under alkaline conditions to form a polydopamine layer which can coat a wide variety of surfaces [23][24]. Polydopamine can covalently react with molecules containing the nucleophilic functional groups R-NH_2 or R-SH to bind covalently to the surface, or can have non-covalent interactions such as π-π or cation-π with the coated substrate [23]. The variety of these interactions allows polydopamine to successfully modify almost any organic or inorganic surface. It has previously been demonstrated that if the coating occurs in a dynamic condition (stirring and shaking), the coating itself can be antibacterial due to the roughness of the surface [25]. Therefore, polydopamine is a promising choice as an antibacterial coating for a commercial collagen-GAG matrix since it can simultaneously achieve two functions: firstly, it can covalently bond the pro-drug (Pro-Cip) onto the collagen surface of

the collagen-GAG matrix. Secondly, the inherent antibacterial activity of the polydopamine may boost the self-disinfecting properties of the modified surface. After covalent attachment of Pro-Cip to the polydopamine layer, this layer acts as a bacteria-responsive antibacterial depot. In the presence of bacteria, bacterial lipases cleave the Pro-Cip ester linkage, releasing the bioactive form of ciprofloxacin. Without bacteria, Pro-Cip remains stably attached.

A critical property of commercial bioengineered collagen-GAG matrix is biodegradation. Since the matrix collagen layer should merge with the regenerating skin, it is suitable that the antibacterial coating also lasts until the skin regenerates/repairs itself. PDA is a biodegradable polymer with unique behavior for degradation. Similar to its polymerization, the degradation of PDA relies on the pH of the microenvironment; alkaline conditions lead to faster degradation of PDA. It has been reported that PDA at pH=13 was degraded entirely after 120 hr; however, the degradation rate at pH=8 decreased significantly [26]. Although healthy skin typically has an acidic pH, open or chronic wounds tend to have neutral to alkaline pH ranging from 6.5-8.9 [27]. Therefore, the biodegradation characteristics of PDA are expected to achieve a balance between sufficient stability to allow for wound healing with sufficient biodegradeability to merge with the regenerating skin and allow for remodeling of the wound. The unique properties of PDA (fast, simple and effective coating, adjustable biodegradation and antibacterial effect), make it well-suited for covalently anchoring pro-Cip onto the commercial bioengineered collagen-GAG matrix. Additionally, PDA can also affect cellular behaviour during wound healing, improve cell adhesion and proliferation, and accelerate the healing [28].

Various techniques can be employed to coat PDA and biomolecules onto desired surfaces. This study presents several approaches for the surface modification of a commercial bioengineered collagen-GAG matrix with polydopamine-anchored Pro-Cip, including: facile one-pot surface

modification, ad-layer coating, and the addition of additives for improved efficacy. The performance of the modified dermal regeneration templates was evaluated based on their antibacterial properties, cytocompatibility, cell adhesion and proliferation.

1.4. Thesis Organization

This thesis is organized into five chapters. Chapter 1 provides an introduction to the project, with a broad overview of the goal to reduce the risk of infection of a commercial bioengineered collagen-GAG matrix as well as the proposed modification strategy with a ciprofloxacin pro-drug via polydopamine-based surface modification chemistry. Chapter 2 defines the objectives and hypothesis. Chapter 3 describes the materials & methods, including detailed experimental design, coating process, and methodology for characterization and performance of the modified dermal regeneration template. Chapter 4 presents the major results of this study including characterization of the pro-drug and polydopamine coating, release behaviour, antibacterial activity and cytocompatibility. Chapter 5 provides a summary of the conclusions of this research, and Chapter 6 makes recommendations for future study.

2. Hypothesis and Objectives

Infection of bioengineered collagen-GAG matrixes during skin regeneration is a concern for physicians: as an example, Integra® remodelling sites experience an infection rate of 16.9% [6]. Infection is of particular concern during the initial stages of wound healing, when the matrix has not vascularized and therefore is not accessible to the immune system or systemic antibiotics. We hypothesize that a surface modification of the collagen-GAG layer with a ciprofloxacin-based pro-drug, “Pro-Cip” will endow the matrix with potent triggerable antibacterial activity in the

presence of lipase-producing wound pathogens such as MRSA and *P. aeruginosa*. Surface modification of the collagen-GAG layer will be achieved through polydopamine coating to covalently anchor Pro-Cip to the collagen. Triggered antibacterial activity will be achieved by exposure of the covalently bound pro-drug to bacterial lipase, which will cleave the ester linkage to release active ciprofloxacin from the modified surface.

The primary objectives of this research will be to demonstrate triggered release of ciprofloxacin from the modified dermal regeneration template in the presence of commercial lipase or lipase-producing bacteria. Antibacterial activity of the coated collagen layer will be confirmed in the presence of *P. aeruginosa* and MRSA. Furthermore, important properties of the commercial bioengineered collagen-GAG matrix such as porosity of the collagen layer, cytocompatibility, cell adhesion and proliferation will be confirmed to ensure that the coating does not compromise the function of the matrix.

The major objectives of this research are summarized as follows:

1. Demonstrate lipase triggered release of ciprofloxacin from Pro-Drug modified commercial bioengineered collagen-GAG matrix.
2. Optimize the antimicrobial potency and overall performance (cell attachment, porosity, colour, etc.) by controlling coating parameters such as reaction duration, static or shaken coating, and ad-layer modification.
3. Explore the potential for inducing lipase activity through the incorporation of organic or inorganic lipase inducers in the coating.

3. Materials and Methods

3.1. Materials

Ethanol (EtOH, ≥95.0%), dopamine hydrochloride (≥98%), methyl oleate, Triton X-100, gum arabic from acacia tree and *Bukholderia cepacia* lipase (≥23,000 U/g) were purchased from Sigma Aldrich (St. Louis, MO, USA). Tris hydrochloride, Tween 80, 4-nitrophenyl palmitate, Integra Miltex Standard 4 mm biopsy punches, LB agar (Lennox), LB broth (Lennox), Mueller-Hinton agar, and Mueller-Hinton broth were purchased from Fisher Scientific (Nepean, ON, Canada). Gibco™ Collagenase type I from *Clostridium histolyticum* was purchased from ThermoFisher Scientific (Grand Island, NY, USA). CyQUANT™ MTT Cell Viability Assay and Invitrogen™ LIVE/DEAD™ Viability/Cytotoxicity Kit were purchased from ThermoFisher Scientific (Eugene, Oregon, USA). Fibroblast basal medium, Fibroblast Growth Kit-Low serum and PCS-201-012 human dermal fibroblasts were purchased from Cedarlane. 6-aminohexyl 1-cyclopropyl-6-fluoro-4-oxo-7-(piperazin-1-yl)-1,4-dihydroquinoline-3-carboxylate ($C_{25}H_{31}FN_4O_3$, "Pro-Cip") was custom synthesized by Alberta Research Chemicals Inc.

3.2. Synthesis of Pro-Cip

Pro-Cip was custom-synthesized by Alberta Research Chemicals Inc (Scheme 1). The chemical structure of Pro-Cip was confirmed by attenuated total reflectance-Fourier transform infrared spectroscopy (ATR-FTIR), ^{1}H nuclear magnetic resonance (^{1}H NMR), and electrospray ionization mass spectrometry (ESI-MS).

Boc-ciprofloxacin: 90 mL 1N NaOH was added to 20 g (60 mmol) of ciprofloxacin in 350 mL of dioxane:water (1:1) followed by the addition of 20 g (91.6 mmol) of di-tert-butyl dicarbonate. The

reaction mixture was stirred at room temperature for 17 hours and filtered. The precipitate was washed with 150 ml of water and then with 50 ml of acetone and then dried under high vacuum overnight to obtain Boc protected ciprofloxacin, **1** (23.93 g 92 %).

tert-butyl (6-hydroxy-hexyl) carbamate: Boc anhydride (37.24 g, 187.7 mmol) was added slowly to a stirred solution of 6-amino hexanol (20 g, 170.64 mmol) in 170 ml of anhydrous DCM at 0 ℃. The reaction mixture was warmed to room temperature and was stirred overnight at room temperature. The clear and colourless solution turned cloudy. After completion of the reaction, which was confirmed by TLC, saturated aqueous sodium bicarbonate was added to the reaction mixture, transferred the reaction mixture into separatory funnel. The organic layer was separated, washed with brine (1x250 ml), dried over Na_2SO_4. It was then filtered, evaporated under reduced pressure, and purified by column chromatography using 1:1 hexane/ethyl acetate to obtain the product, **2** as a sticky oil (35.19 g, 95%).

6-((tert-butoxycarbonyl)amino)hexyl 7-(4-(tert-butoxycarbonyl)piperazin-1-yl)-1-cyclopropyl-6-fluoro-4-oxo-1,4-dihydroquinoline-3-carboxylate: A mixture of compound **1** (40 g, 0.0968 mmol), HBTU (36.7 g, 0.0968 mmol) and catalytic amount of DMAP was dissolved in 1L anhydrous DCM. DIPEA (16.86 ml, 0.0968 mmol) and compound **2** (21 g, 0.0968 mmol) were dissolved in 500 mL DCM and then added to the Ciprofloxacin mixture. The reaction was monitored by the TLC and after stirring overnight and the completion of the reaction, the reaction mixture was washed with water. The organic phase was dried over $MgSO_4$, concentrated under reduced pressure and purified by flash chromatography on silica gel eluting with DCM/MeOH (90:10) to get (56.4 g, 92.4%) pure product, **3** as an off-white solid.

^{1}H NMR (400 MHz, $CDCl_3$): δ 1.05-1.01 (m, 2H), 1.30-1.38 (m, 4H), 1.38-1.40 (m, 2H), 1.40 (s, 9H), 1.50 (s, 9H), 1.58 (s, 2H), 1.72-1,78 (m, 2H), 3.19-3.21 (m, 2H), 3.32-3.38 (m, 4H), 3.50 (m, 1H), 3.63-3.65 (m, 4H), 4.30 (m, 2H), 4.68 (m, 1H), 7.36 (d, J = 7.2 Hz, 1H), 7.90 (d, J = 13.2 Hz, 1H), 8.52 (s, 1H); $C_{33}H_{47}FN_4O_7$: MW: 630.34; MS (ESI): m/z 631[$M+H^+$].

6-aminohexyl 1-cyclopropyl-6-fluoro-4-oxo-7-(piperazin-1-yl)-1,4-dihydroquinoline-3-carboxylate: Compound **3** (56.4 g, 89.47 mmol) was dissolved in 800 ml of DCM, cooled to 0 °C for 10 minutes, 150 ml of TFA was added slowly. After the addition of TFA, the reaction mixture warmed to room temperature and stirred at room temperature overnight. After confirming from TLC all the starting material was consumed, the reaction mixture was evaporated on rotary evaporator to remove DCM. The reaction mixture was co-evaporated with diethyl ether 3 times. To the semi-solid crude residue, 150 ml of ether was added and stirred for 15 min and the resulting solid was collected by filtration. The solid was rinsed thoroughly with excess ether, dried under high vacuum to get the product, Pro-CIP.TFA salt as an off-white solid. (Caution: Entire evaporation on the bath needs to be done at room temperature only). Yield 59 g

^{1}H NMR (400 MHz, DMSO-d_6): δ 1.02-1.01 (m, 2H), 1.22-1.8 (m, 2H), 1.32-1.42 (m, 4H), 1.48-1.58 (m, 2H), 1.60-1.68 (m, 2H), 2.70-2.82 (m, 2H), 3.25-3.36 (m, 4H), 3.38-3.46 (m, 4H), 3.62-3.70 (m, 1H), 4.15 (t, 2H), 7.45 (d, J = 7.2 Hz, 1H), 7.62-7.74 (bs, 3H), 7.80 (d, J = 13.2 Hz, 1H), 8.42 (s, 1H), 8.90-9.00 (bs, 2H); ^{19}F NMR (400 MHz, DMSO-d_6): -69, -71, -74 (main peak); $C_{23}H_{31}FN_4O_3$ (free amine): MW: 430.24; MS (ESI): m/z 431[$M+H^+$].

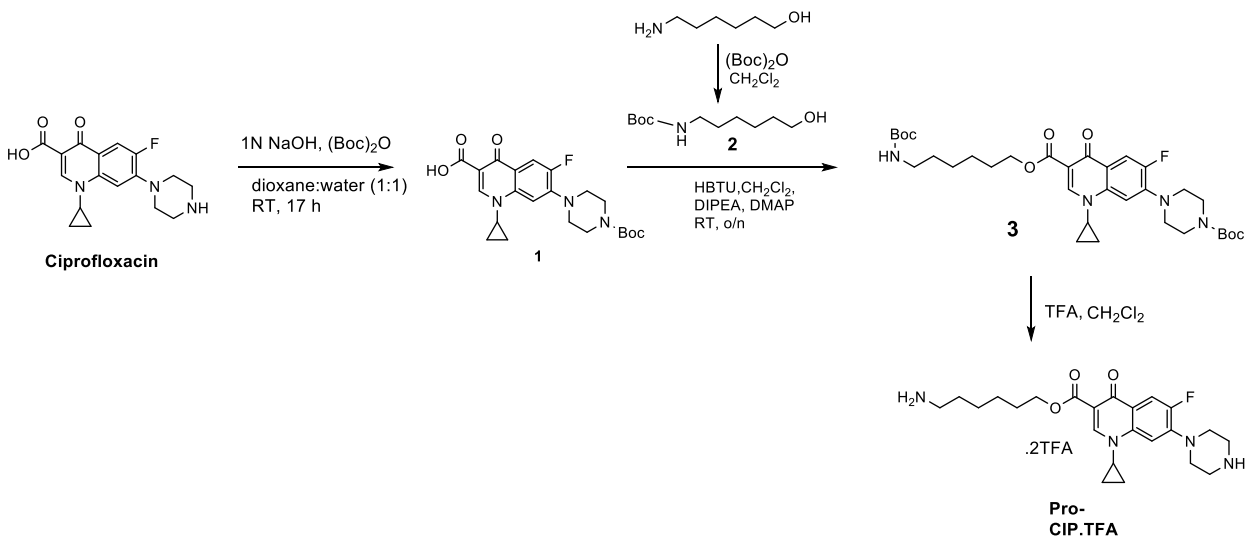

Scheme 1. Synthesis of 6-aminohexyl 1-cyclopropyl-6-fluoro-4-oxo-7-(piperazin-1-yl)-1,4-dihydroquinoline-3-carboxylate (C25H31FN4O3, "Pro-Cip").

3.3 Surface modification of bioengineered collagen-GAG matrix

In the proposed coating design, antibacterial activity primarily arises from the covalent modification of the collagen later of a commercial bioengineered collagen-GAG matrix with a ciprofloxacin-based antibiotic. Due to increased prevalence of the development of resistance of bacteria to antibiotics, a ciprofloxacin based pro-drug has been designed and synthesized. The pro-drug can undergo cleavage by lipase in the presence of bacteria and become an active drug, while in the absence of bacteria, the drug remains inactive (Scheme 2). *Pseudomonas aeruginosa* and *Staphylococcus aureus* (or methicillin-resistant *S. aureus*, MRSA) are the foremost gram negative and gram positive pathogens responsible for burn wound infections, respectively [21]. *P. aeruginosa* and *S. aureus* both produce lipase, as well as other wound pathogens including *Streptococcus agalactiae* [29], *Enterococcus* [30], *Acinetobacter* [31], *E. coli* [32], *Klebsiella pneumoniae* [33], *Staphylococcus epidermidis* [33], *Proteus mirabilis* [33], and *Serratia*

marcescens [34]. Therefore, lipase is of interest of as an indicator of infection and as a trigger for drug release. For this application, we designed an amine-terminated pro-Cip as the pro-drug to facilitate anchoring to the polydopamine matrix [20].

Antibacterial surface modification of the collagen layer of the commercial bioengineered collagen-GAG matrix was achieved via a one-pot method for the alkaline self-polymerization of dopamine with Pro-Cip. Dopamine undergoes autoxidation and self-polymerization under alkaline conditions in the presence of ambient oxygen to form a PDA layer (Scheme 3). Polydopamine can act as an anchor to covalently bond the pro-drug (Pro-Cip) onto the collagen surface (Scheme 4). Possible interactions with collagen are illustrated in Scheme 5.

Several surface modification methods were attempted, including a one-pot reaction, or an ad-layer modification method. These two methods are described as follows.

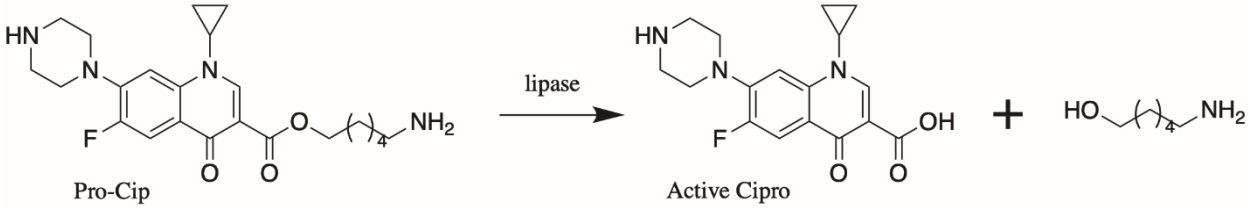

Scheme 2. Structure and lipase-responsive cleavage of the pro-drug “Pro-Cip.”

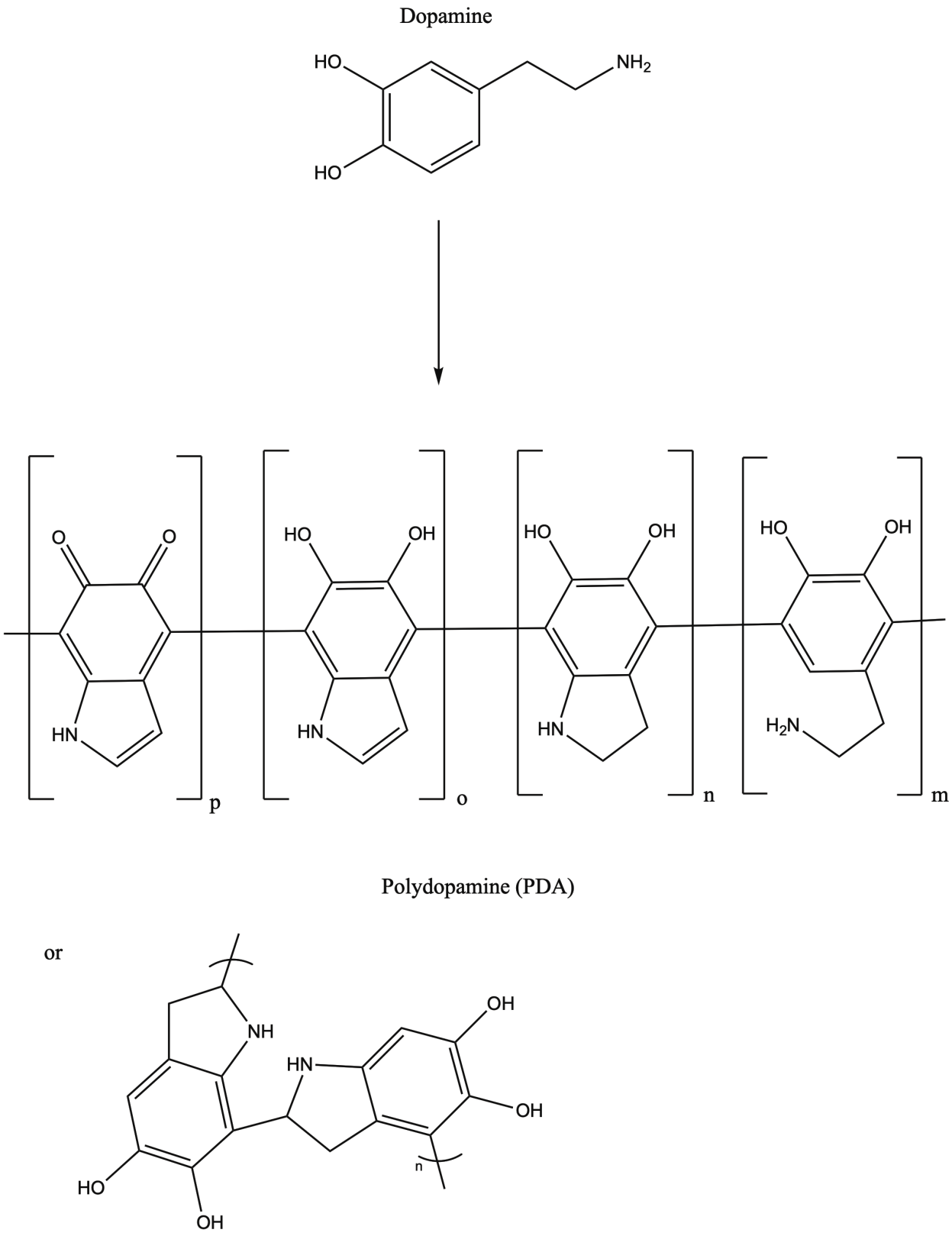

Scheme 3. Self-polymerization of dopamine under alkaline conditions.

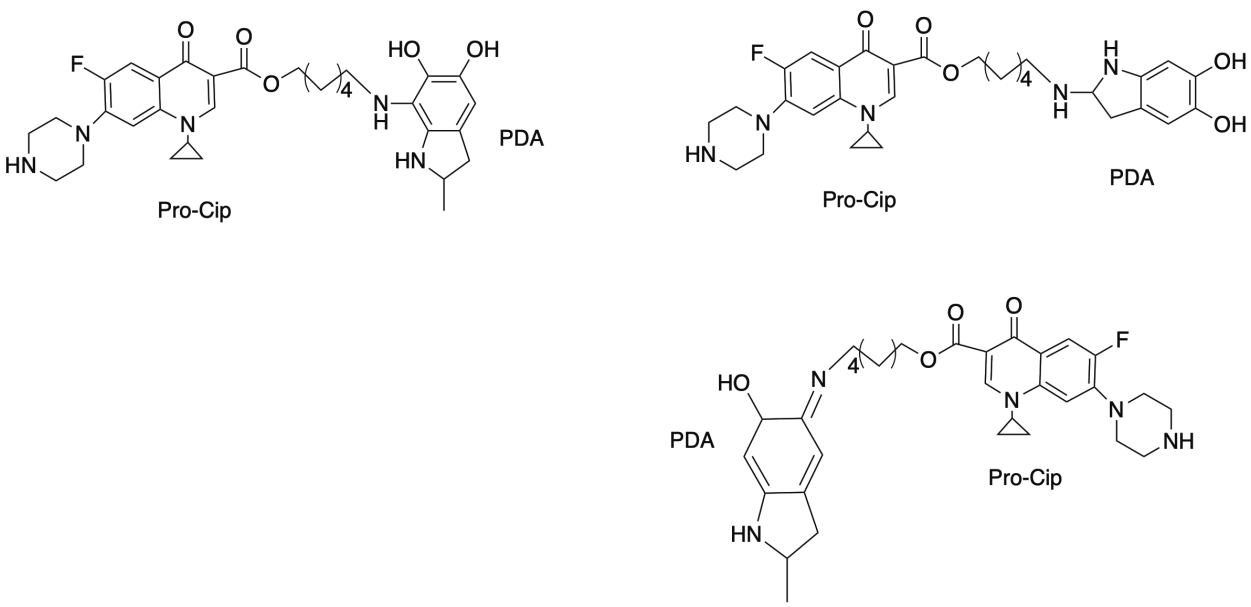

Scheme 4. Possible covalent bonds between Pro-Cip (Pro-drug) and PDA.

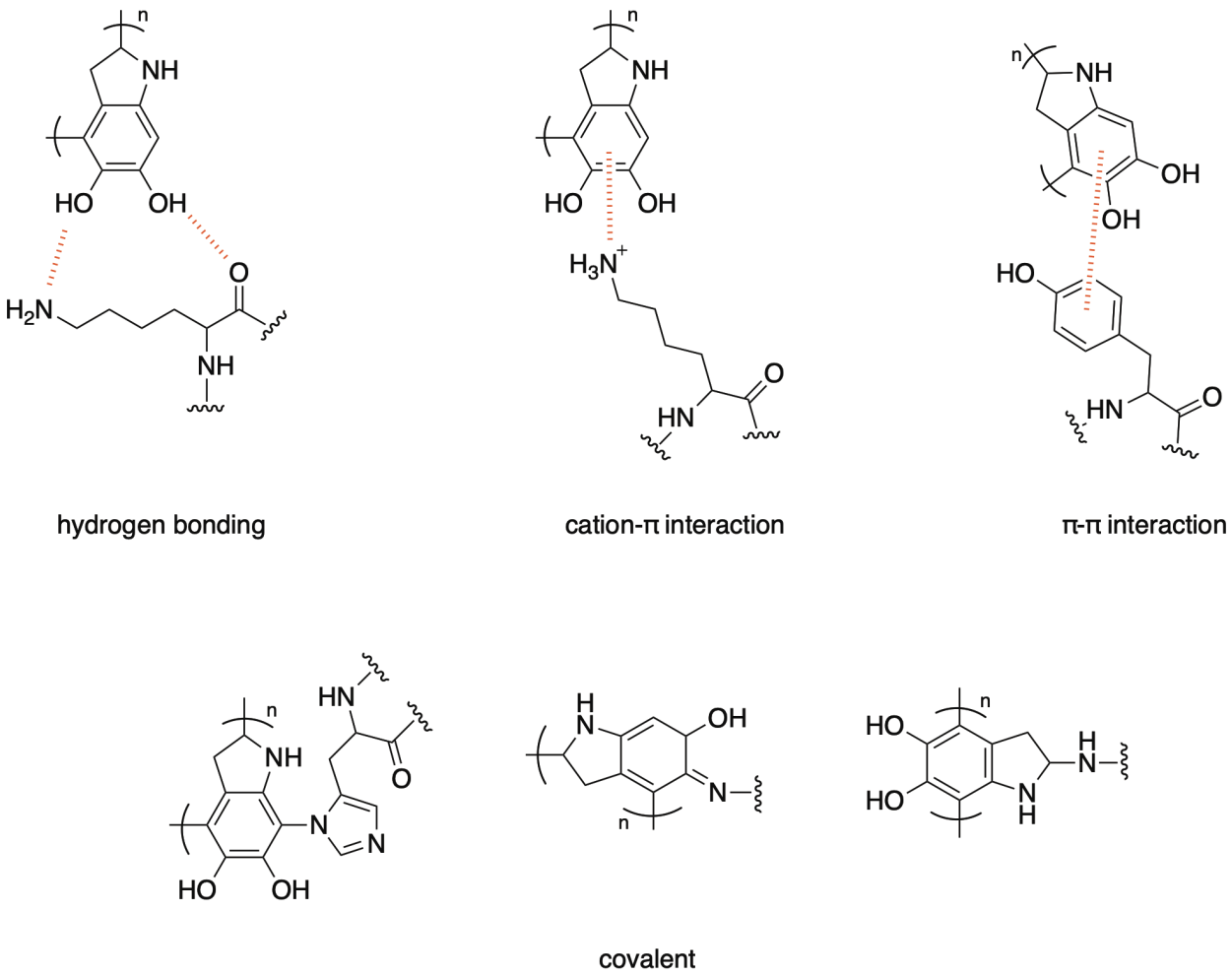

Scheme 5. Possible interactions of PDA and collagen (physical and covalent).

3.3.1 One-pot reaction

One-pot surface modification of the bioengineered collagen-GAG matrix is possible by combining dopamine and the amine-terminated Pro-Cip in alkaline pH 8.5 TRIS buffer in a single reaction (Scheme 6). The collagen surface was immersed in a solution of 0.05-3 mg/mL dopamine with a 1:1 or 10:1 ratio of dopamine:Pro-Cip in 25 mM Tris-HCl buffer, pH 8.5 at room temperature. Shaking and static polymerization were both explored since shaking is known to generate a rough surface texture which can contribute to antibacterial activity (as opposed to static

polymerization) [25]. Shaking speed at 200 rpm was selected for generating the rough coating topography condition. After coating the collagen layer for a duration of 1-18h, the samples were removed from the reaction buffer and rinsed three times with 1X PBS, pH 7.4 with 10 min bath sonication to remove any unreacted or loosely bound Pro-Cip or PDA. In some cases, inducers were added to the coating at ratios of 10:1, 1:1 or 1:3 Pro-Cip:inducer. Inducers included olive oil, methyl oleate, olive oil:Tween80 emulsion, $CaCl_2$, or $MgCl_2$. The olive oil:Tween80 emulsion was prepared by sonication of 1% olive oil with 0.9% Tween80 for 15 min at an amplitude of 100.

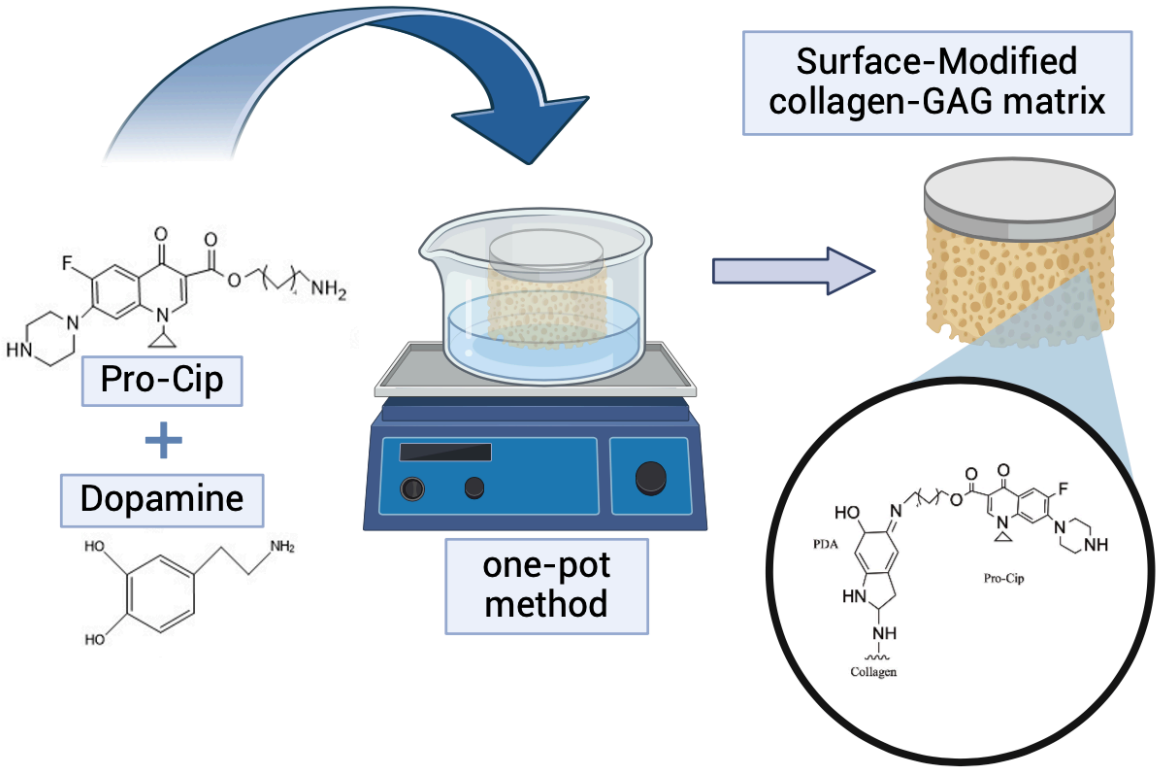

Scheme 6. One-pot surface modification of bioengineered collagen-GAG matrix.

3.3.2 Ad-layer reaction

As an alternative to one-step one-pot coating, ad-layer modification was explored to achieve covalent modification with Pro-Cip as a two-step process (Scheme 7). Firstly, the collagen layer was immersed in 1 mg/mL dopamine in 25 mM TRIS, pH 8.5. After 1h coating in static conditions, the samples were rinsed once in 25 mM TRIS pH 8.5, followed by transferring to a second solution containing 5-10 mg/mL Pro-Cip in 25 mM TRIS at pH 8.5, 9.0, 9.5 or 10.0. The samples were coated for 1-18h with shaking at 200 rpm.

In some cases, inducers $CaCl_2$ or Mg Cl_2 were incorporated in the ad-layer coating. For the inducer coated samples, the first polydopamine coat was achieved with either 0.25 mg/mL or 1 mg/mL dopamine in 25 mM TRIS, pH 8.5. The inducers Ca^{2+} ($CaCl_2$) and Mg^{2+} ($MgCl_2$) were either added to the coating formulation at a 1:3 ratio with the dopamine content during the first step, or added in the second step at a 1:1 ratio with Pro-Cip. After 1h coating in static conditions, the samples were rinsed once in 25 mM TRIS pH 8.5, followed by transferring to a second solution containing 10 mg/mL Pro-Cip in 25 mM TRIS, pH 8.5 for 18h with shaking at 200 rpm. Followed the coating process, the membranes were rinsed three times with 1X PBS, PH 7.4.

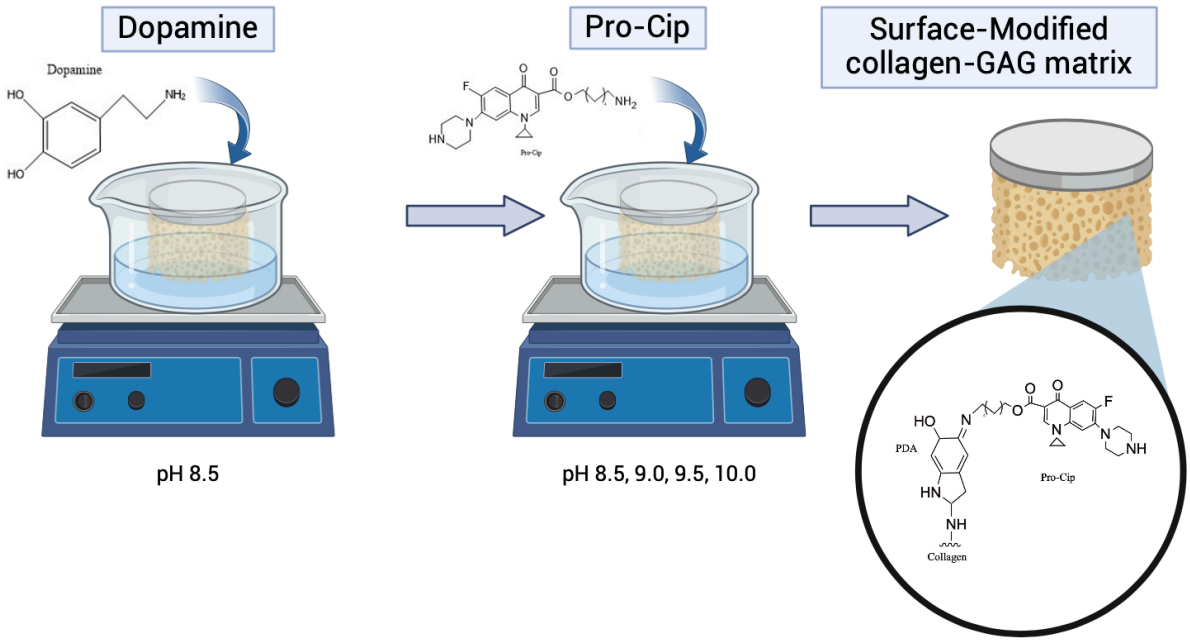

Scheme 7. Ad-layer modification strategy for two-step covalent modification of bioengineered collagen-GAG matrix with polydopamine and Pro-Cip.

3.3.3 Mechanism of release

After covalent attachment of Pro-Cip to the polydopamine layer, cleavage of the Pro-Cip ester linkage by bacterial lipases results in the liberation of the active form of ciprofloxacin, only in the presence of bacteria (Scheme 8).

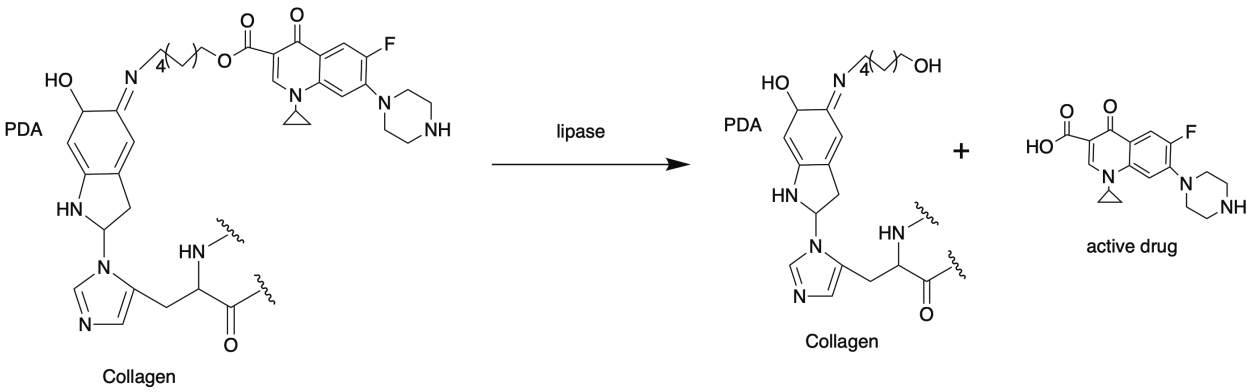

Scheme 8. PDA as a crosslinker between collagen and Pro-Cip. In the presence of bacteria (secretion of lipase), the pro-drug becomes an active drug due to cleavage of the ester linkage.

3.3. Characterization and in vitro testing

The morphology of the coated bioengineered collagen-GAG matrix was characterized by scanning electron microscopy (SEM). Samples were flash-frozen in liquid nitrogen followed by fracturing to reveal cross-sectional morphology and lyophilized at -80ºC prior to imaging. The physical morphology of the samples was characterized by SEM (Nova NanoSEM 450, FEI, Hillsboro, OR) after sputter coating with gold-palladium.

Cumulative release of ciprofloxacin from the coated surfaces was measured in vitro in the presence or absence of lipase. The coated bioengineered collagen-GAG matrix samples were immersed in 1.0 mL of *B. cepacia* commercial lipase solution in pH 7.4 PBS (5 mg/mL lipase concentration), or PBS without lipase. The samples were incubated in the solutions with shaking at 100 rpm, 37ºC. Samples of 0.3 mL were removed at periodic intervals (1h, 3h, 6h, 24h and 48h) and the removed volume was replenished with 0.3 mL fresh buffer, with or without lipase as appropriate. The UV absorbance was quantified at 335 nm to quantify the release of Cip.

The quantity of loaded Cip on the coated bioengineered collagen-GAG matrix was quantified spectrophotometrically after digestion of the collagen layer with collagenase. The collagen layer was removed from the silicon backing using a scalpel, immersed in a 5.0 mL solution of PBS, and homogenized in a tissue homogenizer. Collagenase was added (500 U/mL collagenase) and the solution was incubated with shaking at 200 rpm, 37ºC for 7 days. Collagenase was replenished with fresh enzyme every 2 days. After 7 days of incubation, the loading efficiency was quantified based on the absorbance at 325 nm.

3.4. Antibacterial activity

The antibacterial activity and killing kinetics of the polydopamine coated bioengineered collagen-GAG matrix (with and without Pro-Cip) was analyzed against *P. aeruginosa* (ATCC 27853), MRSA (ATCC 33592) and *E. coli* (ATCC 25922). In some cases, lipase-negative strains *E. coli* Top 10 and *E. coli* DH5α were tested as controls for lipase-responsive antibacterial activity. For bacteria culture, the specified bacteria strains of bacteria were streaked on LB agar and incubated for 18h at 37ºC.

For the preparation of overnight broth culture, colonies were suspended in 0.01 M PBS to a turbidity of 0.5 MF and diluted by a factor of 100X in 0.01 M PBS, followed by adding 15.0 μL of the diluted suspension to 45.0 mL LB broth. The broth culture was incubated for 18 hours at 37ºC with shaking at 140 rpm. Three main assays were used to quantify antibacterial activity: zone of inhibition (ZOI), suspension-based direct contact test, or ex vivo direct contact test.

For the ZOI test, the turbidity of the overnight suspensions were adjusted to 0.5 MF. Bacteria suspension was swabbed onto Mueller-Hinton agar three times, rotating the plate between

each swab. Samples of 6 mm diameter were placed onto the surface of the agar and incubated for 18h at 37ºC. The diameter of the inhibition zones were measured using calipers.

For the suspension-based direct contact test, 1cmx1cm samples of coated or untreated bioengineered collagen-GAG matrix were immersed directly in 1.0 mL of bacteria suspension for a defined time interval (typically 5h unless otherwise specified). The concentration of bacteria were quantified by drop-plating serial dilutions of the suspensions before and after the elapsed contact time with the coated dermal regeneration templates.

For the ex vivo test, pig skins were prepared by excising the layer of fat beneath the skin to achieve a uniform thickness followed by removing the hair with a scalpel. The surface of the skins were cleaned with 70% ethanol prior to burning. Burn wounds were created on pig skins by holding a soldering iron against the skin surface for a period of 15 seconds. The soldering iron was cleaned with 70% ethanol and reheated for 2 min between each burn. After the wounds completely cooled, the skins were sterilized in 70% ethanol for 10 min and dried completely in a Petri dish in the BSC with the lid open prior to use in the experiment. Bacteria suspensions were prepared to 0.5 MF in PBS, and diluted twice by a factor of 10x. The wounds were inoculated with 100 uL of diluted bacteria suspension. 1cmx1cm bioengineered collagen-GAG matrix samples were placed on the inoculated wounds. To maintain a moist environment, 10 mL of PBS was added to the bottom of each Petri dish. The samples were incubated for the desired contact time (18h) at 37ºC prior to biopsy punching the infected surfaces with a 4mm diameter punch. The punched samples were collected in 1 mL PBS, vortexed for 2 minutes to flush bacteria from the surface, and serially diluted for drop-plating to allow for colony counting to quantify the remaining live concentration of bacteria after the 18h contact period.

Various inducers were explored to boost the activity of lipase, including methyl oleate, olive oil, Tween 80, Ca^{2+} and Mg^{2+}. To explore the effects of the inducers on lipase activity, bacteria were grown in a defined medium supplemented with the inducers at various concentrations. The "base medium" consisted of 0.3% yeast, 0.1% bacto-peptone, 0.07% K_2HPO_4, 0.03% KH_2PO_4, 0.01% $MnCl_2$, 0.025% $(NH_4)_2SO_4$, and 2% dextrose. $MgCl_2$, $CaCl_2$ or $MgSO_4$ were added to the base medium at concentrations ranging from 0.01-0.05%. Bacteria were cultured on the supplemented media as previously described to produce overnight cultures, which were then used to inoculate pig skins. The overnight cultures were spun down and diluted in PBS to a concentration of 0.5 MF, then diluted in the supplemented medium by a factor of 1000X (prepared as previously described). Pig skins were inoculated with 100 µL of bacteria in the supplemented medium and incubated for 18h followed by biopsy punching to remove a sample for quantification of lipase activity. The punched samples were collected in 1 mL 50 mM TRIS buffer, pH 7.4 and sonicated for 2 minutes to detach bacteria followed by vortexing for 20 seconds.

Lipase activity of the bacteria recovered from pig skin was quantified by a pNpp-based assay. Briefly, 30 µL of the sample lipase solution was added to a 96-well plate containing 270 µL of substrate solution. Substrate solution was prepared by stirring together a solution of 30 mg of pNPP in 10 mL of isopropanol with a solution of 0.1 g gum Arabic and 0.40 mL Triton X-100 in 90 mL 50 mM TRIS buffer pH 7.4. Lipase activity was quantified based on the absorbance at 410 nm.

3.5. In vitro cytocompatibility and cell proliferation

Since the function of the commercial bioengineered collagen-GAG matrix is to provide a scaffold for cellular migration into the matrix, it is critical that the dressing should retain its cell-

adhesive characteristics after the surface-modification with the polydopamine coating. To study the cell-adhesion and proliferation on the modified matrix, fibroblasts were seeded directly onto the surface and cytocompatibility was evaluated by MTT assay and Live/Dead staining.

PCS-201-012 fibroblasts were maintained at 37ºC, 5% CO_2 in Fibroblast Basal Medium with Fibroblast Growth Kit-Low serum supplemented with 10% fetal bovine serum and 1% penicillin/streptomycin.

For the elution based test, 1cm x 1cm coated or uncoated bioengineered collagen-GAG matrix samples were eluted for 24h in culture medium. After 24h, PCS-201-012 human dermal fibroblasts were treated with the elutions of the coated or uncoated bioengineered collagen-GAG matrices for another 24h, with 100 uL elution medium per well. The positive control was 1.0 M acrylamide, and the negative control was blank cell culture medium. After 24h treatment, an MTT assay was performed to analyze cell viability after exposure to the elutions. Briefly, 5 mg of MTT reagent were dissolved in 1 mL medium, followed by dilution of the 1 mL MTT solution in 9 mL of pre-warmed medium. The old media in the wells were removed and replaced with 100 uL of the MTT medium per well. The plate was covered in foil and incubated at 37ºC for 2 hours. After the incubation period, the medium was replaced with 150 uL DMSO to solubilize the blue formazan crystals at the bottom of the wells. The plate was mixed on a shaker at 120 rpm for 5 min to completely solubilize the crystals. The absorbance was measured at 570 nm.

For the direct contact test, PCS-201-012 fibroblasts were seeded onto the scaffolds (50 000 cells/sample in 50 uL of cell culture medium) and maintained in an incubator for 2h to allow for cell attachment. Subsequently, 1 mL cell culture media was added and cells were cultured for 7 days with media changes every 2 days. After 1, 3, 5 and 7 days, the cell culture medium was removed and the samples were washed twice with D-PBS. For Live/Dead staining, cell culture

medium was removed and the samples were washed twice with D-PBS. The scaffolds were then stained using a Live/Dead Viability/Cytotoxicity Kit with staining solution consisting of 5 µL of calcein AM (green live stain) and 20 µL ethidium homodimer-1 (red dead stain) in 10 mL D-PBS. 300 µL of the staining solution was added directly to the cells on the bioengineered collagen-GAG matrix samples and the cells were incubated for 30 min at room temperature in the dark for staining.

3.6. Data analysis

Data are presented as mean ± standard deviation. The number of replicates is indicated as the *n*-value. Data were analyzed by two-way ANOVA with Tukey's correction ($p<0.05$). Statistical analyses were conducted using Origin (Version 2023b, OriginLab Corporation, Northampton, MA, USA).

4. Results & Discussion

4.1. Characterization of Pro-Cip

Antimicrobial surface modification of the collagen/GAG layer of commercial bioengineered collagen-GAG matrices is desirable to mitigate the risk of infection. Our group has previously reported a ciprofloxacin-based pro-drug, "Pro-Cip" which features a labile ester linkage which can be cleaved by bacterial lipase produced by wound pathogens such as *P. aeruginosa* or MRSA to release the active drug ciprofloxacin only when bacteria are present [20]. To facilitate covalent modification of the collagen/GAG layer with Pro-Cip through reaction with polydopamine, the design of the previously reported Pro-Cip small molecule was adjusted to replace the azide group with a primary amine terminus. Pro-Cip was synthesized by Alberta

Research Chemicals Inc. according to Scheme 1. The product was successfully synthesized as a pale yellow solid with 97% purity (by LC-MS) and characterized by ^{1}H-NMR and ESI-MS.

The lipase-triggerable antimicrobial activity of Pro-Cip was confirmed through investigation of the minimum inhibitory concentration (MIC) of the drug against *E. coli*, MRSA and *P. aeruginosa*, which could be compared to the MIC of commercial ciprofloxacin (Table 1). The MIC of Pro-Cip was evaluated toward a lipase-positive (ATCC 25922) and lipase-negative (Top10) strain of *E. coli*. The MIC of Pro-Cip against the non-lipase producing Top10 strain was 8 μg/mL, compared to 2 μg/mL for the lipase-producing *E. coli* strain ATCC 25922. The increased sensitivity of the lipase-producing *E. coli* strain to Pro-Cip indicates that cleavage of the Pro-drug occurred in the presence of lipase. Comparison of the MIC for ciprofloxacin and the MIC of intact Pro-Cip against *E. coli* Top10 in the absence of lipase revealed that the intact pro-drug was significantly less active against *E. coli* compared to the active drug (<0.0625 μg/mL for ciprofloxacin compared to 8 μg/mL for Pro-Cip). However, the 8 μg/mL MIC of Pro-Cip against *E. coli* Top10 indicated that the intact pro-drug does possess some inherent antimicrobial activity in its non-cleaved state. The MIC of the pro-drug was also evaluated toward two lipase-producing wound pathogens, MRSA and *P. aeruginosa*. MRSA and *P. aeruginosa* were less sensitive to Pro-Cip compared to *E. coli*, with MIC values of 32 μg/mL and 16 μg/mL respectively.

Table 1. Minimum inhibitory concentrations for Cip and Pro-Cip against major wound pathogens.

	Ciprofloxacin	Pro-Cip
E. coli	<0.0625 μg/mL	2 μg/mL
E. coli Top10	<0.0625 μg/mL	8 μg/mL
MRSA	0.25 μg/mL	32 μg/mL
P. aeruginosa	0.125 μg/mL	16 μg/mL

The inhibited antimicrobial activity of the pro-drug can be explained by examining the mechanism of action of ciprofloxacin. Ciprofloxacin inhibits DNA gyrase (topoisomerase II), an enzyme responsible for cleaving and re-ligating the DNA backbone to introduce negative supercoils which are necessary for DNA replication, as well as topoisomerase IV which resolves daughter chromosomes and relaxes DNA supercoils after DNA replication [35]. This inhibition is achieved by binding of ciprofloxacin to the A subunit of DNA gyrase, which is mediated by a water-metal ion bridge of noncatalytic Mg^{2+} ion bridge with four coordinated water molecules which binds the quinolone with the enzyme serine and acid residues [36]. The noncatalytic Mg^{2+} ion is chelated by the keto/acid of the quinolone [37]. Therefore, the modification of the acid group in Pro-Cip with the ester linkage to a C6 alkyl chain can explain the lower activity of the pro-drug, due to impaired binding with DNA gyrase (Scheme 9). In fluoroquinolone drugs the acid group is typically left unmodified due to its critical role binding to DNA gyrase as well as facilitating drug transport into the bacterial cell [38].

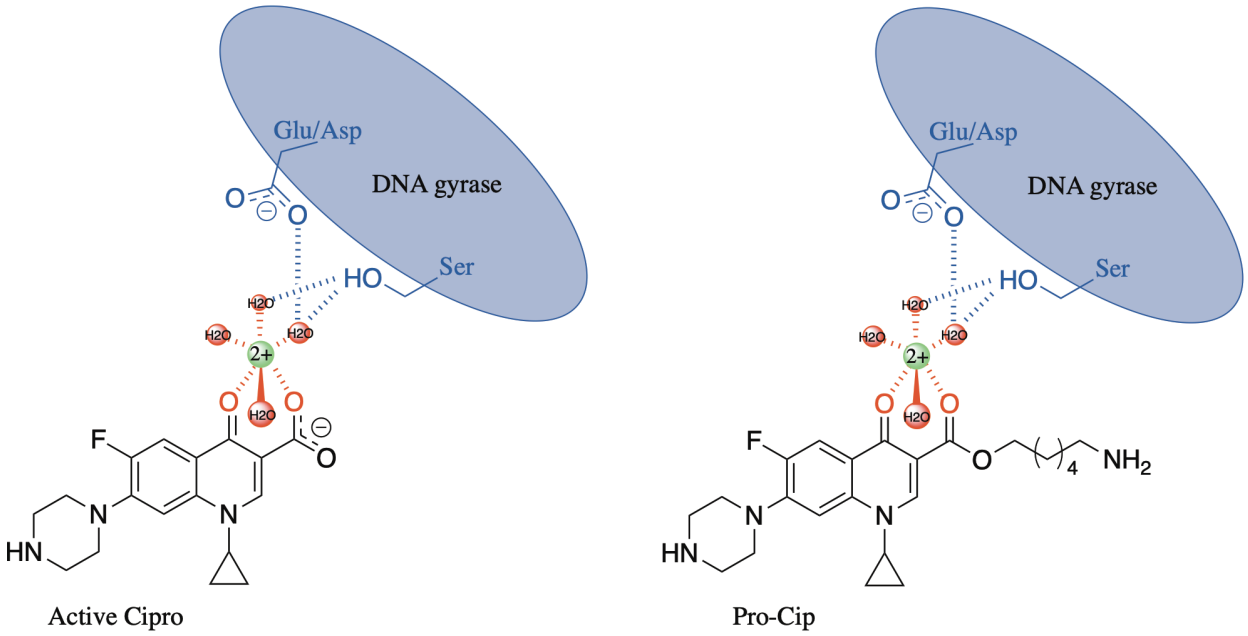

Scheme 9. Binding of ciprofloxacin versus Pro-Cip with DNA gyrase. Adapted from Aldred et al. [37].

Table 2. Viability of PCS-201-012 fibroblasts after exposure to Cip or Pro-Cip.

Dose (mg/mL)	Cell Viability (%)	
	Pro-Cip	Cip
1.0	68 ± 6	39 ± 2
0.5	85 ± 3	55 ± 11
0.25	80 ± 7	65 ± 2
0.125	84 ± 3	73 ± 3
0.0625	90 ± 3	91 ± 11
0.0	100 ± 9	100 ± 9

*LC50 towards PCS-201-012 fibroblasts: LC50 of Pro-Cip > 1.0 mg/mL. LC50 of Cip = 0.67 mg/mL.

To verify that the pro-drug was non-toxic towards human fibroblast cells, the LC50 of free Pro-Cip in fibroblast culture medium was evaluated toward PCS-201-012 human dermal fibroblasts (Table 2). The LC50 of Pro-Cip against PCS-201-012 fibroblasts was >1.0 mg/mL, which exceeds the LC50 of ciprofloxacin toward the same cell line (0.67 mg/mL). Therefore, the free pro-drug can be considered non-toxic to human cells. The risk of cytotoxicity is further mitigated by the design for drug delivery which involves covalent immobilization of the pro-drug to the collagen layer of the commercial bioengineered collagen-GAG matrix. Release of the active ciprofloxacin form of the drug will only occur in the presence of lipase if bacteria are present, which reduces exposure to the active drug. The release of the intact pro-drug Pro-Cip from the dressing should be minimal due to rinsing of the scaffolds after the reaction to flush away any non-covalently bound pro-drug. Release of the intact pro-drug would primarily occur in the case of biodegradation of the polydopamine layer or collagen layer of the commercial bioengineered collagen-GAG matrix throughout the formation of the neodermis.

4.2. One-pot surface modification of bioengineered collagen-GAG matrix with polydopamine anchored Pro-Cip

4.2.1 Comparison of shaken or static reaction conditions to generate rough polydopamine coating

Surface modification of the collagen layer of the bioengineered collagen-GAG matrix to impart self-disinfecting bacteria-responsive antibacterial properties can be achieved in a single step via a one-pot reaction of dopamine and Pro-Cip under alkaline conditions. Bioengineered collagen-GAG matrix samples were immersed collagen-side down in an alkaline solution of dopamine and Pro-Cip at pH 8.5 to catalyze self-polymerization of dopamine with dissolved oxygen as the oxidant.

Polydopamine was selected as an anchoring layer due to its "universal coating properties," as it can interact with the material surface through covalent bonding, π-π interaction, cation-π interaction, catechol metal coordination or hydrogen bonding. Polydopamine coating bears distinct advantages compared to other popular surface modification methods including self-assembled monolayer, layer-by-layer (LbL) assembly and plasma treatment due to its simplicity, versatility, and low cost. Contrary to LbL, polydopamine coating does not require the complex synthesis of specialized polymers for the layering process. Additionally, as a small molecule, dopamine can easily diffuse through the matrix of porous substrates, which is ideal for coating the inner structures of 3D porous materials such as the bioengineered collagen-GAG matrix. Polydopamine is biodegradeable in the presence of oxidants as well as biocompatible [39]. Furthermore, polydopamine is hydrophilic and cell-adhesive.

The reaction was conducted under static conditions or with shaking to generate a rough surface texture. Dopamine solutions are well-known to form particulate aggregates under alkaline conditions for self-polymerization: for example, 2 mg/mL dopamine in 50 mM TRIS pH 8.5 forms anisotropic aggregates of >200 nm diameter after 2h reaction [40]. Shaking during the one-pot reaction prevents particle sedimentation and results in their incorporation in the coating, whereas static conditions particle sedimentation can be observed at the bottom of the reaction vessel. It has previously been reported that polydopamine coating roughness can contribute to enhanced antibacterial activity compared to smooth PDA coatings [25]. Therefore, both static and shaken one-pot reaction conditions were explored. Both of the reaction conditions (static or shaken) resulted in a colour change visible to the naked eye from transparent and colourless to opaque brown or black (Figure 1). The darkness of the obtained coating was proportional to the

concentration of PDA in the reaction solution, and darker colour was achieved by shaking compared to static polymerization.

Polydopamine coatings are characteristically dark brown or black coloured due to their melanin-like structure with delocalized π-electron network which can absorb a broad range of visible light wavelengths. Therefore, achieving transparency in the coating requires either alternative selection of monomer to create polydopamine-like coatings, co-polymerization of dopamine with transparent molecules or polymers, and controlling the thickness and morphology of the coating. Since polydopamine colour intensity increases with thickness, one of the simplest methods to achieve transparency is to control the coating thickness. Coating morphology also affects the darkness and opacity of the coating colour, as Su et al. demonstrated that shaking-assisted formation of rough particle coatings produced darker surface colour compared to smooth films, although it is unclear whether this arises from morphology or thicker coating of polydopamine by avoiding the sedimentation of large particles [25].

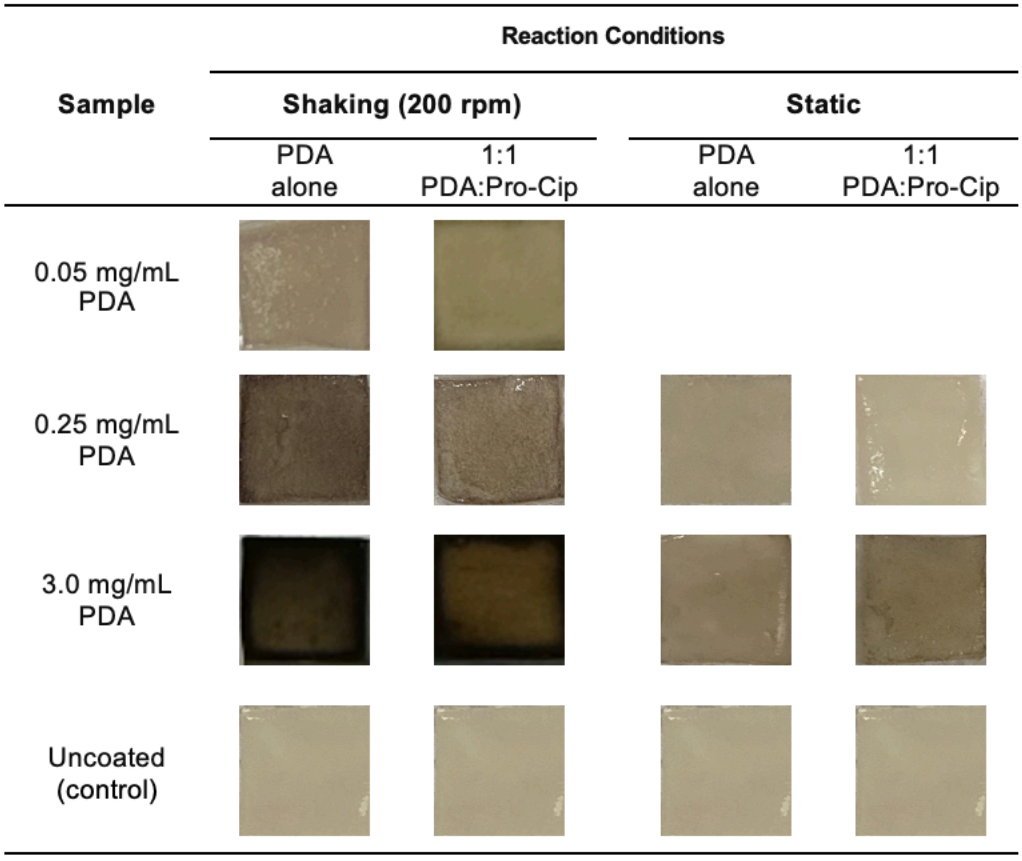

Figure 1. Visual appearance of bioengineered collagen-GAG matrix coated with PDA at concentrations ranging from 0.05 mg/mL-3.0 mg/mL under static or shaken polymerization conditions. Samples coated with one-pot method and 1h coating time.

Polydopamine possesses inherent antibacterial activity, and in some cases can endow the coated surface with antimicrobial potency without further modification with an antibiotic or other antibacterial agent. The mechanism of polydopamine's inherent antibacterial activity has been attributed to the interaction of bacteria with positively charged amine groups in polydopamine [25,41], or by ROS generation [42,43].

Su et al. demonstrated that by shaking throughout the polymerization process, rough polydopamine coatings can be produced which possess inherent antimicrobial activity against *S. aureus*, *E. coli* and *P. aeruginosa* [25]. Although smooth polydopamine coatings were observed to have minor antibacterial effect (≤5%), increasing the shaking rate during polymerization ≥200 rpm resulted in deposition of polydopamine particles (which typically would settle out to the bottom of the reaction vessel) to create rough coatings which had antibacterial activity between 99-100% in exposure to 10^5 CFU/mL bacteria suspensions after 24h contact. The coating roughness was hypothesized to increase contact with the bacteria, resulting in better antibacterial activity of the polydopamine's positively charged amine groups.

The antibacterial activity of coated bioengineered collagen-GAG matrix samples prepared under static or shaken conditions were confirmed via an ex vivo burn model, in order to capture the combined antibacterial activity that may arise from direct contact with PDA alone as well as the release of Cip from Pro-Cip (Table 3). The rough-coated samples obtained with shaking conditions during the one-pot polymerization reaction displayed some inherent antimicrobial activity due to the PDA coating alone, although the effect was less than 1.0 log reduction (0.9 ± 0.1 against *P. aeruginosa* and 0.81 ± 0.04 against MRSA after 18h contact). Increasing the dopamine concentration from 0.05 to 0.25 mg/mL resulted in increased antibacterial activity from the rough polydopamine coated samples, from 0.19 ± 0.06 to 0.9 ± 0.1 for *P. aeruginosa* or 0.77 ± 09 to 0.81 ± 0.04 for MRSA. Formation of polydopamine particles in solution by self-nucleation is concentration-dependent (>0.5 mg/mL) [44]. Furthermore, coating roughness increases with concentration and thickness [45]. Therefore, the observed increase in antibacterial activity with increased concentration under shaken condition could arise from increased coating roughness. Static coated samples did not display inherent antibacterial activity arising from the polydopamine

coating when Pro-Cip was omitted from the coating, with log reduction <0.3 even when the dopamine concentration was increased to 3.0 mg/mL. The absence of inherent antibacterial activity was expected for the 1h static polymerization condition used, since minimizing the coating time <3h typically promotes smooth polydopamine coating formation [23].

For static coated samples, the log reduction for *P. aeruginosa* and MRSA increased significantly when the concentration of PDA and Pro-Cip was increased from 0.25 mg/mL to 3.0 mg/mL. Interestingly, for the samples which reacted under shaken conditions, the antimicrobial activity was not significantly improved by increasing the concentration. This could arise from the polydopamine particle formation which occurs under shaken conditions. Shaking prevents the sedimentation of larger polydopamine particles throughout the self-polymerization of dopamine in the reaction solution, and facilitates their incorporation into the coating. Higher concentration of dopamine in the reaction solution could impact the PDA particle size and resulting release kinetics of Cip and accessibility of Pro-Cip to lipase.

Ultimately, static coatings with 3.0 mg/mL dopamine concentration yielded the optimal balance between acceptable coating colour (Figure 1) and antimicrobial potency with a 4.2 ± 0.6 log reduction against *P. aeruginosa* and 1.2 ± 0.1 log reduction against MRSA (Table 3). The benefit of the inherent antimicrobial activity of polydopamine which could be obtained through conducting the one-pot reaction under shaken conditions to produce a rough surface layer was outweighed by the dark black opaque colour of the rough coatings.

Table 3. Antibacterial activity of PDA/Pro-Cip coated bioengineered collagen-GAG matrix in an ex vivo porcine skin burn model, after 18h contact.

	Sample	Log Reduction		
		E. coli 25922	*P. aeruginosa*	MRSA
Shake	0.05 mg/mL PDA	0.39 ± 0.05	0.19 ± 0.06	0.77 ± 0.09
	0.05 mg/mL PDA 1:1 PDA:Pro-Cip	2.53 ± 0.08	3.08 ± 0.03	1.05 ± 0.04
	0.25 mg/mL PDA	0.04 ± 0.05	0.9 ± 0.1	0.81 ± 0.04
	0.25 mg/mL PDA, 1:1 PDA:Pro-Cip	2.39 ± 0.05	1.7 ± 0.1	0.7 ± 0.5
Static	0.25 mg/mL PDA	0.09 ± 0.04	0.22 ± 0.09	0.9 ± 0.3
	0.25 mg/mL PDA, 1:1 Pro-Cip	2.44 ± 0.09	0.65 ± 0.04	0.5 ± 0.1
	3.0 mg/mL PDA	0.19 ± 0.01	-0.24 ± 0.02	-0.12 ± 0.04
	3.0 mg/mL PDA, 1:1 PDA:Pro-Cip	2.14 ± 0.05	4.2 ± 0.6	1.2 ± 0.1

The ex vivo antibacterial model promoted drying of bioengineered collagen-GAG samples throughout the prolonged exposure period, which could impede the antibacterial activity of the coating by limiting the diffusion of lipase through the porous matrix of the collagen layer, and thus compromise the cleavage of the Pro-drug by lipase for release of the active drug. For this reason, a suspension-based direct contact test was adopted for preliminary screening and testing of the various tested coating formulations. The antibacterial activity of the 3 mg/mL PDA and 3 mg/mL PDA 1:1 PDA:Pro-Cip static coatings were evaluated by immersing 1cmx1cm samples in 1 mL of bacteria suspension for 5h direct contact, followed by quantifying the reduction in bacteria concentration (Table 4). Excellent log reduction of *E. coli* and *P. aeruginosa* were achieved, with

values of 4.38 ± 0.35 and 2.14 ± 0.02 respectively. In comparison, the coated membrane was less effective against MRSA, with only 0.67 ± 0.01 log reduction after 5h contact.

Table 4. Antibacterial activity of static one-pot coated bioengineered collagen-GAG matrix after 5h direct contact with bacteria suspension.

	Log Reduction (inoculum $1.0x10^8$ CFU/mL)		
	E. coli	MRSA	*P. aeruginosa*
3 mg/mL PDA, 1h static	0.02 ± 0.02	0.11 ± 0.02	0.25 ± 0.07
3 mg/mL 1:1 PDA:Pro-Cip, 1h static	4.38 ± 0.35	0.67 ± 0.01	2.14 ± 0.02

The physical morphology of the coated samples was assessed using SEM to assess the surface roughness obtained by the shaken and static coating strategies. The samples which were coated under shaken conditions displayed visible particulates bound to the surface of the collagen matrix (Figure 2). It is well-documented that black PDA particles form in solution during the self-polymerization of dopamine under alkaline conditions. In the case of a static reaction solution, the particles sediment to the bottom of the dish, resulting in a smooth PDA coating on the sample surface. In contrast, shaking allows the PDA particles to remain in suspension throughout the coating process which leads to a rough surface coating which has also been associated with increased antibacterial activity [25].

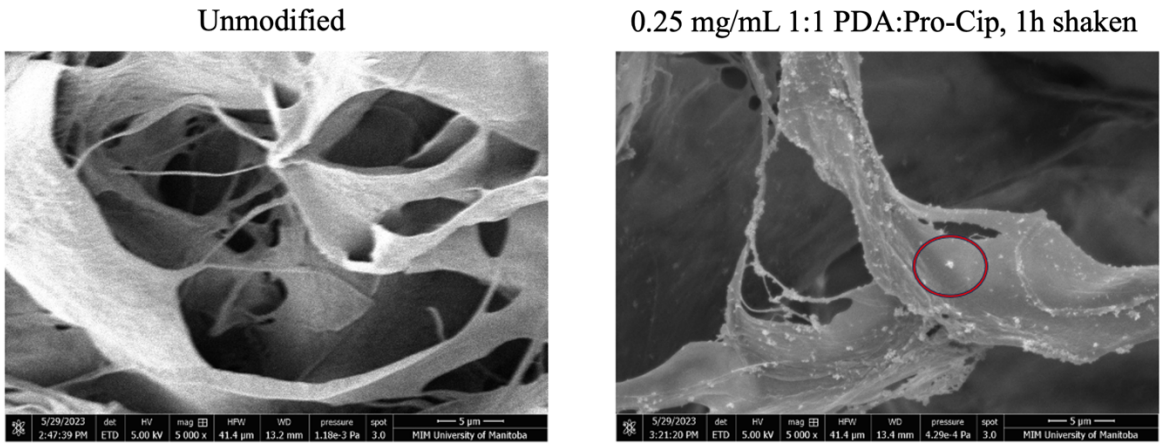

Figure 2. Physical morphology of collagen layer of the bioengineered collagen-GAG matrix after coating (top view). SEM of bioengineered collagen-GAG matrix, either uncoated or after coating with 0.25 mg/mL PDA, 1:1 Pro-Cip under shaken conditions, 1h coating time.

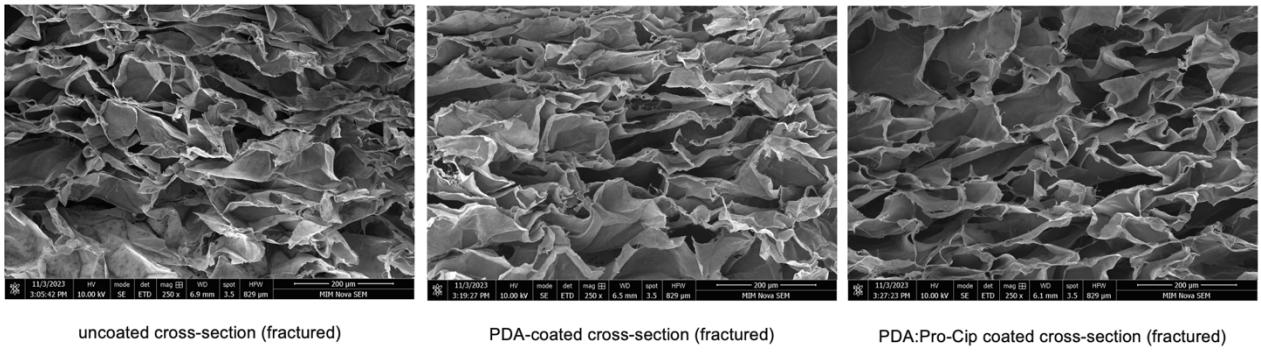

Figure 3. Physical morphology of bioengineered collagen-GAG matrix after coating (cross-sections after fracture with liquid nitrogen). SEM of bioengineered collagen-GAG matrix, either uncoated, coated with 3.0 mg/mL PDA 1h static, or 3.0 mg/mL 1:1 PDA:Pro-Cip 1h static.

The pore structure of the bioengineered collagen-GAG matrix coated under static conditions was assessed by SEM (Figure 3). The pore structure was not significantly impacted by coating with 3.0 mg/mL PDA or 3.0 mg/mL PDA 1:1 Pro-Cip under static conditions compared to the uncoated bioengineered collagen-GAG matrix. This confirms the expectation that the coating would not markedly impact the porosity of the dermal regeneration template since polydopamine coatings typically range from 20-50 nm thickness.

4.2.2 Lipase-responsive behaviour of static coated samples

The lipase-responsive release of ciprofloxacin from the 3.0 mg/mL 1:1 PDA/Pro-Cip static-coated matrix was quantified in the presence or absence of commercial *Burkholderia cepacia* lipase (1 μg/mL or 5 mg/mL) based on UV absorbance at 325 nm (Figure 4). The UV-vis absorbance of ciprofloxacin at 325 nm UV-vis absorbance spectrum was confirmed to be free of interference from the UV-vis absorbance of polydopamine (Supplemental Figure A2). Lipase-responsive cleavage of ciprofloxacin from the covalently bound Pro-drug was successfully confirmed at a lipase concentration of 5 mg/mL, with a release of ciprofloxacin exceeding 8 μg/mL after 192h, compared to <2 μg/mL release after 192h in the absence of lipase.

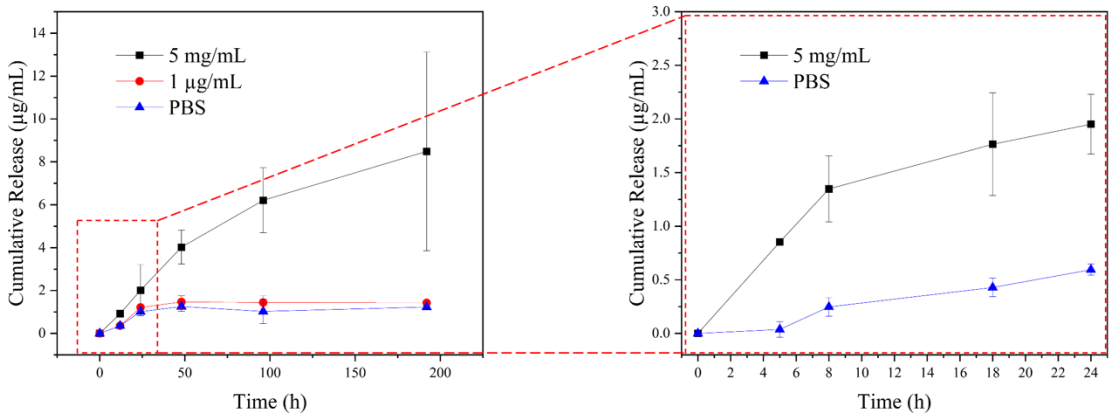

Figure 4. Cumulative release of Cip from 3.0 mg/mL 1:1 Pro-Cip coated bioengineered collagen-GAG matrix.

Table 5. Release of ciprofloxacin from 3 mg/mL 1:1 Pro-Cip:PDA coated matrix in the presence of 5 mg/mL *B. cepacia* lipase, at pH 7.4 and 37ºC.

Time (h)	Released Cip (µg/mL)	
	Lipase (5 mg/mL)	PBS
0	0	0
5	0.85 ± 0.01	0.04 ± 0.07
8	1.3 ± 0.3	0.25 ± 0.09
18	1.8 ± 0.5	0.43 ± 0.09
24	2.0 ± 0.3	0.59 ± 0.05

The MIC of ciprofloxacin against *E. coli*, MRSA and *P. aeruginosa* are <0.0625 µg/mL for *E. coli*, 0.125 µg/mL for *P. aeruginosa*, and 0.25 µg/mL for MRSA (Table 1). The released ciprofloxacin in the presence of 5 mg/mL commercial lipase exceeds the experimentally determined MIC values for the tested bacteria strains (Table 5).

To further explore the lipase-responsive antibacterial activity of the Pro-Cip-coated bioengineered collagen-GAG matrix, the 1h shaken-coated samples were tested against a lipase-producing (ATCC 25922) and non-lipase producing (Top10) strain of *E. coli* (Figure 5, Table 6). The bioengineered collagen-GAG matrix coated with PDA alone (without Pro-Cip) did not exhibit any ZOI against *E. coli* ATCC 25922 or Top10. The absence of a ZOI should not be interpreted as a lack of antibacterial activity, since the PDA coating is covalently bound to the collagen layer and therefore is not mobile to diffuse through the agar to create an inhibition zone. In this case, the ex vivo direct contact test provides a better description of the antimicrobial impact of the polydopamine layer when Pro-Cip is not included in the coating, where a <1.0 log reduction was observed for rough coated membranes. When Pro-Cip was included in the coating, the membranes static-coated with PDA and Pro-Cip did show inhibition zone size of 8.8-9.0 mm toward the lipase-positive *E. coli* ATCC 25922, indicating release of ciprofloxacin from the coating. Since the membranes did not exhibit inhibition zones against a non-lipase producing strain of *E. coli* Top10, the ZOI observed in the lipase-positive strain support the expected cleavage of the pro-drug Pro-Cip by lipase to release the active drug ciprofloxacin.

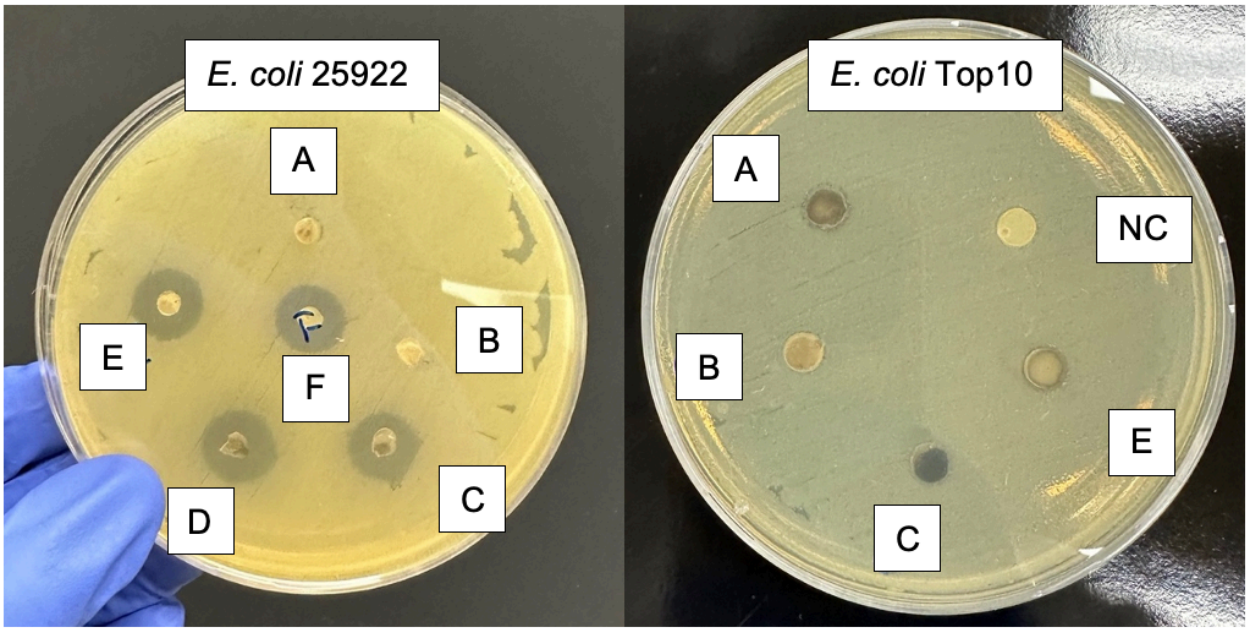

Figure 5. Zone of inhibition of shaken one-pot coated bioengineered collagen-GAG matrix with or without Pro-Cip against *E. coli* 25922 (lipase positive) or *E. coli* Top10 (lipase negative). Coatings were composed of: (A) 0.25 mg/mL PDA 1h shaken, (B) 0.05 mg/mL PDA 1h shaken, (C) 0.25 mg/mL PDA 1:1 PDA:Pro-Cip 1h shaken, (D) 0.25 mg/mL PDA 10:1 PDA:Pro-Cip 1h shaken, (E) 0.05 mg/mL PDA 1:1 PDA:Pro-Cip 1h shaken, (F) 0.05 mg/mL PDA 10:1 PDA:Pro-Cip 1h shaken.

Inhibition zone diameters corresponding to the membranes tested in Figure 5 are noted below in Table 6.

Table 6. Zone of inhibition of 1h shaken one-pot coated bioengineered collagen-GAG matrix against *E. coli* 25922 (lipase positive) and *E. coli* Top10 (lipase negative).

Sample	Treatment	Diameter (mm)	
		E. coli 25922	*E. coli* Top 10
A	0.25 mg/mL PDA, 1h shaken	0	0
B	0.05 mg/mL PDA, 1h shaken	0	0
C	0.25 mg/mL PDA, 1:1 PDA:Pro-Cip, 1h shaken	8.9	0
D	0.25 mg/mL PDA, 10:1 PDA:Pro-Cip, 1h shaken	9.0	-
E	0.05 mg/mL PDA, 1:1 PDA:Pro-Cip, 1h shaken	9.0	0
F	0.05 mg/mL PDA, 10:1 PDA:Pro-Cip, 1h shaken	8.8	-

4.2.3 Cytocompatibility of one-pot polydopamine coatings

PDA/Pro-Cip-coated bioengineered collagen-GAG matrix samples were eluted in growth medium for duration of 24h, followed by treating primary human dermal fibroblasts (PCS-201-012) with the eluted medium for 24h to evaluate the cytotoxicity of released matter from the coating (Figure 6). The cell viability of cells exposed to the PDA or PDA/Pro-Cip elutions was not statistically significantly different compared to the cell viability of elutions from uncoated bioengineered collagen-GAG matrix, and all tested samples had cell viability of >90%.

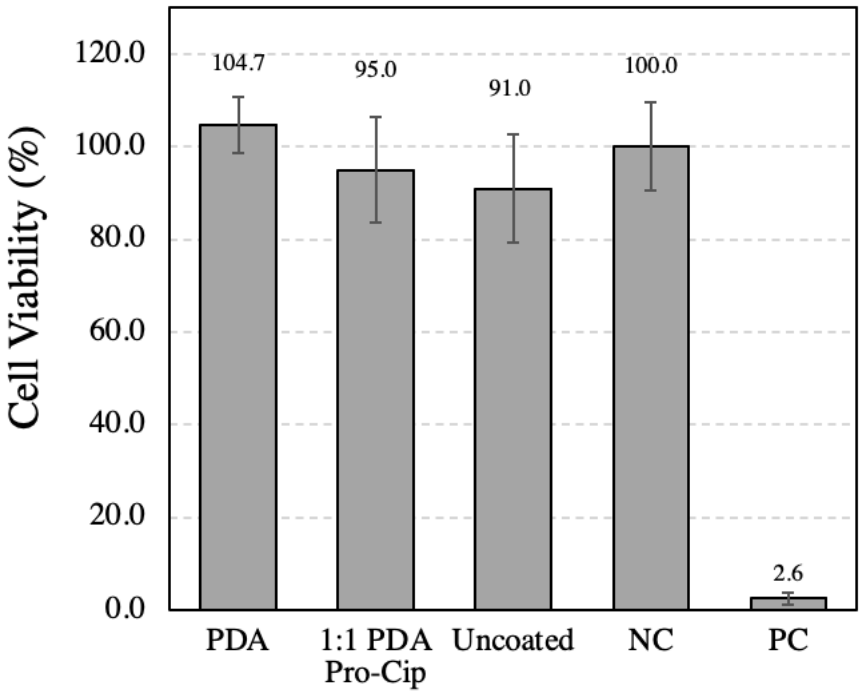

Figure 6. Cytotoxicity of elution from coated bioengineered collagen-GAG matrix towards human dermal fibroblasts. Coated bioengineered collagen-GAG matrices (1.0 cm^2) eluted in culture media for 24h, followed by exposure of PCS-201-012 human dermal fibroblasts to elution for 24h. Coatings included 3.0 mg/mL PDA 1h static ("PDA"), 3.0 mg/mL 1:1 PDA:Pro-Cip ("1:1 PDA Pro-Cip"), untreated, negative control of blank culture medium ("NC") and positive control of 1.0 M acrylamide ("PC").

Typically, cell viability could be quantitatively confirmed through MTT assay of PCS-201-012 fibroblasts cultured in direct contact with the coated samples. However, polydopamine is known to reduce MTT, which interferes with the assay result which is dependent on the reduction of MTT to formazan by dehydrogenases in the mitochondria of living cells [46]. Therefore, cell viability of cells in direct contact with the coated samples was determined based on Live/dead

staining of the cells with calcein-AM and ethidium homodimer-1 (Figure 7). After 48h attachment, the cells in direct contact with the coated surfaces displayed good viability with minimal cell death and elongated and flattened cell morphology and even distribution on the scaffold, with similar appearance to fibroblasts cultured on the uncoated negative control.

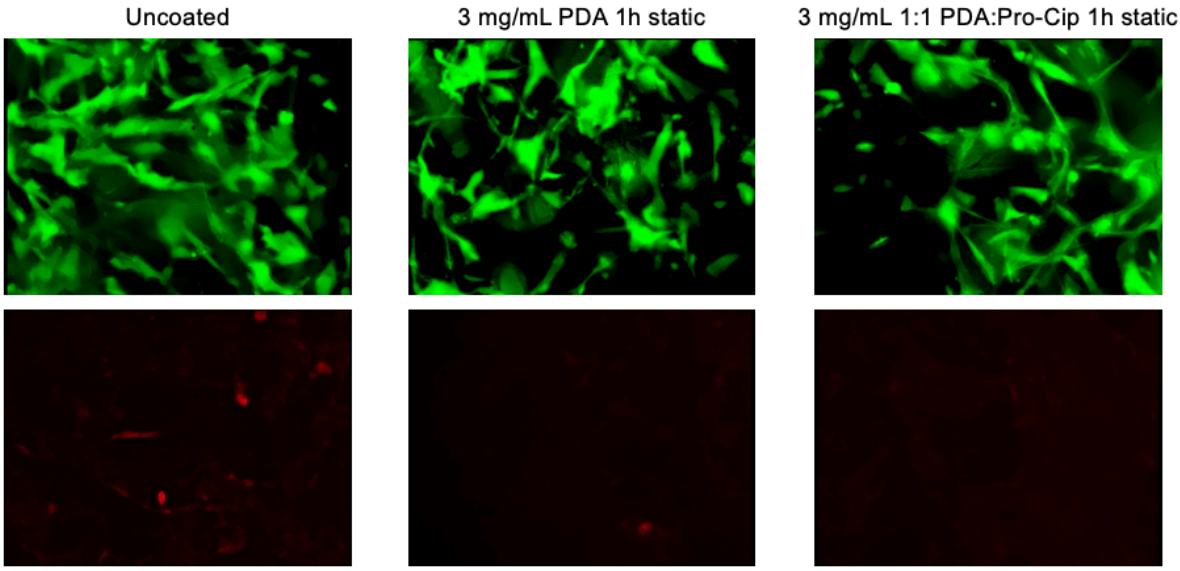

Figure 7. Cell viability of PCS-201-012 human primary dermal fibroblasts on one-pot static-coated bioengineered collagen-GAG matrix samples, 48h after seeding. Live/Dead assay (calcein-AM and ethidium homodimer-1). Samples included uncoated bioengineered collagen-GAG matrix, matrix coated with 3.0 mg/mL PDA 1h static, or matrix coated with 3.0 mg/mL 1:1 PDA:Pro-Cip 1h static.

4.3. Surfactants for boosted lipase activity

As previously discussed, static 1h one-pot coating of bioengineered collagen-GAG matrix with 3 mg/mL PDA 1:1 PDA:Pro-Cip yielded promising antibacterial activity against *E. coli* and

P. aeruginosa, with log reductions of 4.38 ± 0.35 and 2.14 ± 0.02 respectively after 5h contact. However, the antibacterial activity of the 3 mg/mL PDA 1:1 PDA:Pro-Cip static-coated membrane was insufficient against MRSA, with 0.67 ± 0.01 log reduction after the same duration. Therefore, various surfactants were explored as potential additives to improve the cleavage efficiency of the Pro-drug in the presence of MRSA. Nonionic surfactants can increase enzyme catalytic efficiency and interact with the enzyme itself to stabilize the active conformation of lipase (whereas ionic surfactants can have a denaturing effect) [47]. Furthermore, the coating duration was increased from 1h static coating to 18h coating with shaking increase coating thickness. Coating formulations with surfactants are described in Table 6.

Table 6. PDA coating formulations for boosted lipase activity

Sample	PDA	Cip	Additive	Condition
A	3 mg/mL	-	-	1h static
B	3 mg/mL	3 mg/mL	-	1h static
C	3 mg/mL	3 mg/mL	-	18h shaking
D	3 mg/mL	3 mg/mL	Tween 20 (2.5 v/v%)	1h shaking
E	3 mg/mL	3 mg/mL	Tween 80 (2.5 v/v%)	1h shaking
F	3 mg/mL	3 mg/mL	Triton X-100 (2.5 v/v%)	1h shaking
G	3 mg/mL	3 mg/mL	Olive oil (2.5 v/v%)	1h shaking
H	-	-	-	negative control

The antibacterial activity of the surfactant-coated samples was screened by zone of inhibition (Figure 8).

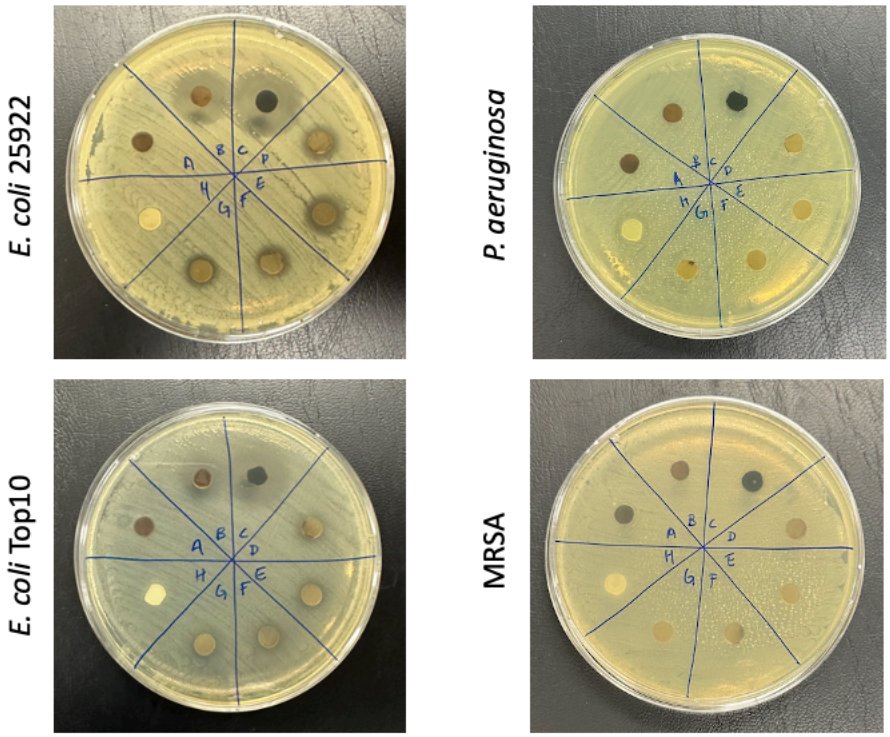

Figure 8. Effect of coatings incorporating surfactants on the ZOI diameter in exposure to one-pot coated bioengineered collagen-GAG matrix. (A) 3 mg/mL PDA 1h static coat, (B) 3 mg/mL 1:1 PDA:Pro-Cip 1h static coat, (C) 3 mg/mL 1:1 PDA:Pro-Cip, 18h shaken coat (D) 3 mg/mL 1:1 PDA:Pro-Cip, 1h shaken coat with Tween 20, (E) 3 mg/mL 1:1 PDA:Pro-Cip, 1h shaken coat with Tween 80, (F) 3 mg/mL 1:1 PDA:Pro-Cip, 1h shaken coat with Triton X-100, (G) 3 mg/mL 1:1 PDA:Pro-Cip, 1h shaken coat with Olive oil, (H) negative control (uncoated).

Zone diameters for the surfactant-coated samples are reported in Table 7. Increasing the coating thickness by extending the duration of the polymerization reaction from 1h static to 18h with shaking increased the ZOI from 15 to 20 mm in *E. coli*, and 8 to 10 mm in *P. aeruginosa*. However, the increased concentration of Pro-Cip in the 18h-coated sample was still insufficient to

produce a discernable ZOI against MRSA. The incorporation of nonionic surfactants Tween 20, Tween 80 and Triton X-100 did not boost the efficacy of cleavage of Pro-Cip by lipase and actually appeared to have a negative effect on the antibacterial activity of the coatings, as evidenced by the smaller ZOI diameter.

Table 7. ZOI of PDA-coated bioengineered collagen-GAG matrix with various surfactant additives.

Sample*	Inhibition Zone Diameter (mm)			
	E. coli	Top 10	MRSA	*P. a.*
A	0	0	0	0
B	15	12	0	8
C	20	16	0	10
D	10	7	0	7
E	11	7	0	7
F	10	7	0	7
G	8	7	0	7
H	0	0	0	0

*(A) 3 mg/mL PDA 1h static coat, (B) 3 mg/mL 1:1 PDA:Pro-Cip 1h static coat, (C) 3 mg/mL 1:1 PDA:Pro-Cip, 18h shaken coat (D) 3 mg/mL 1:1 PDA:Pro-Cip, 1h shaken coat with Tween 20, (E) 3 mg/mL 1:1 PDA:Pro-Cip, 1h shaken coat with Tween 80, (F) 3 mg/mL 1:1 PDA:Pro-Cip, 1h shaken coat with Triton X-100, (G) 3 mg/mL 1:1 PDA:Pro-Cip, 1h shaken coat with Olive oil, (H) negative control (uncoated).

The surfactant-coated samples were further evaluated for antibacterial potency by immersion in bacteria suspension for 5h contact (Table 8). The antibacterial activity against MRSA and *P. aeruginosa* was improved by increasing the coating duration from 1h to 18h (increase in log reduction from 0.67 ± 0.01 to 1.11 ± 0.21 for MRSA, and increase from 2.14 ± 0.02 to 4.56 ± 0.05 for *P. aeruginosa*). Similar to the ZOI results, the incorporation of various surfactants did not boost the antibacterial activity against the three tested bacteria, but actually had a negative impact on the antibacterial activity. The addition of surfactants could potentially compromise the coating process. The addition of surfactant might increase aggregation of PDA particles which form during the self-polymerization of dopamine under alkaline conditions, which could result in increased sedimentation of PDA and Pro-Cip in the reaction solution and decrease the efficiency of coating with the collagen layer of the bioengineered collagen-GAG matrix. Alternatively, the incorporation of surfactant might solubilize PDA oligomers, reducing their ability to deposit as a coherent film.

Table 8. Antibacterial activity of surfactant-containing coatings after 5h direct contact with bacteria suspensions.

		Log Reduction (inoculum $1.0x10^8$ CFU/mL)		
	Sample	*E. coli*	MRSA	*P. aeruginosa*
A	3 mg/mL PDA, 1h static	0.02 ± 0.02	0.11 ± 0.02	0.25 ± 0.07
B	3 mg/mL 1:1 PDA:Pro-Cip, 1h static	4.38 ± 0.35	0.67 ± 0.01	2.14 ± 0.02
C	3 mg/mL 1:1PDA:Pro-Cip,18h shake	4.42 ± 0.28	1.11 ± 0.21	4.56 ± 0.05
D	3 mg/mL 1:1 PDA:Pro-Cip with Tween 20 (2.5 v/v%), 1h shake	3.94 ± 0.19	0.31 ± 0.06	0.32 ± 0.11
E	3 mg/mL 1:1 PDA:Pro-Cip with Tween 80 (2.5 v/v%), 1h shake	3.99 ± 0.11	0.31 ± 0.04	0.74 ± 0.41
F	3 mg/mL 1:1 PDA:Pro-Cip with Triton X-100 (2.5 v/v%), 1h shake	3.71 ± 0.11	0.62 ± 0.21	0.27 ± 0.03
G	3 mg/mL 1:1 PDA:Pro-Cip with Olive oil (2.5 v/v%), 1h shake	4.42 ± 0.28	0.27 ± 0.08	1.79 ± 0.02

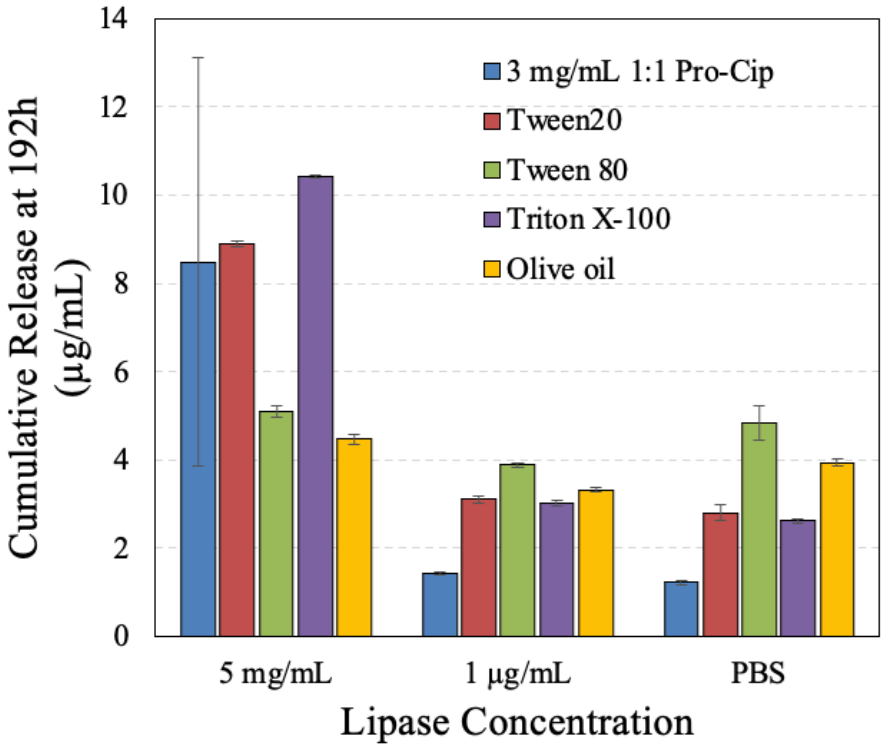

Figure 9. Cumulative release of ciprofloxacin after 192h exposure to lipase from coated bioengineered collagen-GAG matrix containing surfactants. Exposure to 5.0 mg/mL or 1 µg/mL *B. cepacia* lipase, pH 7.4 and 37ºC.

The cumulative release characteristics of the surfactant-coated membranes confirmed that the overall release of ciprofloxacin from lipase-exposed samples was lower in comparison to the formulation which did not include surfactant in the coating (Figure 9). For 18h shaken polymerization condition (without surfactant), the release of ciprofloxacin after 192h exposure to 5 mg/mL commercial *B. cepacia* lipase was 8.5 ± 4.6 µg/mL, compared to 8.90 ± 0.08 µg/mL (Tween 20), 5.1 ± 0.1 µg/mL (Tween 80), 10.43 ± 0.03 µg/mL (Triton X-100) and 4.5 ± 0.1 µg/mL (olive oil). The lower cumulative release of ciprofloxacin from the surfactant-coated membranes was consistent with the lower antibacterial activity observed in the surfactant-coated samples.

4.5. Inducers for boosted lipase activity

Another strategy to boost the antibacterial activity against MRSA involved incorporating inducers in the coating in order to boost the lipase activity: either by boosting production of bacterial lipase by substrate induction, or by enhancing the activity of the enzyme itself. The effects of various inducers (methyl oleate, olive oil, Tween 80, Mg^{2+} and Ca^{2+}) on the lipase activity of *P. aeruginosa* and MRSA were explored in vitro to screen for inducers which may be viable additives for the coating to boost lipase activity on Pro-Cip. The bacteria were grown in the presence of various inducers in broth media followed by culture on ex vivo pig skin for 18h before sampling for lipase activity. Lipase activity was quantified spectrophotometrically using a pNPP-based lipase assay.

For induction of lipase activity in *P. aeruginosa*, methyl oleate and olive oil were both effective carbon sources to boost lipase activity from 0.64 μmol/min/cm^2 in the negative control to 4.11 or 6.66 μmol/min/cm^2 for methyl oleate and olive oil respectively (Figure 10). $CaCl_2$ boosted lipase activity from 1.77 μmol/min/cm^2 to 6.72 μmol/min/cm^2 as the $CaCl_2$ concentration increased from 0.01% to 0.05%. The addition of $MgCl_2$ and $MgSO_4$ to the growth medium also successfully boosted lipase activity in *P. aeruginosa*, with a maximum lipase activity achieved with supplementation of the medium with 0.01% $CaCl_2$ and 0.05% $MgCl_2$. The relationship between Ca^{2+} and Mg^{2+} concentration and the induced lipase activity appears to be complex, as lipase activity does not simply increase with increased concentration of the inducer.

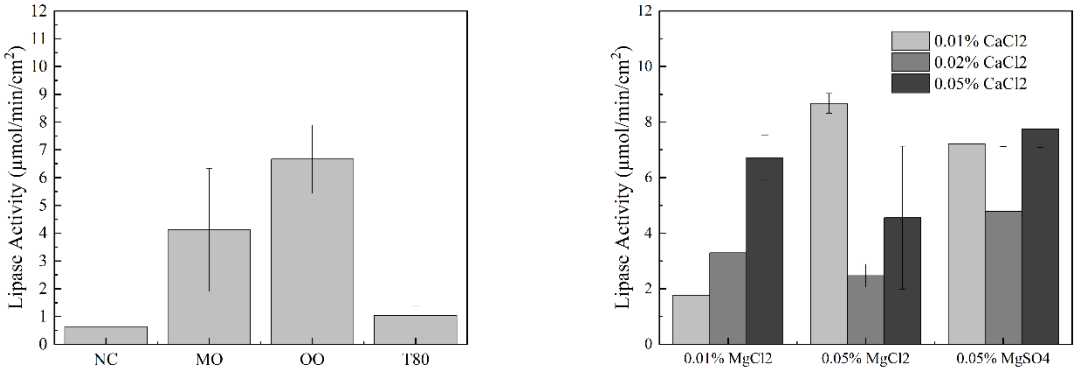

Figure 10. Lipase activity of *P. aeruginosa* grown in the presence of various inducer carbon sources (left) or ions (right).

The induced lipase activity of MRSA was similarly explored in an ex vivo model (Figure 11). Methyl oleate and olive oil effectively boosted the lipase activity from 3.45 µmol/min/cm^2 in the negative control to 7.31 and 7.42 µmol/min/cm^2 respectively for methyl oleate and olive oil. Supplementation with Ca^{2+} and Mg^{2+} also resulted in elevated lipase activity in the ex vivo model, although increasing the inducer concentration did not exhibit a direct relationship with increased lipase activity.

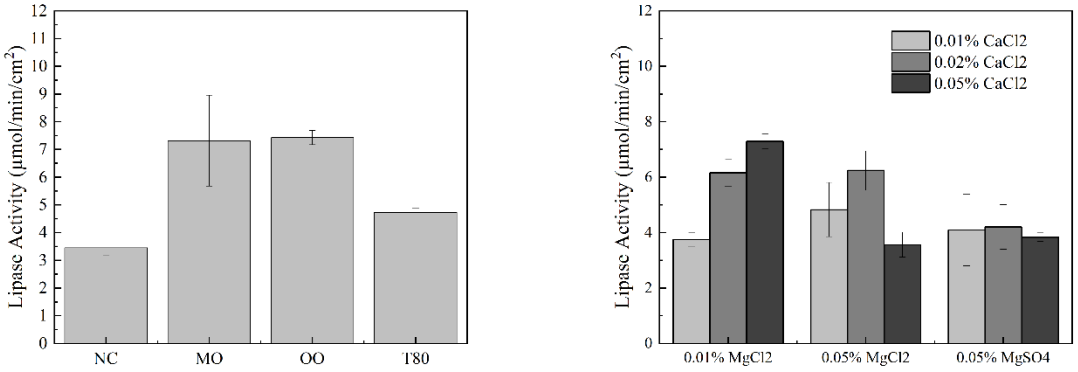

Figure 11. Lipase activity of MRSA grown in the presence of various inducer carbon sources (left) or ions (right).

Various inducers including Ca^{2+}, Mg^{2+} and olive oil (emulsified with Tween-80) were added to the coating formulation at 10:1, 1:1 or 1:3 ratio with the PDA content (Scheme 10). The samples were coated for 18h with shaking at 200 rpm.

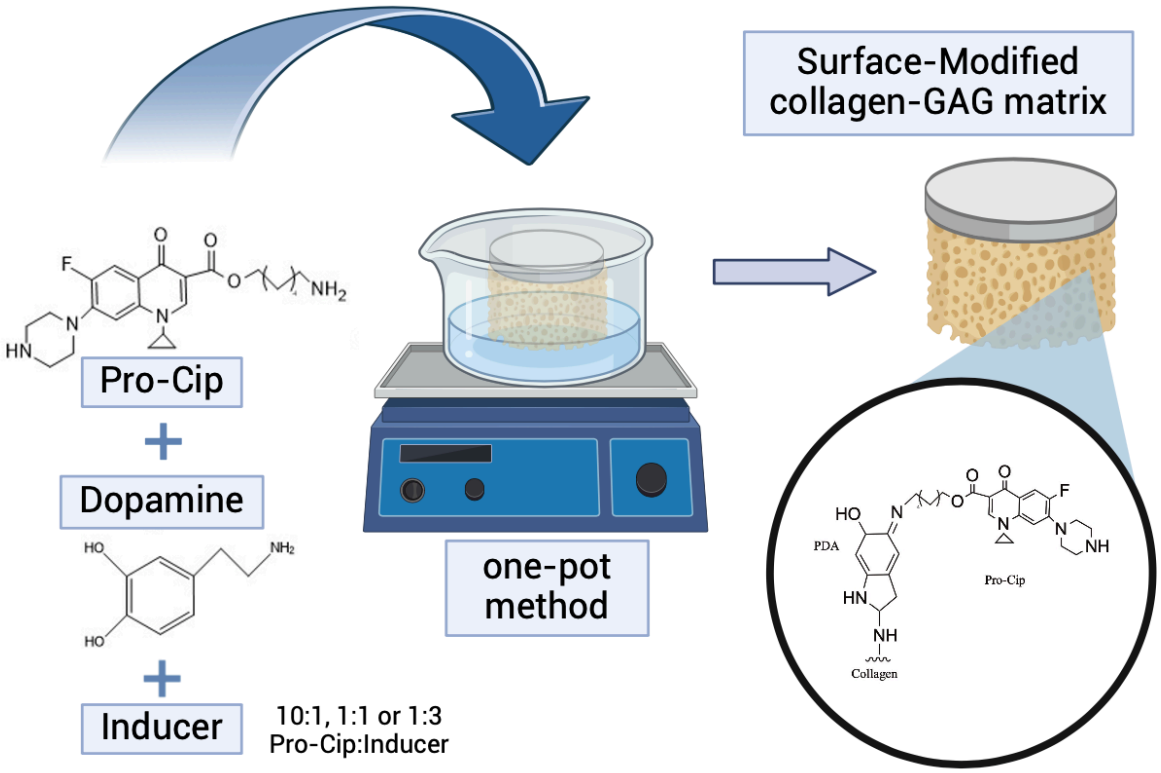

Scheme 10. Incorporation of various inducers to the coating formulation for enhanced lipase activity against Pro-Cip.

The ZOI for inducer-coated bioengineered collagen-GAG matrix samples were tested in response to *E. coli*, *P. aeruginosa* and MRSA (Figure 12, Table 9). $MgCl_2$ and $CaCl_2$ were both effective additives to boost the release of ciprofloxacin from the pro-drug coated membranes, as evidenced by the increase in ZOI diameter from 9 mm to 12 mm in each case (1:3 ratio for $MgCl_2$ or 1:1 ratio for $CaCl_2$). Olive oil/Tween 80 emulsion was also effective in boosting the zone diameter from 9 to 13 mm against MRSA. A subtle increase in zone diameter was observed for inducer-coatings toward *P. aeruginosa*, from 11 to 12 mm in the presence of the additives 1:1 $MgCl_2$, 1:1 $CaCl_2$ or olive oil/Tween 80 emulsion (10:1 and 1:1 ratios). The zone diameter did not directly correspond to inducer concentration, as in some cases the optimal concentration for maximizing zone diameter was at the lowest or intermediate ratio tested (10:1 or 1:1).

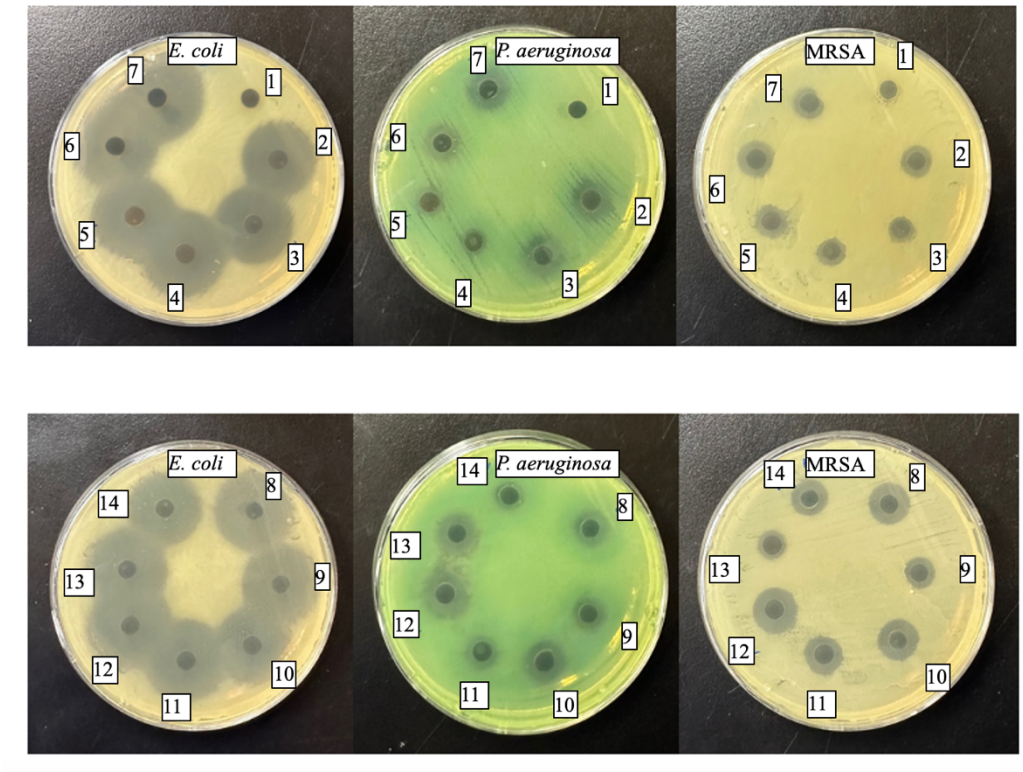

Figure 12. ZOI for inducer-coated bioengineered collagen-GAG matrix samples. (1) 3.0 mg/mL PDA shaken 18h coat, (2) 3.0 mg/mL 1:1 PDA:Pro-Cip shaken 18h coat, (3) 3.0 mg/mL 1:1 PDA:Pro-Cip shaken 18h coat with 10:1 Pro-Cip:OliveOil, (4) 3.0 mg/mL 1:1 PDA:Pro-Cip shaken 18h coat with 1:1 Pro-Cip:OliveOil, (5) 3.0 mg/mL 1:1 PDA:Pro-Cip shaken 18h coat with 1:3 Pro-Cip:OliveOil, (6) 3.0 mg/mL 1:1 PDA:Pro-Cip shaken 18h coat with 10:1 Pro-Cip:$MgCl_2$, (7) 3.0 mg/mL 1:1 PDA:Pro-Cip shaken 18h coat with 1:1 Pro-Cip:$MgCl_2$, (8) 3.0 mg/mL 1:1 PDA:Pro-Cip shaken 18h coat with 1:3 Pro-Cip:$MgCl_2$, (9) 3.0 mg/mL 1:1 PDA:Pro-Cip shaken 18h coat with 10:1 Pro-Cip:$CaCl_2$, (10) 3.0 mg/mL 1:1 PDA:Pro-Cip shaken 18h coat with 1:1 Pro-Cip:$CaCl_2$, (11) 3.0 mg/mL 1:1 PDA:Pro-Cip shaken 18h coat with 1:3 Pro-Cip:$CaCl_2$, (12) 3.0 mg/mL 1:1 PDA:Pro-Cip shaken 18h coat with 10:1 Pro-Cip:OliveOil/Tween80Emulsion, (13) 3.0 mg/mL 1:1 PDA:Pro-Cip shaken 18h coat with 1:1 Pro-Cip:OliveOil/Tween80Emulsion, (14) 3.0 mg/mL 1:1 PDA:Pro-Cip shaken 18h coat with 1:3 Pro-Cip:OliveOil/Tween80Emulsion.

Table 9. ZOI of inducer-coated bioengineered collagen-GAG matrix.

			Zone diameter (mm)		
	Sample	Ratio	MRSA	*P. a.*	*E. coli*
1	PDA	-	0	0	0
2	1:1 Pro-Cip	-	9	11	24
3	OO	10:1	8	11	24
4		1:1	9	8	25
5		1:3	9	8	25
6	$MgCl_2$	10:1	10	10	25
7		1:1	10	12	26
8		1:3	12	10	25
9	$CaCl_2$	10:1	9	10	25
10		1:1	12	12	25
11		1:3	11	10	25
12	OO & T80	10:1	13	12	25
13		1:1	9	12	26
14		1:3	11	8	24

Table 10. Antibacterial activity of inducer-coated bioengineered collagen-GAG matrix after 18h contact with bacteria suspensions (low initial inoculum, ~10^4 CFU/mL).

			Bacteria concentration after 18h (CFU/mL)			
	Sample	Ratio	MRSA	*P. aeruginosa*	*E. coli*	Top10
1	inoculum (time=0)	-	$1.5\pm0.2x10^4$	$2.1\pm0.2x10^4$	$1.4\pm0.2x10^4$	$1.5\pm0.3x10^4$
2	1:1 Pro-Cip	-	0	0	0	0
3	OO	10:1	0	0	0	0
4		1:1	0	0	0	0
5		1:3	0	0	0	0
6	$MgCl_2$	10:1	0	0	0	0
7		1:1	0	0	0	0
9		1:3	0	0	0	0
10	$CaCl_2$	10:1	0	0	0	0
11		1:1	0	$5.6 \pm 1.9 \times 10^1$	0	0
12		1:3	0	$5.9 \pm 0.8 \times 10^3$	0	0
13	OO & T80	10:1	0	$1.6 \pm 1.3 \times 10^3$	0	0
14		1:1	0	$5.7 \pm 0.6 \times 10^2$	0	0
15		1:3	0	$3.3 \pm 3.3 \times 10^1$	0	0

The antibacterial activity of the inducer-coated membranes was evaluated via direct immersion in bacteria suspension. Complete eradication of MRSA and *P. aeruginosa* (no detectable CFU with a detection limit of 33 CFU/mL) was achieved when the coated bioengineered collagen-GAG matrix was inoculated with a low concentration (10^4 CFU/mL) for 18 hours (Table 10). When the initial bacterial concentration reached 10^8 CFU/mL, the coated bioengineered collagen-GAG matrix could attain a 4-4.9 log reduction of two tested bacteria MRSA and *P. aeruginosa* which are the major culprits of wound infection. Specifically, as shown in Table 11, within 8h contact, the log reduction of MRSA was increased from 4.04 ± 0.07 in the sample without inducer (1:1 Pro-Cip) to 4.39 ± 0.08 for the coating containing 1:3 $MgCl_2$ or 4.49 ± 0.06 in the

coating containing $CaCl_2$. Mg^{2+} and Ca^{2+} were also effective inducers for *P. aeruginosa*, and boosted the log reduction from 4.70 ± 0.07 for the 1:1 Pro-Cip sample without inducers to 4.90 ± 0.04 (1:1 $MgCl_2$) or 4.91 ± 0.05 (1:1 $CaCl_2$).

Table 11. Antibacterial activity of inducer-coated bioengineered collagen-GAG matrix after 8h contact with bacteria suspensions, inoculum concentration 10^8 CFU/mL.

			Log reduction after 8h	
	Sample	Ratio	MRSA	*P. aeruginosa*
1	NC	-	9.0 x 10^9 CFU/mL	1.9 x 10^{10} CFU/mL
2	1:1 Pro-Cip	-	4.04 ± 0.07	4.70 ± 0.07
3	OO	10:1	3.91 ± 0.01	4.76 ± 0.01
4		1:1	3.94 ± 0.03	4.73 ± 0.01
5		1:3	3.93 ± 0.02	4.68 ± 0.01
6	$MgCl_2$	10:1	4.30 ± 0.05	4.88 ± 0.01
7		1:1	4.32 ± 0.03	4.90 ± 0.04
9		1:3	4.39 ± 0.08	4.85 ± 0.01
10	$CaCl_2$	10:1	4.27 ± 0.02	4.85 ± 0.01
11		1:1	4.33 ± 0.05	4.91 ± 0.05
12		1:3	4.49 ± 0.06	4.86 ± 0.01
13	OO & T80	10:1	4.25 ± 0.03	4.82 ± 0.02
14		1:1	4.32 ± 0.01	4.81 ± 0.06
15		1:3	4.31 ± 0.04	4.82 ± 0.06

Cumulative release of ciprofloxacin was evaluated for the top performing samples against MRSA (one-pot 18h coating with 1:3 dopamine:$CaCl_2$ or 1:3 dopamine:$MgCl_2$). Release of ciprofloxacin from the coating was evaluated from in vitro in the presence or absence of 5.0 mg/mL commercial *B. cepacia* lipase (Figure 13).

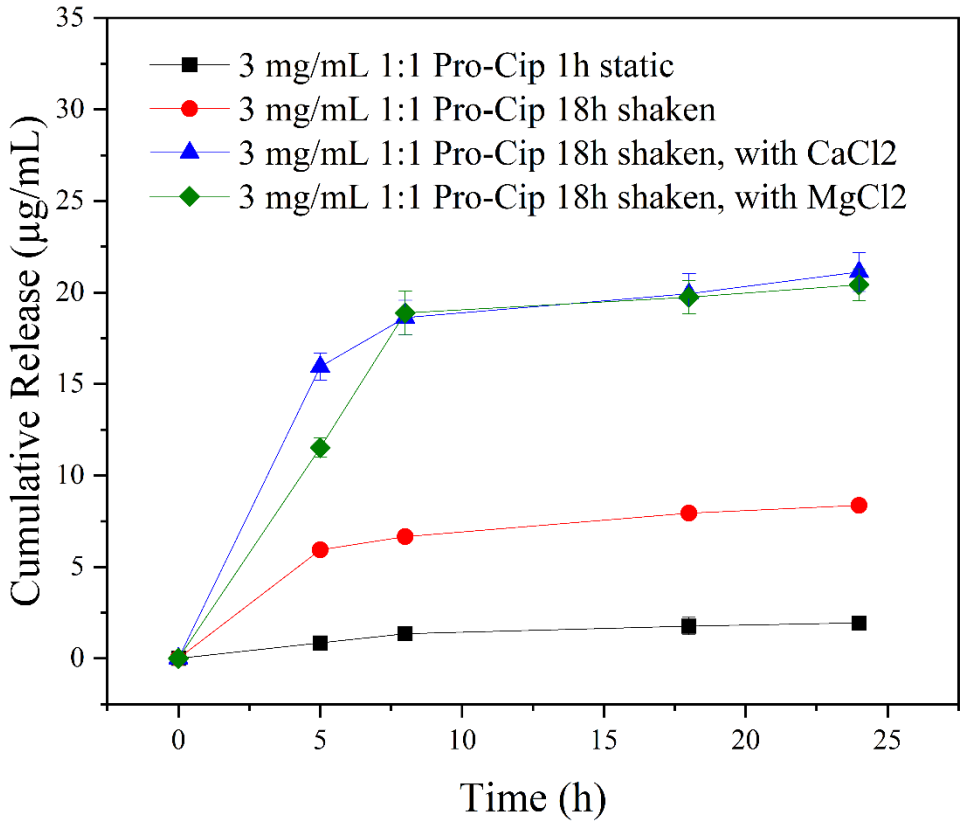

Figure 13. Cumulative release of ciprofloxacin from 18h shaken one-pot coated bioengineered collagen-GAG matrix containing Ca^{2+} or Mg^{2+} inducers, in the presence of 5 mg/mL *B. cepacia* lipase, pH 7.4 and 37ºC.

The cumulative release of ciprofloxacin from the coated bioengineered collagen-GAG matrix containing inducers Ca^{2+} or Mg^{2+} was significantly higher compared to the 18h shaken 1:1 PDA:Pro-Cip coating which was prepared under the same conditions but with the absence of the inducers. The release after 8h for the $CaCl_2$ and $MgCl_2$ coatings were 18.6 ± 0.9 µg and 19 ± 1 µg, respectively. In contrast, release from the coating without $CaCl_2$ or $MgCl_2$ was 6.7 ± 0.2 after 8h. The increased release of ciprofloxacin from the coatings containing divalent cations emphasizes the role of the inducers in boosting cleavage of the pro-drug, which was consistent with the observed antibacterial activity of the inducer-loaded membranes. The *in vitro* release of ciprofloxacin from the Pro-Cip coated bioengineered collagen-GAG matrix cannot be directly compared with the antibacterial result given the differing type and concentration of lipase concentration, but improved antibacterial activity was observed in the same 8h contact period. Against MRSA, after 8h a log reduction of 4.39 ± 0.08 (1:3 dopamine:$MgCl_2$) or 4.49 ± 0.06 (1:3 dopamine:$CaCl_2$) were achieved compared to 4.04 ± 0.07 log reduction in the coated sample without inducers. Similarly, against *P. aeruginosa*, log reductions of 4.85 ± 0.01 (dopamine:$MgCl_2$) or 4.86 ± 0.01 (dopamine:$CaCl_2$) were achieved, compared to 4.70 ± 0.07 without inducers.

Divalent cations Ca^{2+} and Mg^{2+} can increase lipase activity by binding to pockets within the enzyme to influence enzyme structure [48]. *P. aeruginosa* lipase contains a Ca^{2+} binding pocket within its structure which bridges the active site cleft wall to the loop containing His^{251} (part of the catalytic triad) which pushes the histidine residue to the optimal position in the active site of the enzyme [49]. *S. aureus* lipase contains a calcium binding pocket as well [50]. Divalent cations such as Ca^{2+} and Mg^{2+} can stimulate either the production or activity of lipase in some bacteria, but can have an inhibitory effect in others [51]. Zouaoui et al. reported that Ca^{2+} and Mg^{2+} can

increase *P. aeruginosa* lipase activity, while Zn^{2+}, Cu^{2+} and Mn^{2+} inhibit the activity [52]. The lipase activity of *S. aureus* SAL3 is not increased in the presence of Ca^{2+} [53], nor is SAL2, although SAL1 does show Ca^{2+} dependent lipase activity which is higher in the presence of Ca^{2+} [54].

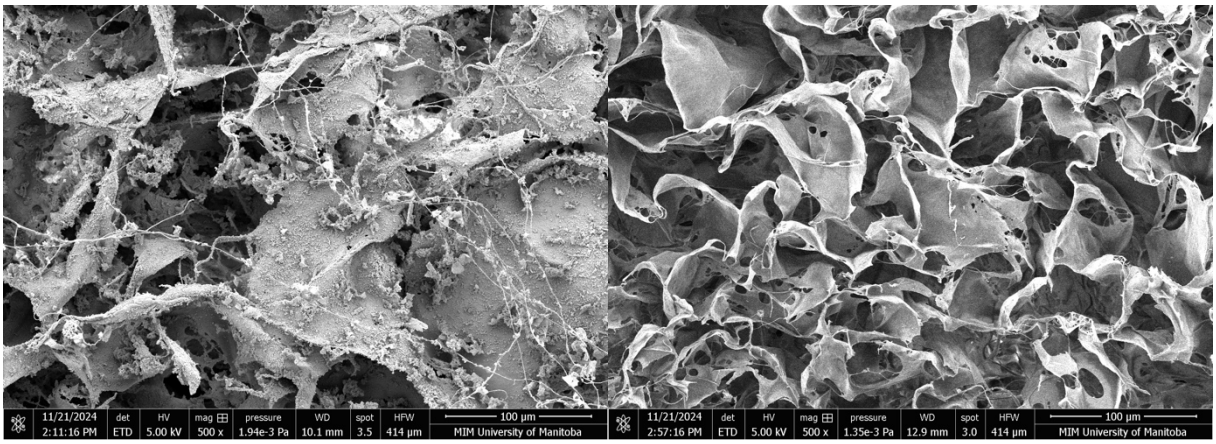

Figure 14. Physical morphology of 1:1 PDA:Pro-Cip 18h shaken coating. SEM of: (Left) Top view of the collagen surface, (Right) cross-section view.

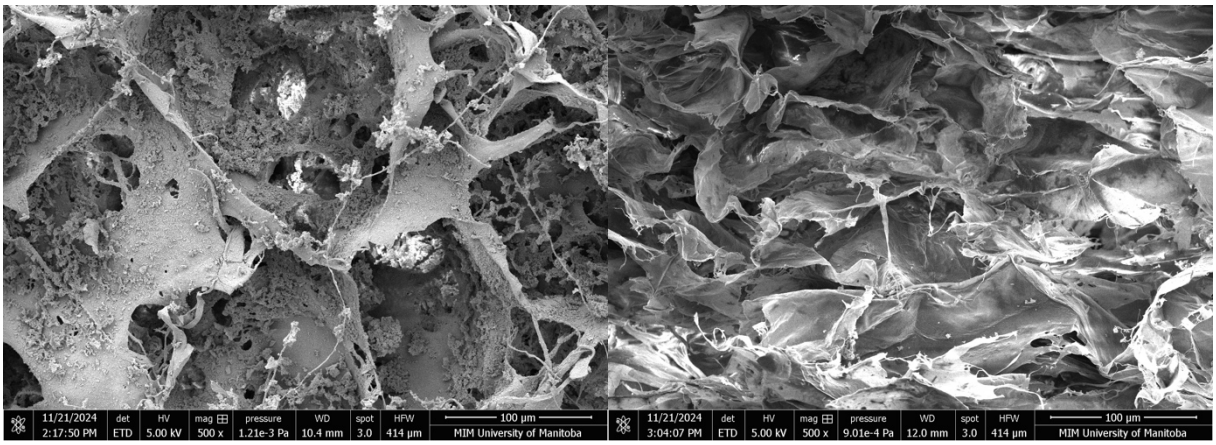

Figure 15. Physical morphology of 1:1 PDA:Pro-Cip 18h shaken coating with $CaCl_2$. SEM of: (Left) Top view of the collagen surface, (Right) cross-section view.

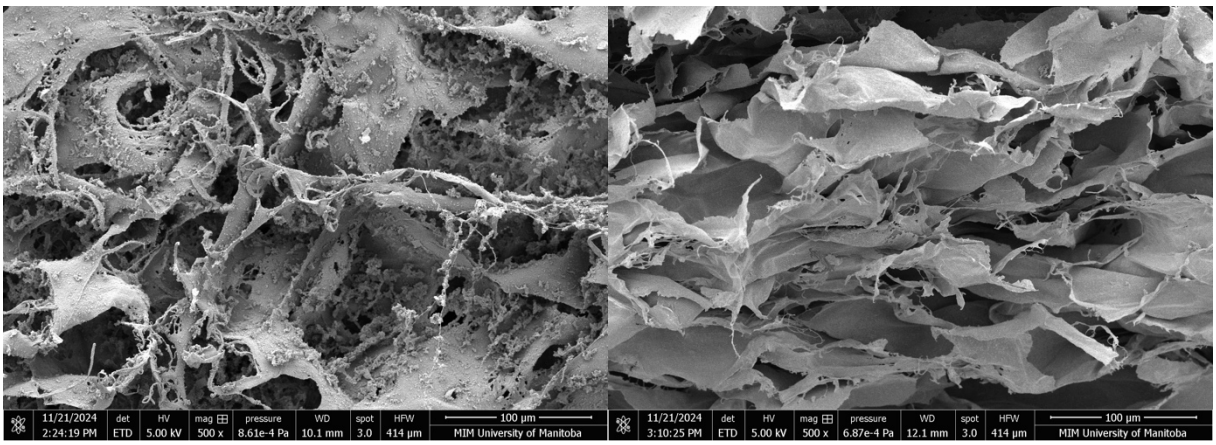

Figure 16. Physical morphology of 1:1 PDA:Pro-Cip 18h shaken coating with $MgCl_2$. SEM of: (Left) Top view of the collagen surface, (Right) cross-section view.

For the samples which were coated with a thick polydopamine layer by shaking for 18h (Figures 14-16), comparison of the top versus cross-section of nitrogen fracture samples of coated bioengineered collagen-GAG matrix revealed that the top surfaces (the outer surface of collagen exposed to the one-pot reaction solution) were coated with abundant polydopamine particle debris. In contrast, the inner pores (visible in the cross-section image) were relatively free of these large particle agglomerations and the inner pore structure remained intact. The agglomerated particle masses were more evident in the 18h shaken samples with $CaCl_2$ and $MgCl_2$.

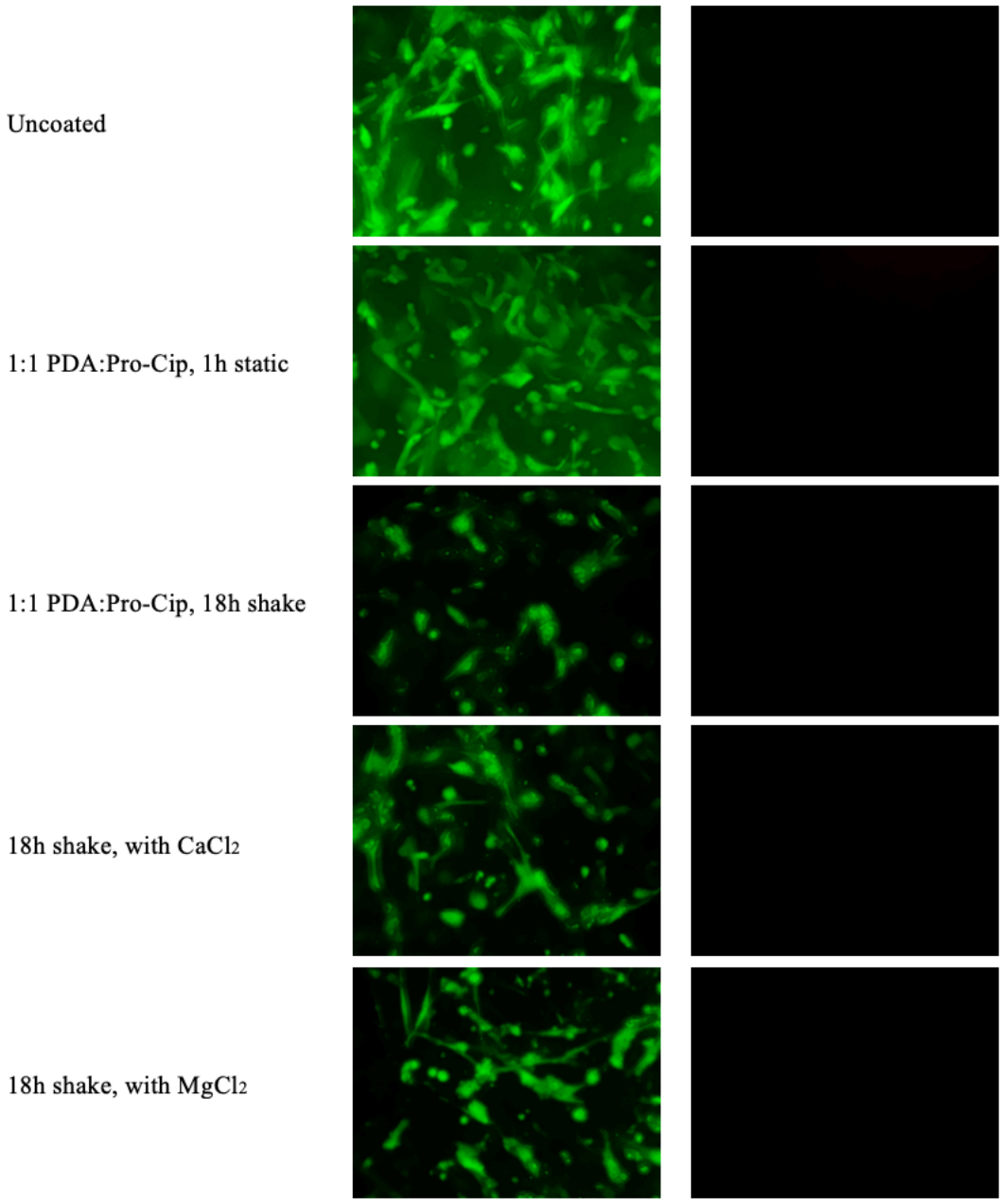

Figure 17. Cell proliferation of PCS-201-012 human primary dermal fibroblasts on coated bioengineered collagen-GAG matrix, 3 days after seeding. Live/Dead assay (calcein-AM and ethidium homodimer-1). High concentration 18h shaken samples, with or without inducers ($MgCl_2$ and $CaCl_2$).

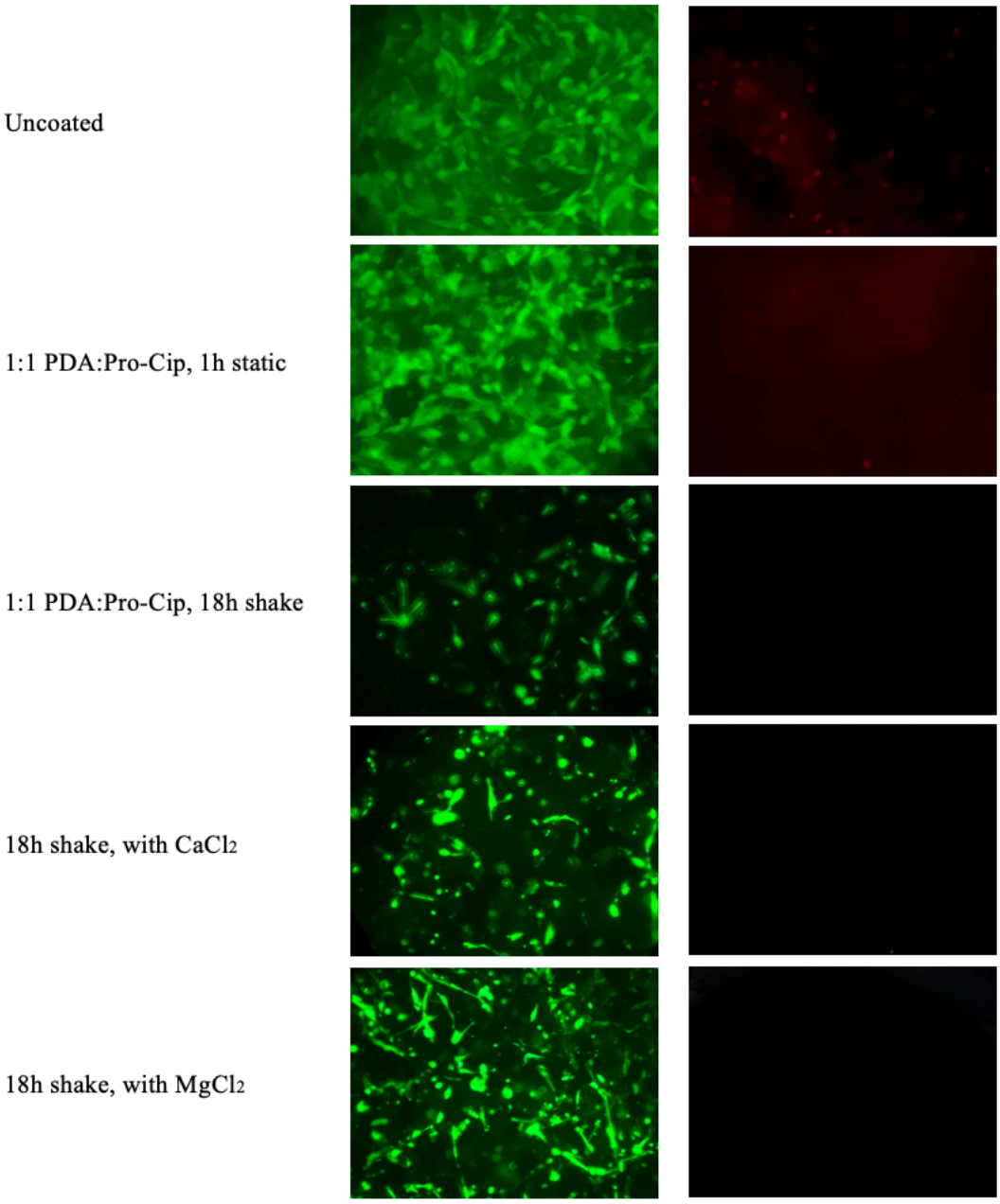

Figure 18. Cell proliferation of PCS-201-012 human primary dermal fibroblasts on coated bioengineered collagen-GAG matrix samples, 7 days after seeding. Live/Dead assay (calcein-AM and ethidium homodimer-1). One-pot 18h shaken samples, with or without inducers ($MgCl_2$ and $CaCl_2$).

After 3 days of direct contact, high densities of viable cells were observed for the ad-layer coated samples as well as the 1:1 Pro-Cip static coated sample (Figure 17). The cell proliferation appeared to be slower on the high-concentration 18h coated samples compared to the samples coated with 1h static condtions (all ad-layer samples as well as the 1:1 Pro-Cip static sample). However, despite lower viable cell density on the 18h shaken coated samples, dead cells were not observed in the red staining with ethidium homodimer-1. After 7 days proliferation on the coated bioengineered collagen-GAG matrices, the one-pot coated dark black samples with the thick 18h shaken polydopamine coatings (with or without $MgCl_2$ or $CaCl_2$) showed lower cell proliferation rate on the coated surfaces compared to the negative control or to the thin 1h static coated membrane (Figure 18). However, the thick one-pot shaken coatings were still cytocompatible as minimal dead cells were observed under red fluorescence.

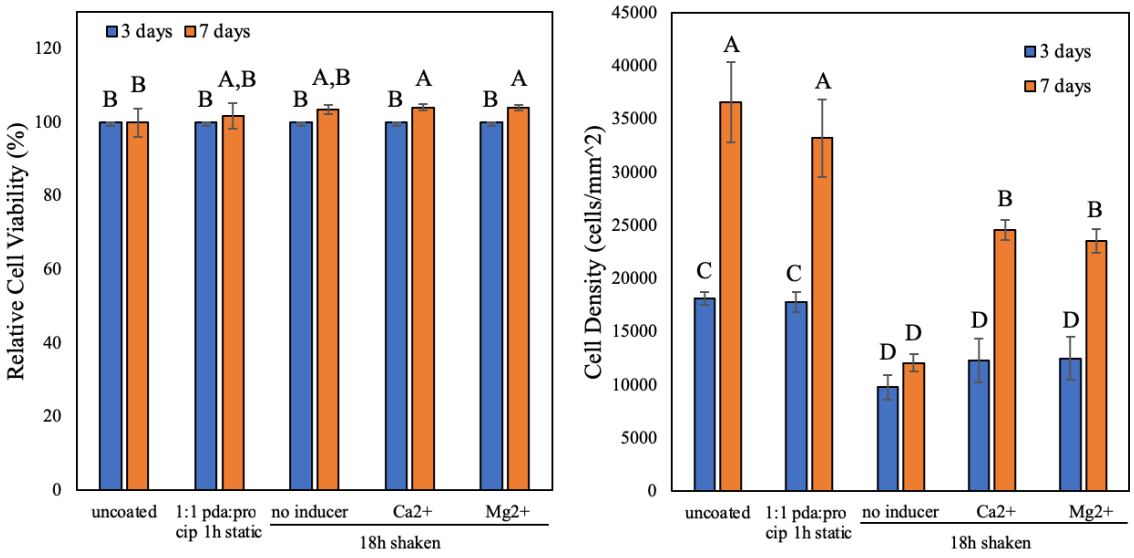

Figure 19. Cell viability of PCS-201-012 fibroblasts after 3-7 days direct contact with one-pot 1h or 18h shaken samples, with or without inducers ($MgCl_2$ and $CaCl_2$). Different letters (A, B, C, D) indicate significant differences by ANOVA with Tukey correction, n=5 ($p<0.05$).

Cell viability and cell density of PCS-201-012 human dermal fibroblasts cultured in direct contact with the coated bioengineered collagen-GAG matrix was evaluated based on enumeration after live/dead staining since typical quantification with MTT assay is not feasible for this application due to interference of polydopamine with the redox-based assay (Figure 19). After 7 days direct contact, there was no significant decrease in cell viability was observed in the coated samples compared to the negative control. Coating with 1:1 PDA:Pro-Cip for 1h (static) did not significantly impact the proliferation rate of the cells compared to uncoated bioengineered collagen-GAG matrix, with a cell density of $3.3 \pm 0.4 \times 10^4$ cells/mm^2 compared to $3.7 \pm 0.4 \times 10^4$ cells/mm^2 in the negative control. The 18h shaken coatings (with or without inducers added) compromised the rate of cell proliferation. Without inducers, 18h shaken coating resulted in a reduction from $3.7 \pm 0.4 \times 10^4$ cells/mm^2 (negative control) to $1.21 \pm 0.08 \times 10^4$ cells/mm^2 after 7 days. With Ca^{2+} or Mg^{2+} incorporated in the 18h shaken coating, cell density was $2.5 \pm 0.1 \times 10^4$ cells/mm^2 or $2.4 \pm 0.1 \times 10^4$ cells/mm^2 after 7 days, respectively.

4.6. Ad-layer coating for boosted loading capacity of Pro-Cip

Increasing the coating time of one-pot static polymerization of dopamine and Pro-Cip from 1h static to 18h with shaking was demonstrated to be effective in increasing the antibacterial activity of the coatings by increasing the thickness of the PDA/Pro-Cip coating, as previously discussed. The addition of inducers for lipase activity further boosted the antibacterial efficacy of the coatings. However, increasing the PDA thickness layer is undesirable for several reasons, including the opaque black colour which is visible to the naked eye and may negatively impact the surface properties of the collagen as well as the acceptability of the product to health care

providers. Consultation with stakeholders such as clinicians and patients would be necessary to determine whether surface colour of the dermal regeneration template impacts perception of the product aesthetically or psychologically, and whether colour would make visual assessment of the wound and monitoring fluid accumulation or infection more difficult. To mitigate the colour change to the dermal regeneration template imbued by the coating process, an ad-layer coating strategy was implemented to achieve a higher concentration of Pro-Cip on the bioengineered collagen-GAG matrix with reduced polydopamine content (Figure 20). Rather than incorporating dopamine and Pro-Cip in a one-pot reaction under alkaline conditions to achieve self-polymerization in one step, a two-step process was implemented where the collagen layer was coated with polydopamine under alkaline conditions as the first step. As a second step, the PDA-coated bioengineered collagen-GAG matrix was immersed in a Pro-Cip solution under alkaline conditions. The polydopamine surface remains active after deposition and can be further modified by reaction with amine terminated small molecules in alkaline buffer solution [23]. Various pH ranging from 8.5-10.0 were implemented in the second step to explore the effect of pH on the efficiency of Pro-Cip modification due to the nucleophilic primary amine. The nucleophilic ad-layer modification of the polydopamine coating depends on the pKa of the nucleophilic amine as well as the chemical equilibrium of catechol/quinone in the coated layer, which is shifted toward the quinone under alkaline conditions [55,56]. The appearance of the ad-layer coated samples was similar to the unmodified bioengineered collagen-GAG matrix, with minor visible brown discoloration due to the polydopamine modification (Figure 20).

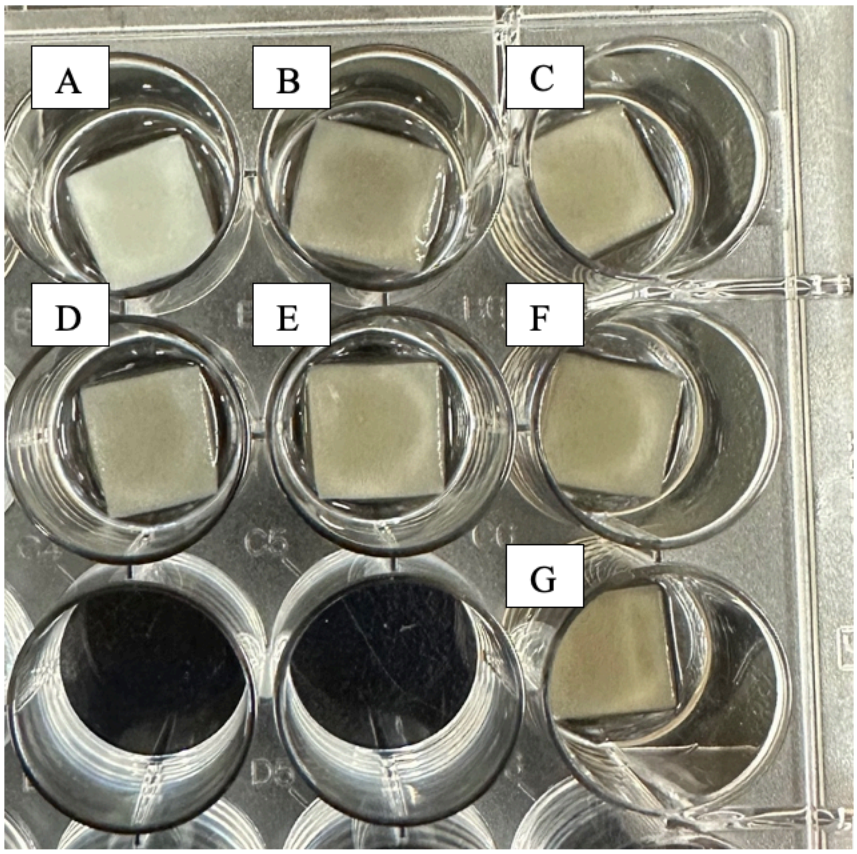

Figure 20. Appearance of Ad-layer coated bioengineered collagen-GAG matrix. (A) uncoated bioengineered collagen-GAG matrix, (B) 3.0 mg/mL PDA 1h static coat, (C) 3.0 mg/mL 1:1 PDA:Pro-Cip 1h static coat, (D) Ad-layer pH 8.5, (E) Ad-layer pH 9.0, (F) Ad-layer pH 9.5, (G) Ad-layer pH 10.0.

The loading of Pro-Cip was quantified based on the absorbance of ciprofloxacin at 325 nm after digestion of the modified collagen layer with collagenase (Table 12). Compared to the one-pot method of coating the collagen with PDA/Pro-Cip, the ad-layer method resulted in higher loading capacity of Pro-Cip to the sample, with 51.7 $\mu g/cm^2$ of Pro-Cip present within the collagen layer compared to 40.1 ± 14.5 $\mu g/cm^2$ in the one-step coating. The coating efficiency was lower at

pH 9.5, potentially indicating depolymerization of polydopamine which can occur under strongly alkaline conditions approaching pH 10-11 [26,57].

Table 12. Loading Pro-Cip to one-pot or ad-layer coated bioengineered collagen-GAG matrix.

	Loaded Pro-Cip (μg/cm^2)
3 mg/mL 1:1 PDA:Pro-Cip (One-pot method, 1h static)	40.1 ± 14.5
3 mg/mL 1:1 PDA:Pro-Cip (Ad-layer pH 8.5)	51.7 ± 6.4
3 mg/mL 1:1 PDA:Pro-Cip (Ad-layer pH 9.5)	13.9± 8.8

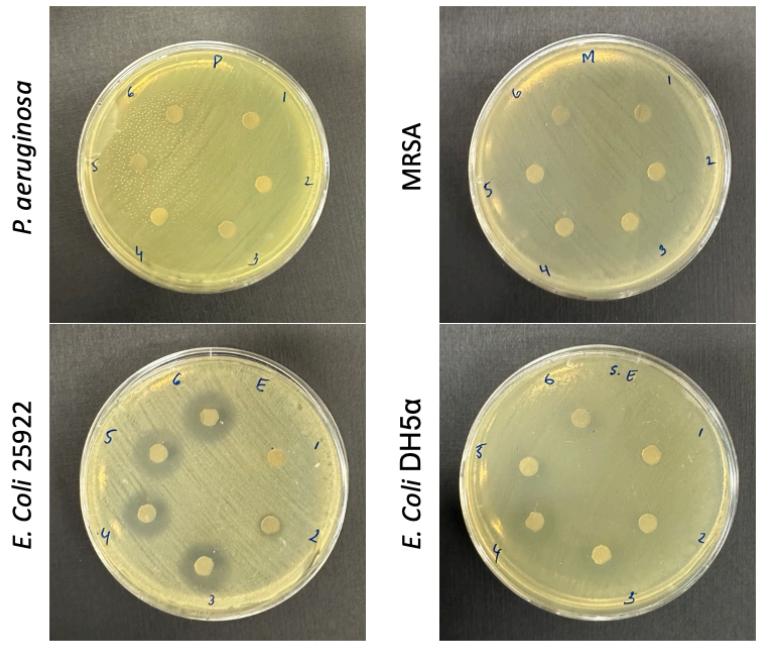

Figure 21. ZOI of ad-layer coated bioengineered collagen-GAG matrix at various pH during the second ad-layer coating step. (1) 3.0 mg/mL PDA 1h static coat, (2) 3.0 mg/mL 1:1 PDA:Pro-Cip 1h static coat, (3) ad-layer pH 8.5, (4) ad-layer pH 9.0, (5) ad-layer pH 9.5, (6) ad-layer pH 10.0.

ZOI testing of the ad-layer coated samples revealed that despite higher concentration of Pro-Cip loaded to the ad-layer pH 8.5 coated sample, there was still no detectable ZOI against MRSA (Figure 21, Table 13).

ZOI for the ad-layer coated membranes are reported in Table 6 as follows. No zone was measurable for MRSA or *P. aeruginosa*.

Table 13. ZOI of PDA-coated ad-layer coated bioengineered collagen-GAG matrix at various pH during the second coating step.

		Inhibition Zone Diameter (mm)			
		E.Coli 25922	*E. Coli* DH5α	MRSA	*P. a.*
1	3.0 mg/mL PDA 1h static	0	0	0	0
2	3.0 mg/mL 1:1 PDA:Pro-Cip 1h static	8	0	0	0
3	Ad-layer pH 8.5	14	9	0	0
4	Ad-layer pH 9.0	14	9	0	0
5	Ad-layer pH 9.5	15	9	0	7
6	Ad-layer pH 10.0	16	9	0	7

* *E. coli* DH5α is a non-lipase producing strain

Given the limited efficacy of the ad-layer coatings against MRSA, the reaction time with Pro-Cip in the second step was extended to 18h with shaking at 200 rpm in 10 mg/mL Pro-Cip.

The incubation time was extended with shaking to increase the coated amount of Pro-Cip without increasing the darkness of the black colour of the polydopamine coating. Given the efficacy of adding inducers $MgCl_2$ and $CaCl_2$ to the coating when the one-pot method was implemented, the divalent cations were incorporated in the ad-layer coatings (either in the first or second step). Finally, two dopamine concentrations for the first coating step were compared – 1.0 mg/mL or 0.25 mg/mL dopamine under static conditions for 1h, 25mM TRIS pH 8.5. The physical appearance of the ad-layer coated samples are illustrated in Table 14.

Table 14. Physical appearance of ad-layer coated bioengineered collagen-GAG matrix compared to 18h shaken coatings.

Method	Sample	Coating Colour
One-pot	3 mg/mL PDA, 1:1 Pro-Cip static 1h coat	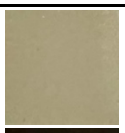
	3 mg/mL PDA, 1:1 Pro-Cip shaken 18h coat	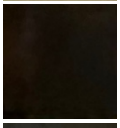
	3 mg/mL PDA, 1:1 Pro-Cip shaken 18h coat, with $MgCl_2$	
	3 mg/mL PDA, 1:1 Pro-Cip shaken 18h coat, with $CaCl_2$	
Ad-layer with 1.0 mg/mL dopamine in initial reaction solution	Ad-layer 10mg/mL 18h coating	
	Ad-layer 10mg/mL 18h coating, with $MgCl_2$ incorporated in the first coating step	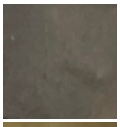
	Ad-layer 10mg/mL 18h coating, with $CaCl_2$ incorporated in the first coating step	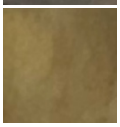
	Ad-layer 10mg/mL 18h coating, with 10 mg/mL $MgCl_2$ incorporated in the second coating step	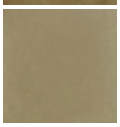
	Ad-layer 10mg/mL 18h coating, with 10 mg/mL $CaCl_2$ incorporated in the second coating step	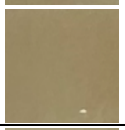
Ad-layer with 0.25 mg/mL dopamine in initial reaction solution	Ad-layer 10mg/mL 18h coating, with 10 mg/mL $MgCl_2$ incorporated in the second coating step	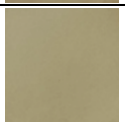
	Ad-layer 10mg/mL 18h coating, with 10 mg/mL $CaCl_2$ incorporated in the second coating step	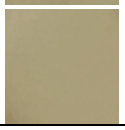

Each of the ad-layer coatings were less opaque and lighter in colour compared to the 18h shaken coatings which were opaque black. The addition of $MgCl_2$ and $CaCl_2$ during the first coating step resulted in a darker surface colour compared to the corresponding 1.0 mg/mL dopamine coated sample without inducers. Incorporating the inducers in the second step successfully mitigated the darker coating colour which occurred when inducers were added concurrently with dopamine (relative to the 1.0 mg/mL dopamine sample without inducers added). The 1.0 mg/mL coatings with inducers added in the second step were still darker in colour compared to the uncoated bioengineered collagen-GAG matrix, so the same strategy of adding $MgCl_2$ and $CaCl_2$ in the second step was implemented with a reduction in the dopamine concentration in the first coating step from 1.0 mg/mL to 0.25 mg/mL. The lower concentration resulted in very acceptable coating colour which was similar to the unmodified bioengineered collagen-GAG matrix.

Cumulative release of ciprofloxacin from the coated surfaces was measured in vitro in the presence or absence of lipase. The coated bioengineered collagen-GAG matrix samples were immersed in 1.0 mL of *B. cepacia* commercial lipase solution in pH 7.4 PBS (5 mg/mL lipase concentration), or PBS without lipase (Figure 22).

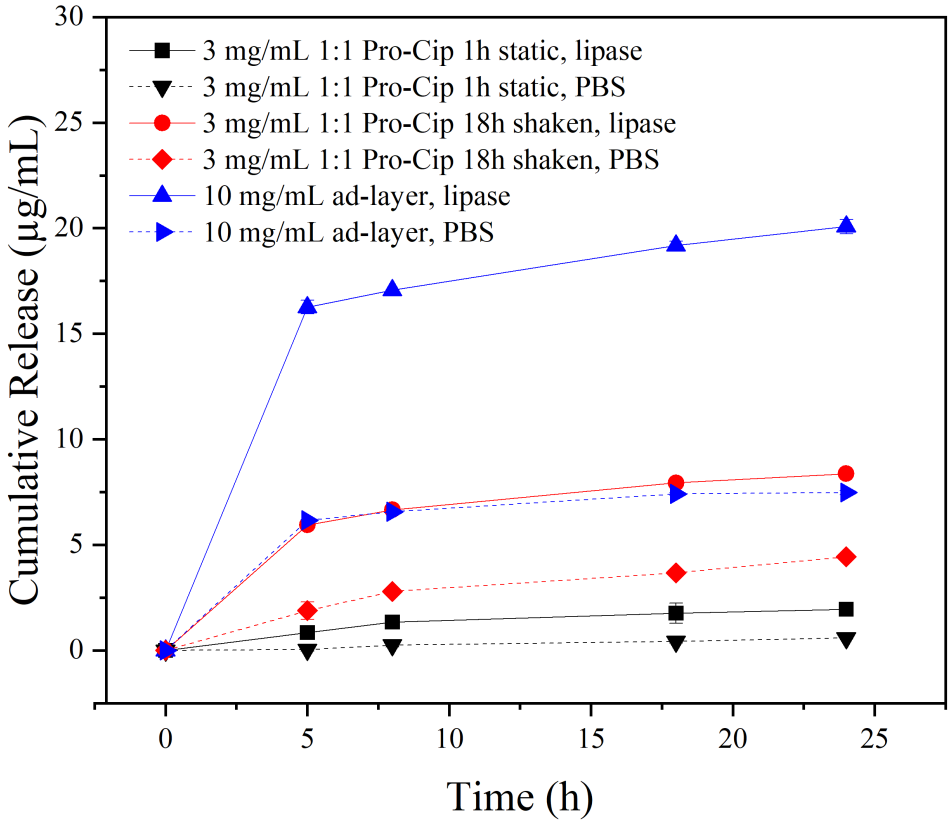

Figure 22. Release of ciprofloxacin from 18h shaken coated and 10 mg/mL ad-layer coated bioengineered collagen-GAG matrix in the presence of commercial lipase. Exposure to 5.0 mg/mL *B. cepacia* lipase. pH 7.4 and 37ºC.

The 10 mg/mL ad-layer coating (1.0 mg/mL dopamine, 18h Pro-Cip coat without inducers) had a similar release profile to the 18h shaken one-pot $CaCl_2$ and $MgCl_2$ coated bioengineered collagen-GAG matrix samples, but with the advantage of a much lighter surface colour similar to the appearance of uncoated bioengineered collagen-GAG matrix. The ad-layer coating released 16.3 ± 0.3 µg/mL after 5h exposure to 5 mg/mL *B. cepacia* lipase, compared to 15.9 ± 0.7 µg/mL

and 11.5 ± 0.5 µg/mL for the 18h shaken one-pot $CaCl_2$ and $MgCl_2$ coated bioengineered collagen-GAG matrix, respectively. This result appears to be very promising as similar antibacterial activity should be achievable without the dark surface colour. The inducers $CaCl_2$ and $MgCl_2$ were then incorporated in the ad-layer coating to further boost the lipase activity. Release was evaluated from the inducer-coated membranes in the presence of 5 mg/mL commercial *B. cepacia* lipase (Figure 23). The incorporation of Ca^{2+} and Mg^{2+} to the coating boosted the release of ciprofloxacin from 16.3 ± 0.3 µg/mL to 24.5 ± 0.5 µg/mL and 24.9 ± 0.7 µg/mL, respectively.

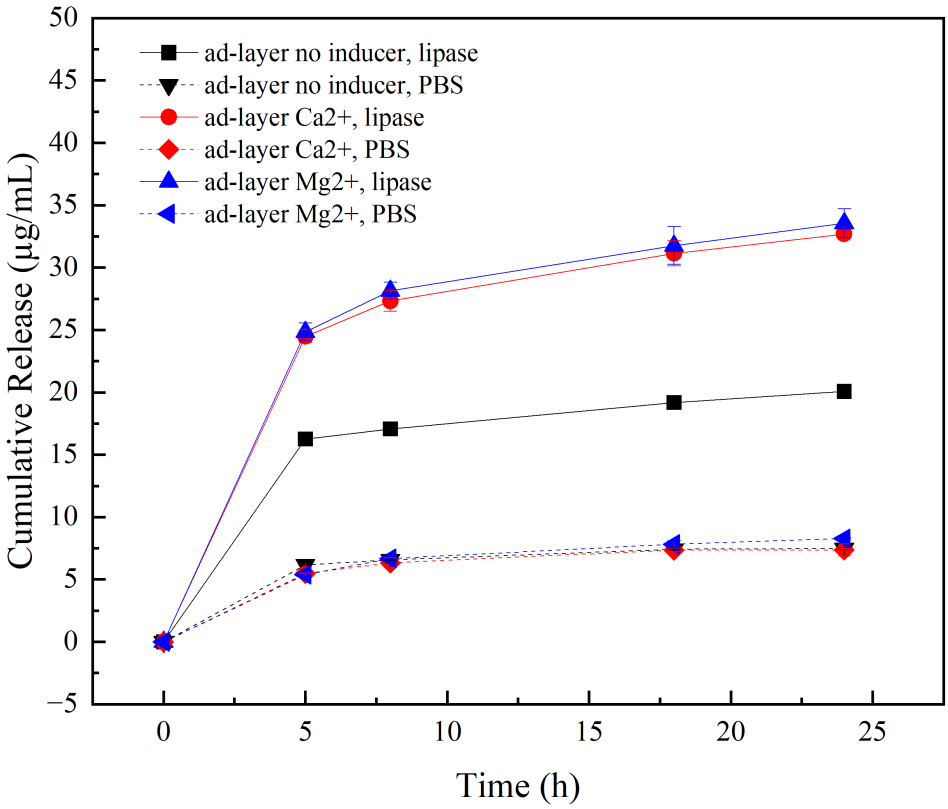

Figure 23. Release of ciprofloxacin from 10 mg/mL ad-layer coatings with CaCl2 and MgCl2 lipase inducers incorporated in the first coating step with dopamine in the presence of commercial lipase. Exposure to 5.0 mg/mL *B. cepacia* lipase. pH 7.4 and 37ºC.

In an effort to mitigate colour change to the coated bioengineered collagen-GAG matrix surface, Mg^{2+} and Ca^{2+} were added in the second step along with lowering the dopamine concentration to 0.25 mg/mL (Figure 24). No significant difference was observed between the cumulative release of ciprofloxacin from the surfaces coated with 1.0 mg/mL dopamine versus 0.25 mg/mL dopamine, indicating that the ad-layer method can be used to fine-tune polydopamine layer thickness (and hence coating opacity) without impacting release characteristics. However, incorporating the inducers in the second ad-layer reaction concurrently with Pro-Cip reduced the cumulative release, with the release limited to a range of 2.1-2.4 μg/mL after 24h.

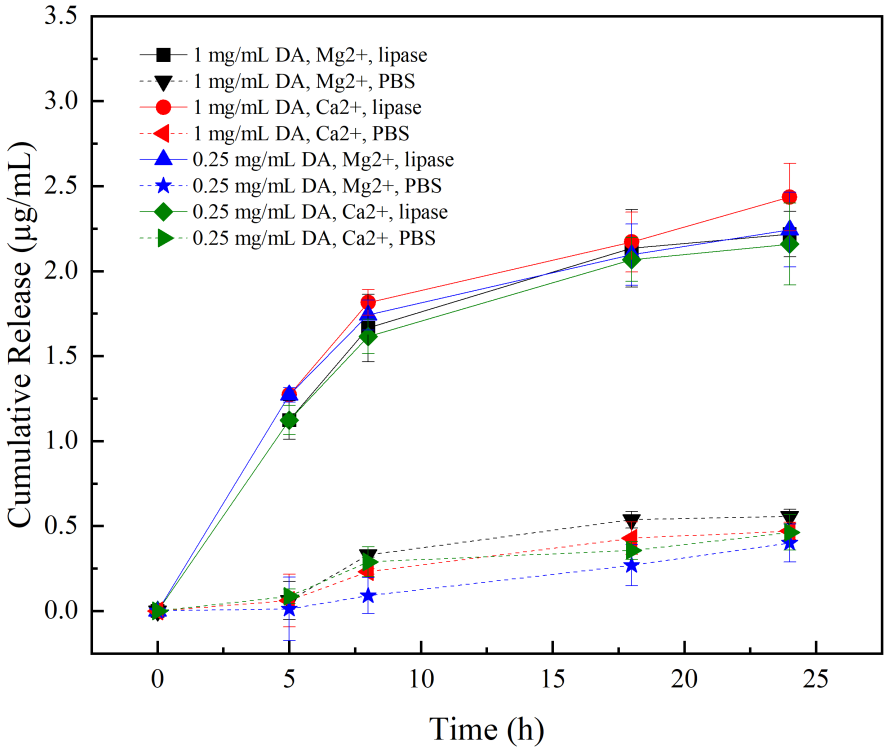

Figure 24. Release of ciprofloxacin from ad-layer coated bioengineered collagen-GAG matrix with Ca2+ and Mg2+ added in second ad-layer coating step in the presence of commercial lipase. Exposure to 5.0 mg/mL *B. cepacia* lipase. pH 7.4 and 37ºC.

Table 15. ZOI of inducer-loaded ad-layer coatings on bioengineered collagen-GAG matrix.

Method	Inducers added	Dopamine (mg/mL)	Sample	Log Reduction		
				E. coli	MRSA	*P. a*
One-pot		3 mg/mL	static 1h coat	23	0	8
			shaken 18h coat	21	9	8
			shaken 18h coat, with $MgCl_2$	22	7	8
			shaken 18h coat, with $CaCl_2$	22	11	8
Ad-layer	1st step	1.0	10mg/mL 18h coating	25	11	8
Ad-layer with inducers	1st step		1:3 dopamine:$CaCl_2$	25	12	9
			1:3 dopamine:$MgCl_2$	24	10	7
	2nd step	1.0	10 mg/mL $MgCl_2$	18	0	8
			10 mg/mL $CaCl_2$	19	0	8
		0.25	10 mg/mL $MgCl_2$	17	0	8
			10 mg/mL $CaCl_2$	17	0	8

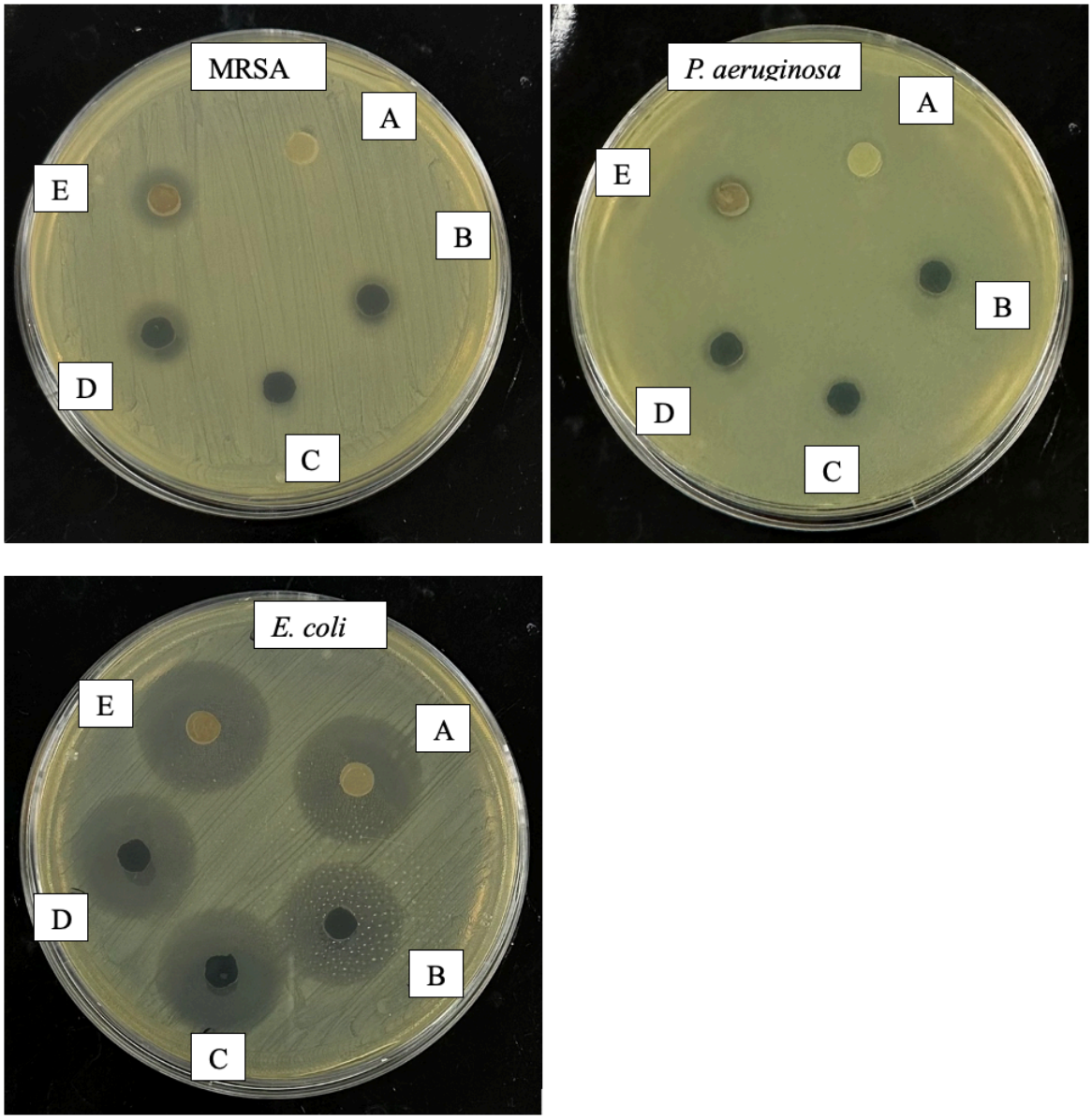

Figure 25. ZOI of 18h shaken coating with or without inducers in the coating. (A) 3 mg/mL 1:1 PDA:Pro-Cip 1h static coat, (B) 3 mg/mL 1:1 PDA:Pro-Cip 18h shaken coat, (C) 3 mg/mL 1:1 PDA:Pro-Cip 18h shaken coat with $MgCl_2$, (D) 3 mg/mL 1:1 PDA:Pro-Cip 18h shaken coat with $CaCl_2$, (E) 10 mg/mL ad-layer coating pH 8.5.

The antibacterial activity of the ad-layer coated bioengineered collagen-GAG matrix was analyzed against *P. aeruginosa* (ATCC 27853), MRSA (ATCC 33592) and *E. coli* (ATCC 25922). ZOI diameters are reported in Table 15 and indicated further in Figures 25-27.

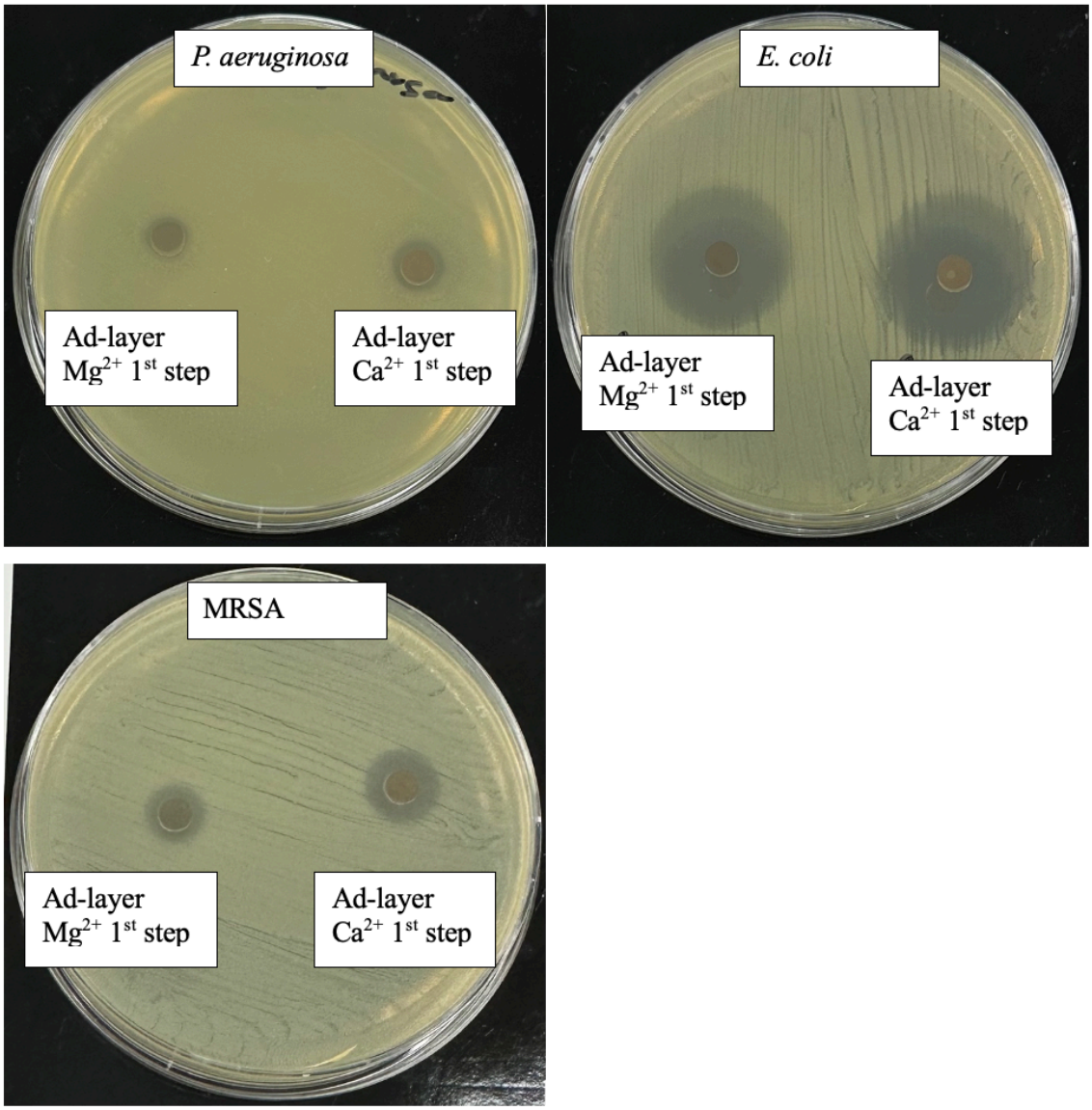

Figure 26. ZOI of 10 mg/mL ad-layer coated bioengineered collagen-GAG matrix with Ca2+ and Mg2+ incorporated in the first coating step.

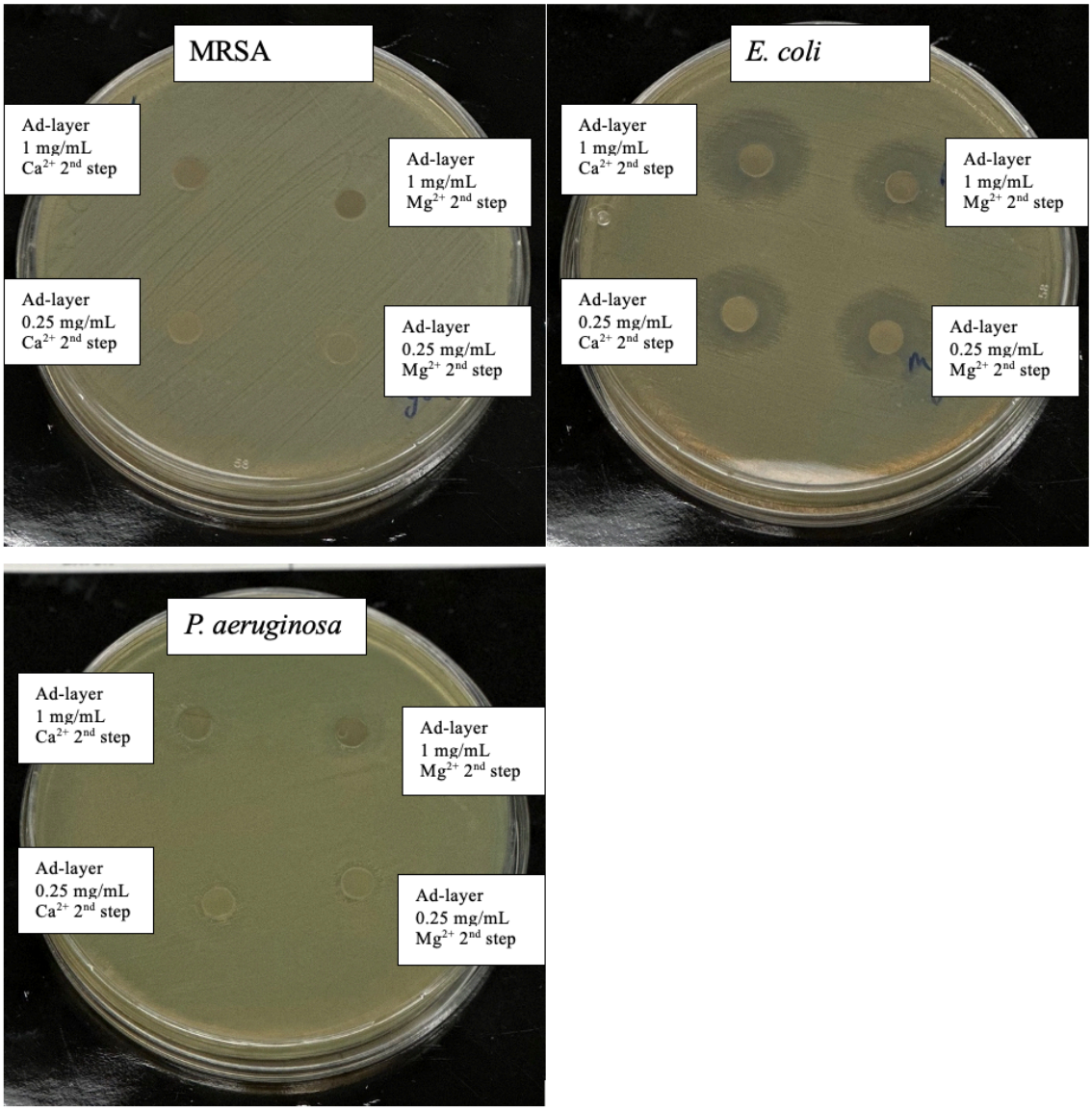

Figure 27. ZOI of 1.0 mg/mL and 0.25 mg/mL ad-layer coated bioengineered collagen-GAG matrix with inducers added in the second step (1:1 Pro-Cip:MgCl2 or 1:1 Pro-Cip:CaCl2).

The ad-layer 10 mg/mL coated membrane had similar zone of inhibition diameter to the highly concentrated 18h coatings with the inducers, with the additional benefit of being much lighter in colour. The ad-layer coating outperformed the static coated membrane (3 mg/mL 1:1

Pro-Cip 1h static coating) against MRSA with an increase in ZOI from 0 to 11mm against MRSA (no improvement was observed against *P. aeruginosa*). The addition of $CaCl_2$ to the ad-layer coating was effective in boosting the ZOI from 11 to 12 mm in MRSA or 8 to 9 mm in *P. aeruginosa*. The addition of $MgCl_2$ within the coating did not exhibit improved zone diameter compared to the ad-layer coating without inducers added. Deposition of the inducers to the coating during the second coat with Pro-Cip proved to be detrimental to the performance of the coating, as no ZOI was observed against MRSA (compared to 8 mm in the ad-layer coating without inducers added).

The antibacterial activity of the ad-layer coated bioengineered collagen-GAG matrix was further analyzed against *P. aeruginosa* (ATCC 27853), MRSA (ATCC 33592) and *E. coli* (ATCC 25922) in a suspension-based test. 1cmx1cm samples of coated or untreated bioengineered collagen-GAG matrix were immersed directly in 1.0 mL of bacteria suspension for 5h. The concentration of bacteria was quantified by drop-plating serial dilutions of the suspensions before and after the elapsed contact time with the coated dermal regeneration templates (Table 16).

Table 16. Antibacterial activity of ad-layer coated bioengineered collagen-GAG matrix with or without inducers, 5h contact time.

	Log Reduction		
	E. coli	MRSA	*P. a*
Inoculum (CFU/mL)	4.3×10^8	3.1×10^9	4.8×10^8
3 mg/mL PDA, 1:1 Pro-Cip static 1h coat	3.27 ± 0.08	1.26 ± 0.01	1.86 ± 0.03
3 mg/mL PDA, 1:1 Pro-Cip shaken 18h coat	3.53 ± 0.06	2.36 ± 0.03	2.47 ± 0.09
3 mg/mL PDA, 1:1 Pro-Cip shaken 18h coat, with $MgCl_2$	3.57 ± 0.03	2.41 ± 0.06	2.32 ± 0.08
3 mg/mL PDA, 1:1 Pro-Cip shaken 18h coat, with $CaCl_2$	3.47 ± 0.02	2.48 ± 0.04	2.13 ± 0.13
Ad-layer 10mg/mL 18h coating	3.66 ± 0.04	2.49 ± 0.09	4.10 ± 0.07
Inoculum (CFU/mL)	3.2×10^7	1.1×10^8	1.02×10^8
Ad-layer $MgCl_2$	7.5 (100%)	8.0 (100%)	8.0 (100%)
Ad-layer $CaCl_2$	7.5 (100%)	8.0 (100%)	8.0 (100%)
Inoculum (CFU/mL)	1.73×10^8	3.36×10^8	4.51×10^8
Ad-layer Coat 1: 1.0 mg/mL dopamine, Coat 2: 1:1 Pro-Cip:$MgCl_2$	2.78 ± 0.03	1.44 ± 0.03	2.85 ± 0.01
Ad-layer Coat 1: 1.0 mg/mL dopamine, Coat 2: 1:1 Pro-Cip:$CaCl_2$	2.81 ± 0.09	1.48 ± 0.02	2.80 ± 0.05
Ad-layer Coat 1: 0.25 mg/mL dopamine, Coat 2: 1:1 Pro-Cip:$MgCl_2$	2.84 ± 0.07	1.48 ± 0.03	2.89 ± 0.01
Ad-layer Coat 1: 0.25 mg/mL dopamine, Coat 2: 1:1 Pro-Cip:$CaCl_2$	2.89 ± 0.07	1.49 ± 0.03	2.85 ± 0.03

*Double line divides separate experiments, as inoculum concentration varied with each experiment.

The 10 mg/mL 18h ad-layer coating (without inducers) performed similarly or better to the one-pot 18h shaken coatings with inducers added. Log reduction of 2.49 ± 0.09 was achieved against MRSA after 5h contact, as well as 4.10 ± 0.07 log reduction against *P. aeruginosa* (a marked improvement over the one-pot shaken coatings with inducers which exhibited a 2.32 ± 0.08 log reduction with $MgCl_2$ or 2.13 ± 0.13 with $CaCl_2$). Incorporating inducers into the ad-layer coating further boosted the antibacterial potency. No colonies were detected in any of the plates after the 5h contact period. (Complete 100% kill after 5h). The inoculum concentrations were $1.02x10^8$ CFU/mL for *P. aeruginosa*, $1.1x10^8$ CFU/mL for MRSA, and $3.2x10^7$ CFU/mL for *E. coli*.

Adding $MgCl_2$ and $CaCl_2$ in the second step with Pro-Cip reduced the antibacterial potency of the coatings compared to when it was added in the first step, as the log reductions ranged from ~2.7-2.9 for *E. coli* and *P. aeruginosa*, and ~1.4-1.5 for MRSA (compared to 100% reduction when inducers were added in the first coating step with dopamine). Adding the inducers in the second step may reduce the loaded quantity of the inducers within the coating. Furthermore, it seems that the incorporation of $MgCl_2$ and $CaCl_2$ in the second step during the Pro-Cip coating may have interfered with the modification of the coating with Pro-Cip, since higher antibacterial activity was observed for the ad-layer coating prepared without any inducers added (log reductions were 3.66 ± 0.04 for *E. coli*, 2.49 ± 0.09 for MRSA and 4.10 ± 0.07 for *P. aeruginosa*).

Physical morphology of the ad-layer coated bioengineered collagen-GAG matrix was examined by SEM (Figure 28).

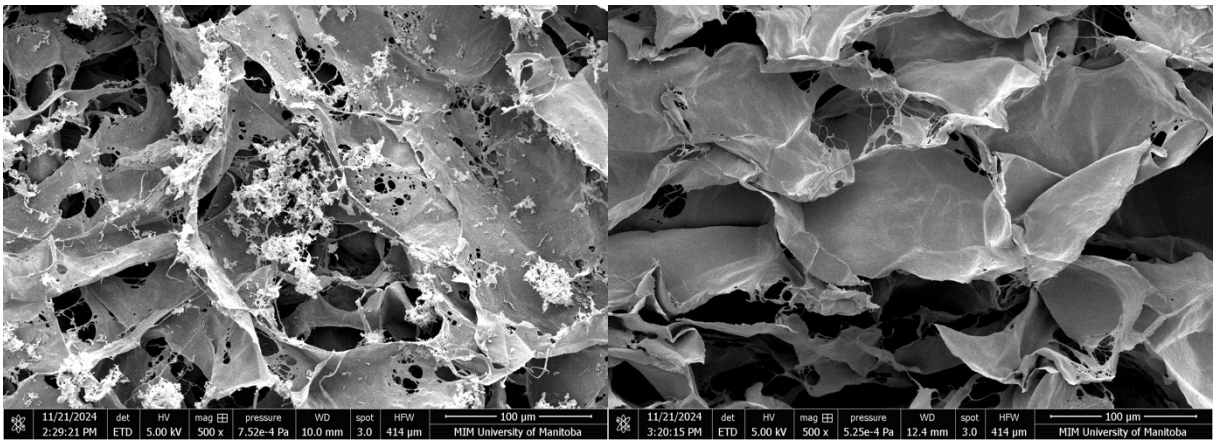

Figure 28. Physical morphology of ad-layer coated bioengineered collagen-GAG matrix (coated with 1.0mg/mL dopamine & 10 mg/mL Pro-Cip). (Left) Top view of the collagen surface, (Right) cross-section view.

The 1.0 mg/mL dopamine, 10 mg/mL Pro-Cip ad-layer coating (Figure 28) had less surface particle surface debris compared to the 18h shaken samples, as expected due to the lower concentration of dopamine, shorter reaction time and static polymerization conditions used to prepare the dopamine layer. The inner pore structure was free of particle debris and retained the expected pore structure. In future work, lower concentrations of dopamine may be explored for fabrication of the initial ad-layer to see if a uniform smooth coating can be obtained on the top layer of the sample.

PCS-201-012 human dermal fibroblasts were seeded onto the coated bioengineered collagen-GAG matrix samples to verify cell attachment, viability, and proliferation after 3 and 7 days of direct contact (Figures 29 and 30).

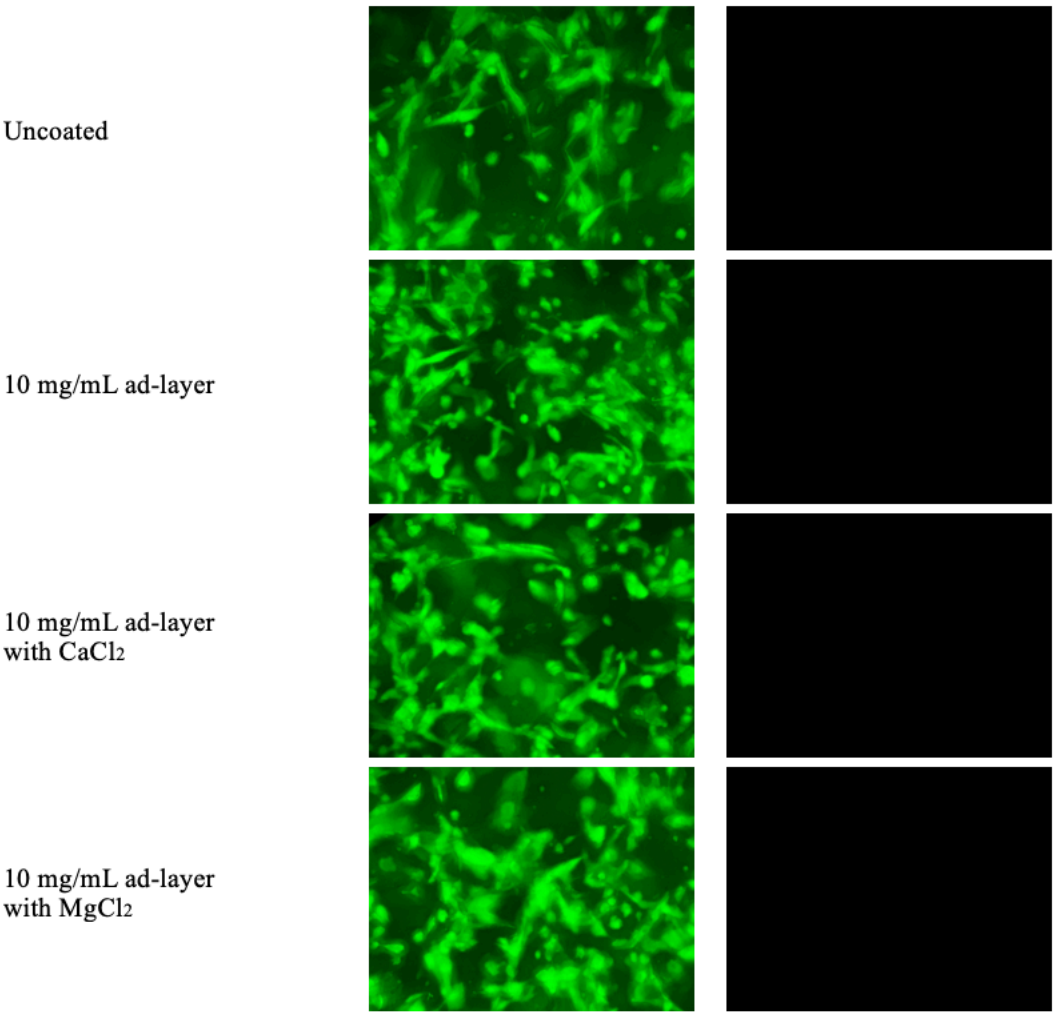

Figure 29. Cell proliferation of PCS-201-012 human primary dermal fibroblasts on ad-layer coated bioengineered collagen-GAG matrix samples with or without inducers incorporated in the first step, 3 days after seeding. Live/Dead assay (calcein-AM and ethidium homodimer-1).

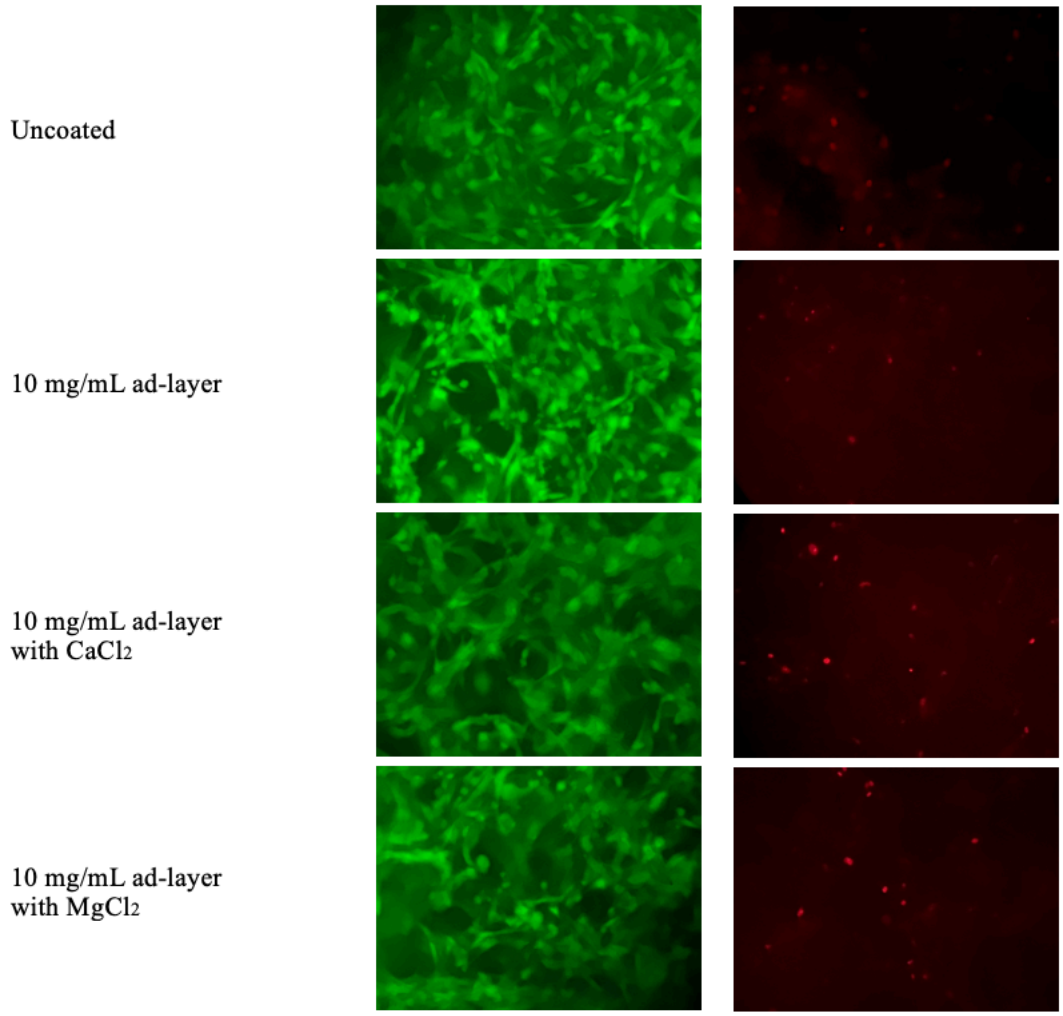

Figure 30. Cell proliferation of PCS-201-012 human primary dermal fibroblasts on ad-layer coated bioengineered collagen-GAG matrix samples with or without inducers incorporated in the first step, 7 days after seeding. Live/Dead assay (calcein-AM and ethidium homodimer-1).

The ad-layer coated samples demonstrated excellent cytocompatibility and cell attachment. After 3 and 7 days attachment to the ad-layer coatings, good proliferation was observed as the cell density was similar to the uncoated negative control. Several dead cells could be observed after ethidium homodimer-1 red staining after 7 days direct contact with the ad-layer coated surfaces (with or without $CaCl_2$ and $MgCl_2$), indicating that the ad-layer coatings did slightly negatively impact cell viability after 7 days. Cell viability of PCS-201-012 human dermal fibroblasts was not significantly different from the uncoated bioengineered collagen-GAG matrix (Figure 31). After 3 days direct contact, similar cell density was observed on the ad-layer coated samples to the untreated bioengineered collagen-GAG matrix, with or without divalent cation inducers incorporated in the coating. When the contact period was extended to 7 days, proliferation rate on the coated sample appeared to be impacted with lower final cell density on the ad-layer coatings, with $3.7\pm0.4 \times 10^4$ cells/mm^2 on the untreated bioengineered collagen-GAG matrix compared to $2.96\pm0.08 \times 10^4$ cells/mm^2 on the 10 mg/mL ad-layer coating, $3.1\pm0.2 \times 10^4$ cells/mm^2 with the incorporation of Ca^{2+}, and $3.0\pm0.2 \times 10^4$ cells/mm^2 with the incorporation of Mg^{2+}.

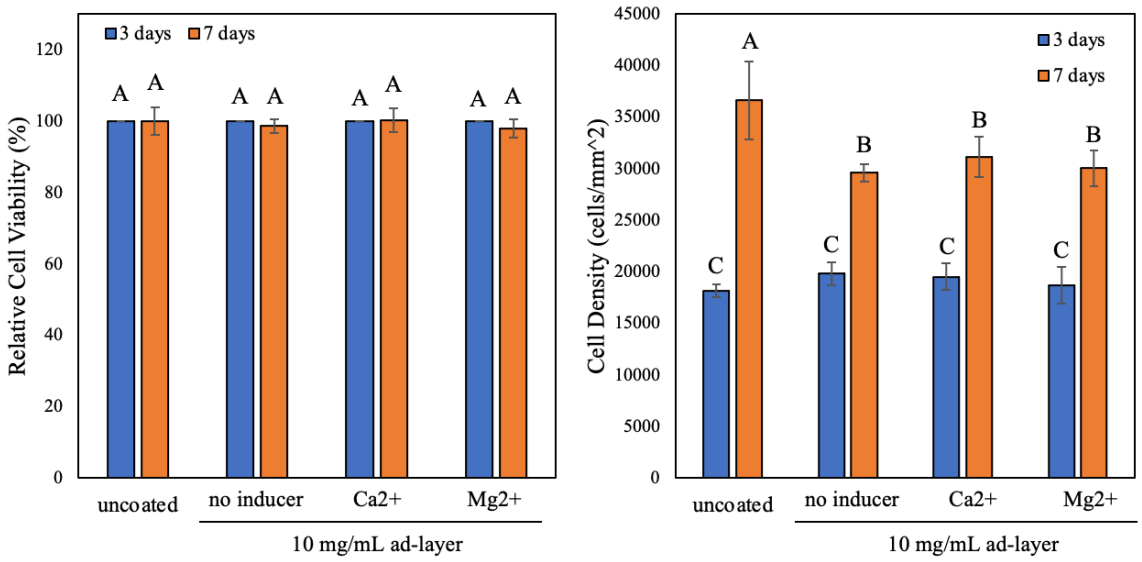

Figure 31. Cell viability of PCS-201-012 fibroblasts after 3-7 days direct contact with ad-layer coated bioengineered collagen-GAG matrix. Ca^{2+} and Mg^{2+} incorporated in the first ad-layer coating step. Different letters (A, B, C, D) indicate significant differences by ANOVA with Tukey correction, n=5 ($p<0.05$).

Cytocompatibility, cell attachment and proliferation were similarly quantified for ad-layer coatings in which $CaCl_2$ and $MgCl_2$ were incorporated in the second step (Figures 32 and 33).

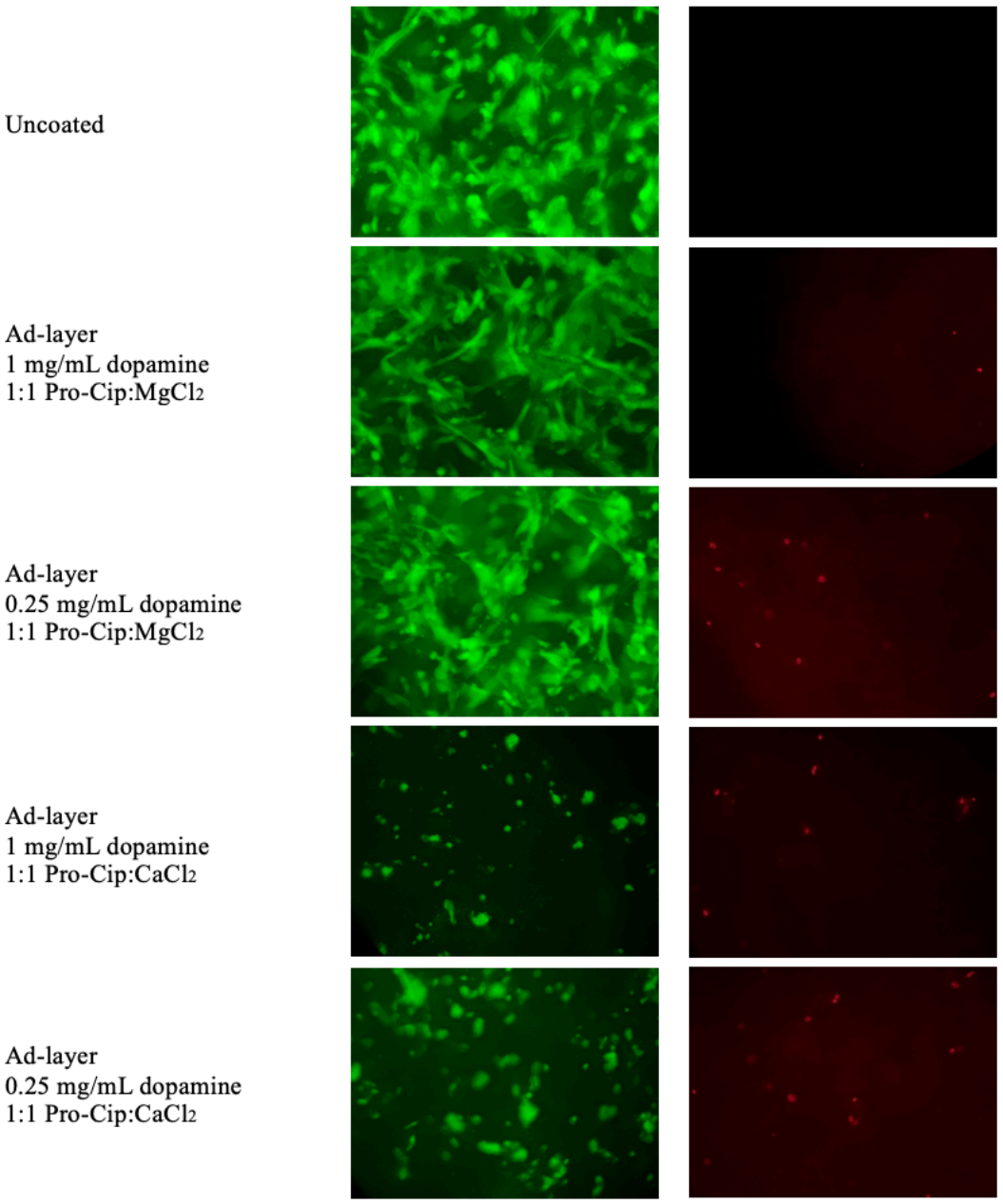

Figure 32. Cell proliferation of PCS-201-012 human primary dermal fibroblasts on ad-layer coated bioengineered collagen-GAG matrix. Ca^{2+} and Mg^{2+} incorporated in the second ad-layer coating step. 3 days after seeding. Live/Dead assay (calcein-AM and ethidium homodimer-1).

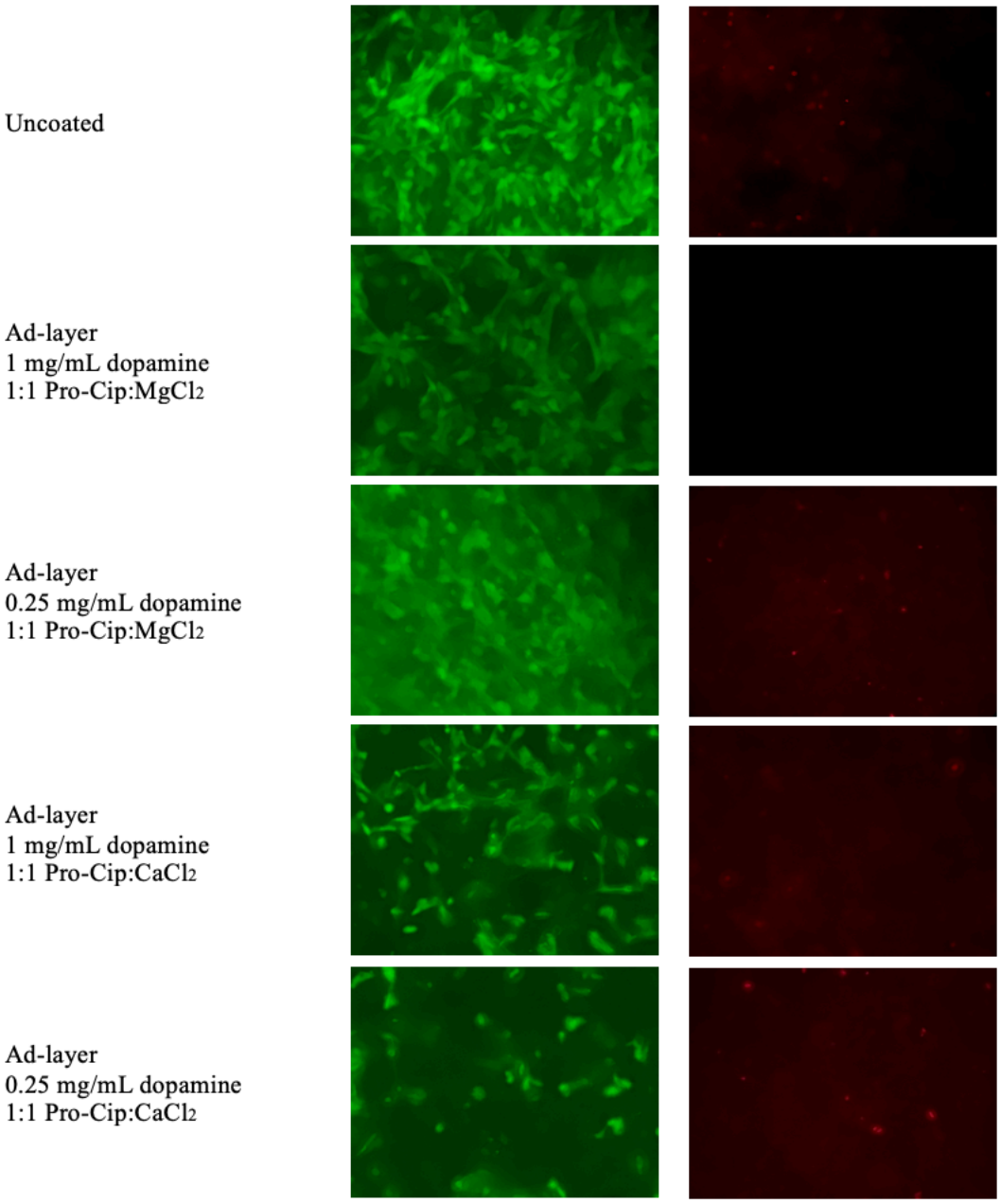

Figure 33. Cell proliferation of PCS-201-012 human primary dermal fibroblasts on ad-layer coated bioengineered collagen-GAG matrix. Ca^{2+} and Mg^{2+} incorporated in the second ad-layer coating step. 7 days after seeding. Live/Dead assay (calcein-AM and ethidium homodimer-1).

The samples coated with $MgCl_2$ in the second step showed similar cell proliferation to the uncoated negative control with minimal cytotoxicity after 3 days of direct contact, with minimal dead cells observed under red fluorescence and similar cell density of 1.9 ± 0.1 x10^4 cells/mm^2 and 1.7 ± 0.1 x10^4 cells/mm^2 for the ad-layer Mg^{2+} coatings produced with 1.0 mg/mL or 0.25 mg/mL dopamine, respectively (compared to 1.78 ± 0.08 x10^4 cells/mm^2 in the negative control) (Figure 34). The cell viability and proliferation on the samples that were coated with $CaCl_2$ in the second step appeared to be compromised, even after 3 days contact. Cell density was lower in the $CaCl_2$ coated samples after 3 days contact, with a reduction from 1.78 ± 0.08 x10^4 cells/mm^2 in the negative control to 0.75 ± 0.06 x10^4 cells/mm^2 or 0.94 ± 0.06 x10^4 cells/mm^2 for the ad-layer Ca^{2+} coatings produced with 1.0 mg/mL or 0.25 mg/mL dopamine, respectively. Furthermore, observation of the cell shape under live/dead fluorescent staining revealed a round morphology as opposed to the typical flattened and extended morphology which is observed in healthy fibroblasts after successful attachment. Interestingly, the $CaCl_2$ sample with the inducer added in the first coating step (with the dopamine) did not exhibit the same issues, where there was no significant difference in cell viability between the coating and the negative control. Chelation of calcium by the polydopamine catechol groups may limit release of calcium, which may be more prevalent when calcium is incorporated in the first step and co-deposited during polymerization of dopamine. When calcium is loaded to the polydopamine layer in the second step, loose adsorption of the calcium ions to the coating may facilitate release resulting in the sensitivity of the fibroblasts to the coating.

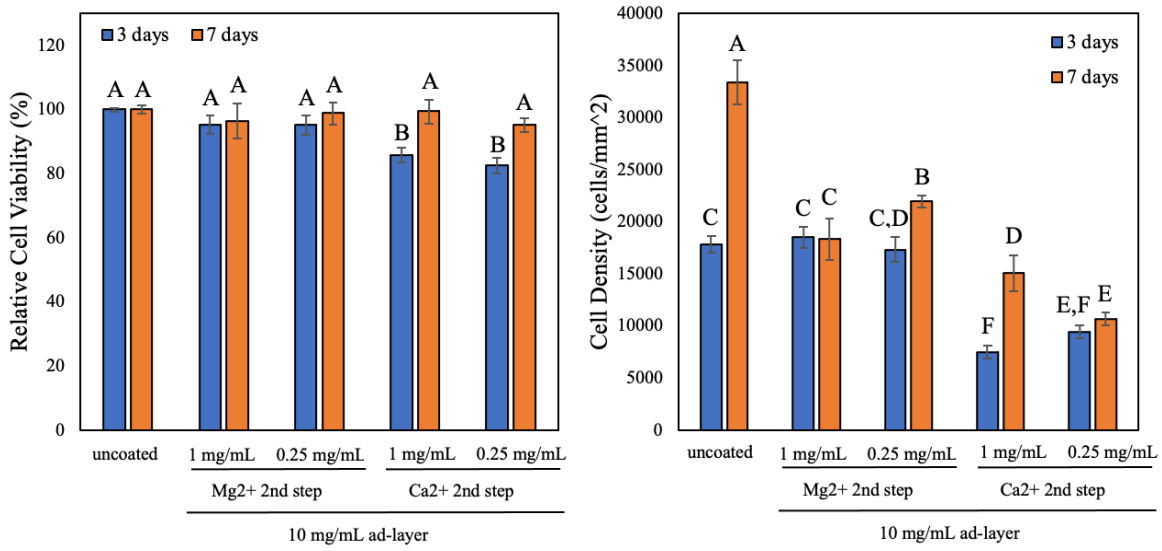

Figure 34. Cell viability of PCS-201-012 fibroblasts after 3-7 days direct contact with ad-layer coated bioengineered collagen-GAG matrix, Ca^{2+} and Mg^{2+} incorporated in the second ad-layer coating step. Different letters (A, B, C, D) indicate significant differences by ANOVA with Tukey correction, n=5 ($p<0.05$).

4.7. Pro-Cip Triglyceride

The structure of the small-molecule pro-drug Pro-Cip features ciprofloxacin covalently modified by an alkyl chain via a labile ester linkage for cleavage by lipase, with a $-NH_2$ to allow for covalent modification of the polydopamine layer and anchoring to the bioengineered collagen-GAG matrix. We explored the performance of an alternative pro-drug structure with a ciprofloxacin-modified glycerol backbone with the hypothesis that cleavage efficiency may be higher toward a pro-drug substrate which more closely resembles the native triglyceride substrate of lipase (Scheme 11). The alkyl chain length for the amine-terminated anchor of the pro-drug for covalent reaction with polydopamine was selected based on the dimension of the hydrophobic pocket of *P. aeruginosa* lipase which accommodates a chain length of 8-10 carbons [49].

Ciprofloxacin

Triglyceride

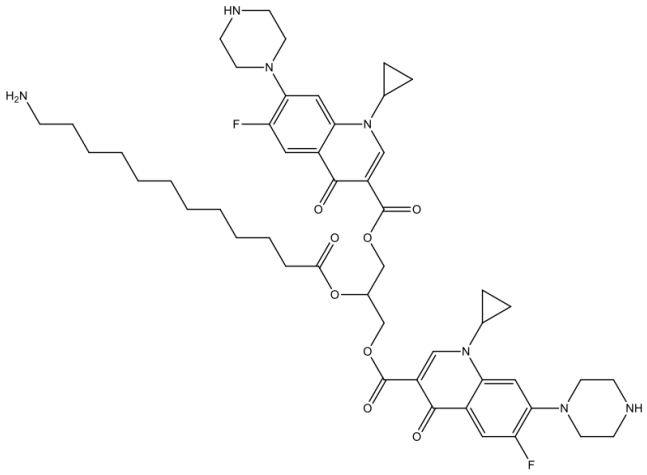

Scheme 11. Structure of ciprofloxacin-based triglyceride pro-drug.

The MIC of the novel Pro-Cip triglyceride was evaluated in comparison to the performance of the small-molecule Cip pro-drug (Table 17). The novel Pro-Cip triglyceride did exhibit lipase-responsive antibacterial activity towards *E. coli* 25922 and *E. coli* Top10, as evidenced by the lower MIC value after exposure to commercial lipase. However, the triglyceride pro-drug did not exhibit lipase-responsive cleavage in the presence of MRSA or P. aeruginosa as evidenced by the high MIC of 26.5 μM for *P. aeruginosa* or >26.5 μM for MRSA.

Table 17. MIC for lipase-exposed Pro-Cip and Pro-Cip-Gly.

	Lipase exposure*	MIC (μM)			
		P. aeruginosa	*E. coli*	MRSA	Top10
Cipro	0	0.38	<0.19	0.75	<0.19
Pro-Cip	0	37.2	4.6	74.3	18.6
	5 h	37.2	2.3	37.2	9.3
	24 h	37.2	2.3	37.2	9.3
Pro-Cip-Gly	0	26.5	6.6	>26.5	26.5
	5 h	26.5	3.3	>26.5	6.6
	24 h	26.5	3.3	>26.5	3.3

*Pro-drugs were pre-exposed to 10 mg/mL *B. cepacia* lipase (≥30,000 U/g) for the specified duration (0h, 5h or 24h) prior to testing for MIC. Concentration reflects the dose of pro-drug concentration prior to lipase exposure.

Ultimately, anchoring the small molecule Pro-Cip to a thin-layer polydopamine coating applied to the bioengineered collagen-GAG matrix by the ad-layer method proved to be the most effective strategy for endowing the bioengineered collagen-GAG matrix with potent lipase-responsive antibacterial activity. Pro-Cip activation only happens in the presence of bacteria which reduces the chance of resistance and since Pro-Cip is covalently bonded to the PDA-collagen there is a low chance of migration to other tissues. This gives the Pro-Cip coating strategy an advantage over other commercial antimicrobial DRT products, such as PriMatrix® Ag Antimicrobial Dermal Repair Scaffold. Primatrix® Ag is an acellular dermal matrix consisting of Type III collagen from

fetal bovine dermis, which is enriched with ionic silver for antimicrobial action. However, it is worth noting that despite providing protection against microbial colonization, the action of ionic silver does not prevent endotoxin. In fact, PriMatrix® Ag Antimicrobial Dermal Repair Scaffold was recalled on May 22, 2023 due to potentially high endotoxin levels. The antimicrobial mechanism of action of silver nanoparticles has been attributed to various phenomena, including: uptake of free Ag^+ which can disturb production of ATP and DNA replication, generation of ROS, and damage to cellular membranes [58]. As an antimicrobial agent, ionic silver bears several disadvantages such as sustained leaching from the wound dressing. As ionic silver is highly reactive with chloride anions which are abundant in wound fluid, they rapidly form AgCl which depletes the concentration of active Ag^+ in the dressing [10,11]. Silver can also bind with ECM proteins such as collagen through interaction with carboxylic acid groups, imidazole, sulfhydryl and amines [11,12] which may reduce its efficacy. Further, ionic silver poses a risk of cytotoxicity towards keratinocytes and fibroblasts and can hinder cell proliferation by increasing ROS and damaging DNA [11,13–17]. Even in intact skin, silver nanoparticles with size of >30 nm can penetrate the stratum corneum to reach the epidermis, with higher permeation in damaged tissues [58]. Furthermore, bacterial resistance can form to Ag^+ [10,11,58–61], which also increases the chance of other antibiotic resistance [60–65].

5. Conclusions

Burn wounds are at a high risk of infection, which jeopardizes patients' health. Although utilizing a bioengineered collagen-GAG matrix can promote the healing procedure, the chance of infection remains. The presence of bacteria in the wound under bioengineered collagen-GAG matrices is hard to monitor. By the time infection is identified, removal of the matrix is required,

bringing complications and discomfort to the patient, extra work for healthcare workers and increasing costs.

Here, we report a polydopamine-based surface modification of a commercially available bioengineered collagen-GAG matrix with a bacteria-responsive pro-drug which is inert when bacteria are not present, and undergoes cleavage by lipase in the presence of pathogenic bacteria to release an active antibiotic, ciprofloxacin. This responsive antibacterial coating achieved an impressive log reduction of bacteria against two major wound pathogens MRSA and *P. aeruginosa*, with up to 100% (8.0 log reduction) achieved against MRSA and *P. aeruginosa* after 5h contact. Importantly, the coatings exhibited minimal impact on cell attachment and proliferation assessed *in vitro*. The incorporation of Pro-Cip is a promising bacteria-responsive method for the control of high-risk infections that compromise wound healing.

Key performance metrics such as lipase-responsive bacterial killing, and cytocompatibility were demonstrated:

1. Responsive bacterial killing: the surface of the bioengineered collagen-GAG matrix could be endowed with lipase-responsive bacterial killing capabilities using the PDA/Pro-Cip one-pot coating. This means that the surface of the matrix could be activated to release antibacterial drugs when exposed to bacteria.
2. The antibacterial activity of the matrix could be fine-tuned by extending the coating duration or by using a two-step coating process involving ad-layer PDA layer modification with Pro-Cip.
3. The PDA/Pro-Cip coating used in the study is non-toxic to skin cells and doesn't compromise cell attachment or viability.

4. Several inducers have been successfully incorporated into the dermal matrix to further optimize the responsive bacterial killing capabilities.

6. Future Work

Future work for the development of a polydopamine/Pro-Cip self-disinfecting coating for a bioengineered collagen-GAG matrix should focus on the wholistic evaluation of the coating formulations using an appropriate animal model. Preliminary assessment should focus on the impact of the polydopamine coating alone, to address concerns over whether polydopamine interferes with cell interaction with the collagen layer of the dermal regeneration template due to the modified surface chemistry after coating. Furthermore, this design can be used for other bioactive molecules of bioagents such as anti-scar drugs, vascularization drugs, endotoxin-encapsulating molecules, or other antibiotics.

Future work may include an exploration of altering the polydopamine coating chemistry to achieve a transparent and colourless coating. Dopamine derivatives such as polynorepinephrine may also offer lighter coating colour due to differences in coating morphology. For example, Tan et al. demonstrated that polynorepinephrine coatings were lighter in colour relative to polydopamine, potentially arising from thinner and smoother coating morphology [66]. Copolymerization of dopamine with other monomers or peptides has been explored as a strategy reduce colour opacity. Copolymerization can disrupt the conjugation of the PDA network, decreasing its visible light-absorbing properties. Kohri et al. achieved colorless polydopamine coating by 2:1 of 2-bromoisobutyryl-substituded dopamine in a 2:1 ratio with dopamine, where the 2-bromoisobutyryl-substituded dopamine reacts with the dopamine amine group to prevent cyclization and reduce colour [67]. Due to reaction with the amine group the coating thickness was

compromised, but high transparency of 80% was achieved at 450 nm. Chen et al. reported a dibutylamine-DOPA-lysine-DOPA (DbaYKY) tripeptide which achieved universal surface modification after 5 min coating in TRIS pH 8.5 with no visible colour change [68]. The tripeptides were terminated with RGD sequence or a cell-adhesive β-peptide polymer to further promote cell adhesion. Post-synthesis treatments have been explored to modify the PDA structure after its formation in order to reduce visible light absorbance. Lu et al. used alkaline solution (pH 12.5) to partially disassemble polydopamine to oligomer structures which can be used to prepare transparent films (in this case, cast with PVA) which enabled visible light transmittance of 75.9% [69]. Alternative "universal" coating chemistries to polydopamine have been developed which do not confer a dark black or brown colour to the surface. For example, polyphenol coatings derived from phenolic compounds in plants such as pyrogallol, tannic acid, epigallocatechin gallate, epicatechin gallate and epigallocatechin can form polydopamine-like coatings in a similar auto-oxidation process, with the advantage of being colourless [23]. The polyphenol coatings of 10-65 nm thickness spontaneously form due to auto-oxidation in alkaline pH (pH 7.8) in the presence of dissolved oxygen, and display characteristics which are valued in polydopamine coatings such as cytocompatibility, antibacterial properties, and ROS scavenging antioxidant ability [70]. In a different strategy, Liu et al. reported a universal surface modification strategy based on polymerization of bis(vinyl sulfonyl)methane to produce coatings which are transparent white or colourless [71]. Surfaces such as silicon wafers, glass, metals (steel, titanium, and gold), metal oxide (Al_2O_3), polypropylene and PDMS were successfully coated, although the materials required pre-treatment with oxygen plasma. Similar to polydopamine coatings, the PBVS coatings were cell adhesive and could be functionalized with amine- or thiol- containing molecules by Michael addition.

Different antibiotics may be explored for development of new pro-drugs to improve the performance against gram positive bacteria such as MRSA. For example, it is known that modification of the fluoroquinolone substituents can impact the drug's activity. Substitution of fluoroquinolone at C5 and C7 can be controlled to add gram positive activity [38]. The structure-activity relationship is dependent on the composition of the side-chain moieties. Caution should be employed to ensure that the eventual release of the pro-drug or cleaved product after biodegradation of the bioengineered collagen-GAG matrix does not increase the risk of emergence of antibiotic-resistant strains.

Other potential inducers may be explored for boosted lipase activity. These inducers may include (but are not limited to) divalent cations, non-ionic surfactants (Tweens, Triton X-100, Spans), fatty acids (stearic acid, arachidic acid, triacetin, tripropionin, tricaprylin, tricaprin, palmitic acid, linolenic acid and oleic acid), oils (olive oil, palm oil, coconut oil, soybean oil), methyl oleate, soybean lecithin, fatty alcohols (decanoyl alcohol, lauryl alcohol, myristyl alcohol, palmityl alcohol, stearyl alcohol, oleyl alcohol), methyl stearate, ethyl stearate, n-butyl stearate, n-dodecyl stearate, methyl oleate, ethyl oleate, n-butyl oleate, 1,2-propanediol 1-stearate, glycerol 1-stearate, POE 8 monostearate Myrj 45, POE 8 bis(stearate), POE 2 palmity ether Brij 52, POE 2 stearyl ether Brij 72, POE 2 oleyl ether Brij 92, POE 10 palmityl ether Brij 56, POE 10 stearyl ether Brij 76, POE 10 oleyl ether Brij 97, POE 20 palmityl ether Brij 58, POE 20 stearyl ether Brij 78, and POE 20 oleyl ether Brij 98.

Finally, the versatility of polydopamine chemistry enables the use of this design for other bioactive molecules such as anti-scar drugs, vascularization drugs, and other antibiotics. This design has the potential to incorporate materials that can encapsulate endotoxin and prevent toxicity such as platelet membrane [72], cationic polymers (polyethyleneimine, poly(L-lysine) and

poly(L-histidine)[73], polymyxin B [74,75], lipopolyamines [76] or histidine [77]. Later on, they can be eliminated by cleaning the wound or eschar removal.

7. References

[1] M. Asuku, T.-C. Yu, Q. Yan, E. Böing, H. Hahn, S. Hovland, M.B. Donelan, Split-thickness skin graft donor-site morbidity: A systematic literature review, Burns. 47 (2021) 1525–1546. doi:10.1016/j.burns.2021.02.014.

[2] J.A. Anyanwu, R. Cindass, Burn Debridement, Grafting, and Reconstruction, StatPearls Publishing, Treasure Island, FL, 2023.

[3] S. Pripotnev, A. Papp, Split thickness skin graft meshing ratio indications and common practices, Burns. 43 (2017) 1775–1781. doi:10.1016/j.burns.2017.04.024.

[4] M.G. Jeschke, M.E. van Baar, M.A. Choudhry, K.K. Chung, N.S. Gibran, S. Logsetty, Burn injury, Nat. Rev. Dis. Prim. 6 (2020). doi:10.1038/s41572-020-0145-5.

[5] D.M. DeBruler, B.N. Blackstone, K.L. McFarland, M.E. Baumann, D.M. Supp, J.K. Bailey, H.M. Powell, Effect of skin graft thickness on scar development in a porcine burn model, Burns. 44 (2018) 917–930. doi:10.1016/j.burns.2017.11.011.

[6] S.R. Gonzalez, K.G. Wolter, J.C. Yuen, Infectious Complications Associated with the Use of Integra: A Systematic Review of the Literature, Plast. Reconstr. Surg. - Glob. Open. (2020) 1–4. doi:10.1097/GOX.0000000000002869.

[7] D. Church, S. Elsayed, O. Reid, B. Winston, R. Lindsay, Burn wound infections, Clin. Microbiol. Rev. 19 (2006) 403–434.

[8] J. Maitz, J. Merlino, S. Rizzo, G. McKew, P. Maitz, Burn wound infections microbiome and novel approaches using therapeutic microorganisms in burn wound infection control,

Adv. Drug Deliv. Rev. 196 (2023) 114769. doi:10.1016/j.addr.2023.114769.

[9] R. Edwards, K.G. Harding, Bacteria and wound healing, Curr. Opin. Infect. Dis. 17 (2004) 91–96.

[10] S.L. Percival, P.G. Bowler, D. Russell, Bacterial resistance to silver in wound care, J. Hosp. Infect. 60 (2005) 1–7. doi:10.1016/j.jhin.2004.11.014.

[11] B.S. Atiyeh, M. Costagliola, S.N. Hayek, S.A. Dibo, Effect of silver on burn wound infection control and healing: Review of the literature, Burns. 33 (2007) 139–148. doi:10.1016/j.burns.2006.06.010.

[12] M. Walker, D. Parsons, The biological fate of silver ions following the use of silver-containing wound care products - a review, Int. Wound J. 11 (2014) 496–504. doi:10.1111/j.1742-481X.2012.01115.x.

[13] N. Hadrup, A.K. Sharma, K. Loeschner, Toxicity of silver ions, metallic silver, and silver nanoparticle materials after in vivo dermal and mucosal surface exposure: A review, Regul. Toxicol. Pharmacol. 98 (2018) 257–267. doi:10.1016/j.yrtph.2018.08.007.

[14] V.K.M. Poon, A. Burd, In vitro cytotoxity of silver: Implication for clinical wound care, Burns. 30 (2004) 140–147. doi:10.1016/j.burns.2003.09.030.

[15] A.B. Lansdown, A. Williams, How safe is silver in wound care?, J. Wound Care. 13 (2004) 131–136. doi:10.12968/jowc.2004.13.4.26596.

[16] E. Hidalgo, C. Domínguez, Study of cytotoxicity mechanisms of silver nitrate in human dermal fibroblasts, Toxicol. Lett. 98 (1998) 169–179. doi:10.1016/S0378-4274(98)00114-3.

[17] M.M. Cortese-Krott, M. Münchow, E. Pirev, F. Heßner, A. Bozkurt, P. Uciechowski, N. Pallua, K.D. Kröncke, C. V. Suschek, Silver ions induce oxidative stress and intracellular

zinc release in human skin fibroblasts, Free Radic. Biol. Med. 47 (2009) 1570–1577. doi:10.1016/j.freeradbiomed.2009.08.023.

[18] S. Saghazadeh, C. Rinoldi, M. Schot, S.S. Kashaf, F. Sharifi, E. Jalilian, K. Nuutila, G. Giatsidis, P. Mostafalu, H. Derakhshandeh, K. Yue, W. Swieszkowski, A. Memic, A. Tamayol, A. Khademhosseini, Drug delivery systems and materials for wound healing applications, Adv. Drug Deliv. Rev. 127 (2018) 138–166. doi:10.1016/j.addr.2018.04.008.

[19] A.J. Whittam, Z.N. Maan, D. Duscher, V.W. Wong, J.A. Barrera, M. Januszyk, G.C. Gurtner, Challenges and Opportunities in Drug Delivery for Wound Healing, Adv. Wound Care. 5 (2016) 79–88. doi:10.1089/wound.2014.0600.

[20] H. Singh, W. Li, M.R. Kazemian, R. Yang, C. Yang, S. Logsetty, S. Liu, Lipase-Responsive Electrospun Theranostic Wound Dressing for Simultaneous Recognition and Treatment of Wound Infection, ACS Appl. Bio Mater. 2 (2019) 2028–2036.

[21] W. Norbury, D.N. Herndon, J. Tanksley, M.G. Jeschke, C.C. Finnerty, Infection in burns, Surg. Infect. (Larchmt). 17 (2016) 250–255. doi:10.1089/sur.2013.134.

[22] I. Singh, G. Dhawan, S. Gupta, P. Kumar, Recent Advances in a Polydopamine-Mediated Antimicrobial Adhesion System, Front. Microbiol. 11 (2021). doi:10.3389/fmicb.2020.607099.

[23] J.H. Ryu, P.B. Messersmith, H. Lee, Polydopamine Surface Chemistry: A Decade of Discovery, ACS Appl. Mater. Interfaces. 10 (2018) 7523–7540. doi:10.1021/acsami.7b19865.

[24] M. Liu, T. Liu, X. Chen, J. Yang, J. Deng, W. He, X. Zhang, Q. Lei, X. Hu, G. Luo, J. Wu, Nano-silver-incorporated biomimetic polydopamine coating on a thermoplastic polyurethane porous nanocomposite as an efficient antibacterial wound dressing, J.

Nanobiotechnology. 16 (2018) 1–19. doi:10.1186/s12951-018-0416-4.

[25] L. Su, Y. Yu, Y. Zhao, F. Liang, X. Zhang, Strong Antibacterial Polydopamine Coatings Prepared by a Shaking-assisted Method, Sci. Rep. 6 (2016) 24420. doi:10.1038/srep24420.

[26] X. Chen, W. Yang, J. Zhang, L. Zhang, H. Shen, D. Shi, Alkalinity triggered the degradation of polydopamine nanoparticles, Polym. Bull. 78 (2021) 4439–4452. doi:10.1007/s00289-020-03312-2.

[27] L. Bennison, C. Miller, R. Summers, A. Minnis, G. Sussman, W. McGuiness, The pH of wounds during healing and infection: a descriptive literature review, Wound Pract. Res. 25 (2017) 63–69.

[28] J. Zhao, F. Han, W. Zhang, Y. Yang, D. You, L. Li, Toward improved wound dressings: Effects of polydopamine-decorated poly(lactic-co-glycolic acid) electrospinning incorporating basic fibroblast growth factor and ponericin G1, RSC Adv. 9 (2019) 33038–33051. doi:10.1039/c9ra05030b.

[29] G.L. Kim, T.T. Luong, S.S. Park, S. Lee, J.A. Ha, C.T. Nguyen, J.H. Ahn, K.T. Park, M.J. Paik, Suhkneung-Pyo, D.E. Briles, D.K. Rhee, Inhibition of autolysis by lipase LipA in Streptococcus pneumoniae sepsis, Mol. Cells. 40 (2017) 935–944. doi:10.14348/molcells.2017.0201.

[30] G.G. de Fernando, Lactic Acid Bacteria | Enterococcus in Milk and Dairy Products, in: J.W. Fuquay (Ed.), Encycl. Dairy Sci. (Second Ed., Academic Press, 2011: pp. 153–159.

[31] E.A. Snellman, R.R. Colwell, Acinetobacter lipases: Molecular biology, biochemical properties and biotechnological potential, J. Ind. Microbiol. Biotechnol. 31 (2004) 391–400. doi:10.1007/s10295-004-0167-0.

[32] G. Nantel, P. Proulx, Lipase activity in E. coli, Biochim. Biophys. Acta (BBA)/Lipids Lipid

Metab. 316 (1973) 156–161. doi:10.1016/0005-2760(73)90005-2.

[33] A. Rahman, S. Sardar, Z. Niaz, A. Khan, S. Sheheryar, A.F. Alrefaei, M. Hamayun, S. Ali, Lipase and Protease Production Ability of Multi-drug Resistant Bacteria Worsens the Outcomes of Wound Infections, Curr. Pharm. Des. 30 (2024) 1307–1316. doi:10.2174/0113816128302189240402043330.

[34] D. Murata, H. Okano, C. Angkawidjaja, M. Akutsu, S.I. Tanaka, K. Kitahara, T. Yoshizawa, H. Matsumura, Y. Kado, E. Mizohata, T. Inoue, S. Sano, Y. Koga, S. Kanaya, K. Takano, Structural Basis for the Serratia marcescens Lipase Secretion System: Crystal Structures of the Membrane Fusion Protein and Nucleotide-Binding Domain, Biochemistry. 56 (2017) 6281–6291. doi:10.1021/acs.biochem.7b00985.

[35] A. Rehman, W.M. Patrick, I.L. Lamont, Mechanisms of ciprofloxacin resistance in Pseudomonas aeruginosa: New approaches to an old problem, J. Med. Microbiol. 68 (2019) 1–10. doi:10.1099/jmm.0.000873.

[36] S. Correia, P. Poeta, M. Hébraud, J.L. Capelo, G. Igrejas, Mechanisms of quinolone action and resistance: where do we stand?, J. Med. Microbiol. 66 (2017) 551–559. doi:10.1099/jmm.0.000475.

[37] K.J. Aldred, R.J. Kerns, N. Osheroff, Mechanism of quinolone action and resistance, Biochemistry. 53 (2014) 1565–1574. doi:10.1021/bi5000564.

[38] J.M. Domagala, Structure-activity and structure-side-effect relationships for the quinolone antibacterials, J. Antimicrob. Chemother. 33 (1994) 685–706.

[39] M.K. Yazdi, M. Zare, A. Khodadadi, F. Seidi, S.M. Sajadi, P. Zarrintaj, A. Arefi, M.R. Saeb, M. Mozafari, Polydopamine Biomaterials for Skin Regeneration, ACS Biomater. Sci. Eng. 8 (2022) 2196–2219. doi:10.1021/acsbiomaterials.1c01436.

[40] F. Bernsmann, O. Ersen, J.C. Voegel, E. Jan, N.A. Kotov, V. Ball, Melanin-Containing Films: Growth from Dopamine Solutions versus Layer-by-Layer Deposition, ChemPhysChem. 11 (2010) 3299–3305. doi:10.1002/cphc.201000384.

[41] R. Batul, T. Tamanna, A. Khaliq, A. Yu, Recent progress in the biomedical applications of polydopamine nanostructures, Biomater. Sci. 5 (2017) 1204–1229. doi:10.1039/c7bm00187h.

[42] X. He, E. Obeng, X. Sun, N. Kwon, J. Shen, J. Yoon, Polydopamine, harness of the antibacterial potentials-A review, Mater. Today Bio. 15 (2022) 100329. doi:10.1016/j.mtbio.2022.100329.

[43] H. Liu, X. Qu, H. Tan, J. Song, M. Lei, E. Kim, G.F. Payne, C. Liu, Role of polydopamine's redox-activity on its pro-oxidant, radical-scavenging, and antimicrobial activities, Acta Biomater. 88 (2019) 181–196. doi:10.1016/j.actbio.2019.02.032.

[44] B. Fei, B. Qian, Z. Yang, R. Wang, W.C. Liu, C.L. Mak, J.H. Xin, Coating carbon nanotubes by spontaneous oxidative polymerization of dopamine, Carbon N. Y. 46 (2008) 1795–1797. doi:10.1016/j.carbon.2008.06.049.

[45] V. Ball, D. Del Frari, V. Toniazzo, D. Ruch, Kinetics of polydopamine film deposition as a function of pH and dopamine concentration: Insights in the polydopamine deposition mechanism, J. Colloid Interface Sci. 386 (2012) 366–372. doi:10.1016/j.jcis.2012.07.030.

[46] A.K. Awasthi, S. Gupta, K.R. Namdev, A. Banerjee, A. Srivastava, Polydopamine and dopamine interfere with tetrazolium-based cytotoxicity assays and produce exaggerated cytocompatibility inferences, Biomater. Sci. 9 (2021) 3300–3305. doi:10.1039/d1bm00140j.

[47] D. Goswami, Lipase Catalysis in Presence of Nonionic Surfactants, Appl. Biochem.

Biotechnol. 191 (2020) 744–762. doi:10.1007/s12010-019-03212-w.

[48] N.H. Shirazi, B. Ranjbar, K. Khajeh, T.T. Moghadam, Structure-function analysis of a new bacterial lipase: Effect of local structure reorganization on lipase activity, Int. J. Biol. Macromol. 54 (2013) 180–185. doi:10.1016/j.ijbiomac.2012.12.020.

[49] M. Nardini, D.A. Lang, K. Liebeton, K.-E. Jaeger, B.W. Dijkstra, Crystal structure of Pseudomonas aeruginosa lipase in the open conformation. The prototype for family I.1 of bacterial lipases, J. Biol. Chem. 275 (2000) 31219–31225. doi:10.1074/jbc.M003903200.

[50] K. Kitadokoro, M. Tanaka, T. Hikima, Y. Okuno, M. Yamamoto, S. Kamitani, Crystal structure of pathogenic Staphylococcus aureus lipase complex with the anti-obesity drug orlistat, Sci. Rep. 10 (2020) 5469. doi:10.1038/s41598-020-62427-8.

[51] R. Gupta, N. Gupta, P. Rathi, Bacterial lipases: An overview of production, purification and biochemical properties, Appl. Microbiol. Biotechnol. 64 (2004) 763–781. doi:10.1007/s00253-004-1568-8.

[52] B. Zouaoui, A. Bouziane, B. Raho Ghalem, Isolation, purification and properties of lipase from Pseudomonas aeruginosa, African J. Biotechnol. 11 (2012) 12415–12421. doi:10.5897/ajb11.3951.

[53] N.G. Kumar, D. Contaifer, D.S. Wijesinghe, K.K. Jefferson, Staphylococcus aureus lipase 3 (SAL3) is a surface-associated lipase that hydrolyzes short chain fatty acids, PLoS One. 16 (2021) e0258106. doi:10.1371/journal.pone.0258106.

[54] D. Francis, A. Bhairaddy, A. Joy, G.V. Hari, A. Francis, Secretory proteins in the orchestration of microbial virulence: The curious case of Staphylococcus aureus, 1st ed., Elsevier Inc., 2023. doi:10.1016/bs.apcsb.2022.10.004.

[55] H. Lee, J. Rho, P.B. Messersmith, Facile conjugation of biomolecules onto surfaces via

mussel adhesive protein inspired coatings, Adv. Mater. 21 (2009) 431–434. doi:10.1002/adma.200801222.

[56] H. Lee, N.F. Scherer, P.B. Messersmith, Single-molecule mechanics of mussel adhesion, Proc. Natl. Acad. Sci. U. S. A. 103 (2006) 12999–13003. doi:10.1073/pnas.0605552103.

[57] H.A. Lee, E. Park, H. Lee, Polydopamine and Its Derivative Surface Chemistry in Material Science: A Focused Review for Studies at KAIST, Adv. Mater. 32 (2020) 1907505. doi:10.1002/adma.201907505.

[58] K. Kalantari, E. Mostafavi, A.M. Afifi, Z. Izadiyan, H. Jahangirian, R. Rafiee-Moghaddam, T.J. Webster, Wound dressings functionalized with silver nanoparticles: Promises and pitfalls, Nanoscale. 12 (2020) 2268–2291. doi:10.1039/c9nr08234d.

[59] V. Pareek, R. Gupta, J. Panwar, Do physico-chemical properties of silver nanoparticles decide their interaction with biological media and bactericidal action? A review, Mater. Sci. Eng. C. 90 (2018) 739–749. doi:10.1016/j.msec.2018.04.093.

[60] S.L. Percival, A.M. Salisbury, R. Chen, Silver, biofilms and wounds: resistance revisited, Crit. Rev. Microbiol. 45 (2019) 223–237. doi:10.1080/1040841X.2019.1573803.

[61] J. Lu, Y. Wang, M. Jin, Z. Yuan, P. Bond, J. Guo, Both silver ions and silver nanoparticles facilitate the horizontal transfer of plasmid-mediated antibiotic resistance genes, Water Res. 169 (2020) 115229. doi:10.1016/j.watres.2019.115229.

[62] S. Sütterlin, P. Edquist, L. Sandegren, M. Adler, T. Tängdén, M. Drobni, B. Olsen, Å. Melhus, Silver resistance genes are overrepresented among Escherichia coli isolates with CTX-M production, Appl. Environ. Microbiol. 80 (2014) 6863–6869. doi:10.1128/AEM.01803-14.

[63] B. Schäfer, J. Vom Brocke, A. Epp, M. Götz, F. Herzberg, C. Kneuer, Y. Sommer, J.

Tentschert, M. Noll, I. Günther, U. Banasiak, G.F. Böl, A. Lampen, A. Luch, A. Hensel, State of the art in human risk assessment of silver compounds in consumer products: A conference report on silver and nanosilver held at the BfR in 2012, Arch. Toxicol. 87 (2013) 2249–2262. doi:10.1007/s00204-013-1083-8.

[64] L. Jakobsen, A.S. Andersen, A. Friis-Møller, B. Jørgensen, K.A. Krogfelt, N. Frimodt-Møller, Silver resistance: An alarming public health concern?, Int. J. Antimicrob. Agents. 38 (2011) 454–455. doi:10.1016/j.ijantimicag.2011.07.005.

[65] A. Davin-Regli, J.M. Pagès, Cross-resistance between biocides and antimicrobials: An emerging question, OIE Rev. Sci. Tech. 31 (2012) 89–104. doi:10.20506/rst.31.1.2101.

[66] X. Tan, P. Gao, Y. Li, P. Qi, J. Liu, R. Shen, L. Wang, N. Huang, K. Xiong, W. Tian, Q. Tu, Poly-dopamine, poly-levodopa, and poly-norepinephrine coatings: Comparison of physico-chemical and biological properties with focus on the application for blood-contacting devices, Bioact. Mater. 6 (2021) 285–296. doi:10.1016/j.bioactmat.2020.06.024.

[67] M. Kohri, H. Kohma, Y. Shinoda, M. Yamauchi, S. Yagai, T. Kojima, T. Taniguchi, K. Kishikawa, A colorless functional polydopamine thin layer as a basis for polymer capsules, Polym. Chem. 4 (2013) 2696–2702. doi:10.1039/c3py00181d.

[68] Q. Chen, X. Zhang, D. Zhang, G. Liu, K. Ma, J. Liu, K. Ma, M. Chen, Y. Li, R. Liu, Universal and One-Step Modification to Render Diverse Materials Bioactivation, J. Am. Chem. Soc. 145 (2023) 18084–18093. doi:10.1021/jacs.3c05928.

[69] J. Lu, J. Fang, J. Li, L. Zhu, Engineering highly transparent UV-shielding films with disassembled polydopamine oligomers as light adsorber, Appl. Surf. Sci. 550 (2021) 149284. doi:10.1016/j.apsusc.2021.149284.

[70] T.S. Sileika, D.G. Barrett, R. Zhang, K.H.A. Lau, P.B. Messersmith, Colorless

multifunctional coatings inspired by polyphenols found in tea, chocolate, and wine, Angew. Chemie - Int. Ed. 52 (2013) 10766–10770. doi:10.1002/anie.201304922.

[71] B. Liu, H. Liu, F. Cheng, C. Liu, F. Shao, C. Li, G. Cheng, H. Wang, Development and post-functionalization of a colorless universal coating using Bis(vinyl sulfonyl)methane, Prog. Org. Coatings. 172 (2022) 107081. doi:10.1016/j.porgcoat.2022.107081.

[72] Z. Peng, X. Zhang, L. Yuan, T. Li, Y. Chen, H. Tian, D. Ma, J. Deng, X. Qi, X. Yin, Integrated endotoxin-adsorption and antibacterial properties of platelet-membrane-coated copper silicate hollow microspheres for wound healing, J. Nanobiotechnology. 19 (2021) 1–17. doi:10.1186/s12951-021-01130-w.

[73] Y. Ding, Z. Sun, R. Shi, H. Cui, Y. Liu, H. Mao, B. Wang, D. Zhu, F. Yan, Integrated Endotoxin Adsorption and Antibacterial Properties of Cationic Polyurethane Foams for Wound Healing, ACS Appl. Mater. Interfaces. 11 (2019) 2860–2869. doi:10.1021/acsami.8b19746.

[74] R. Coudroy, D. Payen, Y. Launey, A.C. Lukaszewicz, M. Kaaki, B. Veber, O. Collange, A. Dewitte, L. Martin-Lefevre, M. Jabaudon, T. Kerforne, M. Ferrandiere, E. Kipnis, C. Vela, S. Chevalier, J. Mallat, S. Charreau, J.C. Lecron, R. Robert, Modulation by polymyxin-B hemoperfusion of inflammatory response related to severe peritonitis, Shock. 47 (2017) 93–99. doi:10.1097/SHK.0000000000000725.

[75] X. Cao, B. Zhu, X. Zhang, H. Dong, Polymyxin B immobilized on cross-linked cellulose microspheres for endotoxin adsorption, Carbohydr. Polym. 136 (2016) 12–18. doi:10.1016/j.carbpol.2015.09.012.

[76] D. Sil, L. Heinbockel, Y. Kaconis, M. Rössle, P. Garidel, T. Gutsmann, S.A. David, K. Brandenburg, Biophysical Mechanisms of the Neutralization of Endotoxins by

Lipopolyamines, Open Biochem. J. 7 (2013) 82–93. doi:10.2174/1874091x01307010082.

[77] L. Mack, B. Brill, N. Delis, B. Groner, Endotoxin depletion of recombinant protein preparations through their preferential binding to histidine tags, Anal. Biochem. 466 (2014) 83–88. doi:10.1016/j.ab.2014.08.020.

Appendix A. Supplementary Data

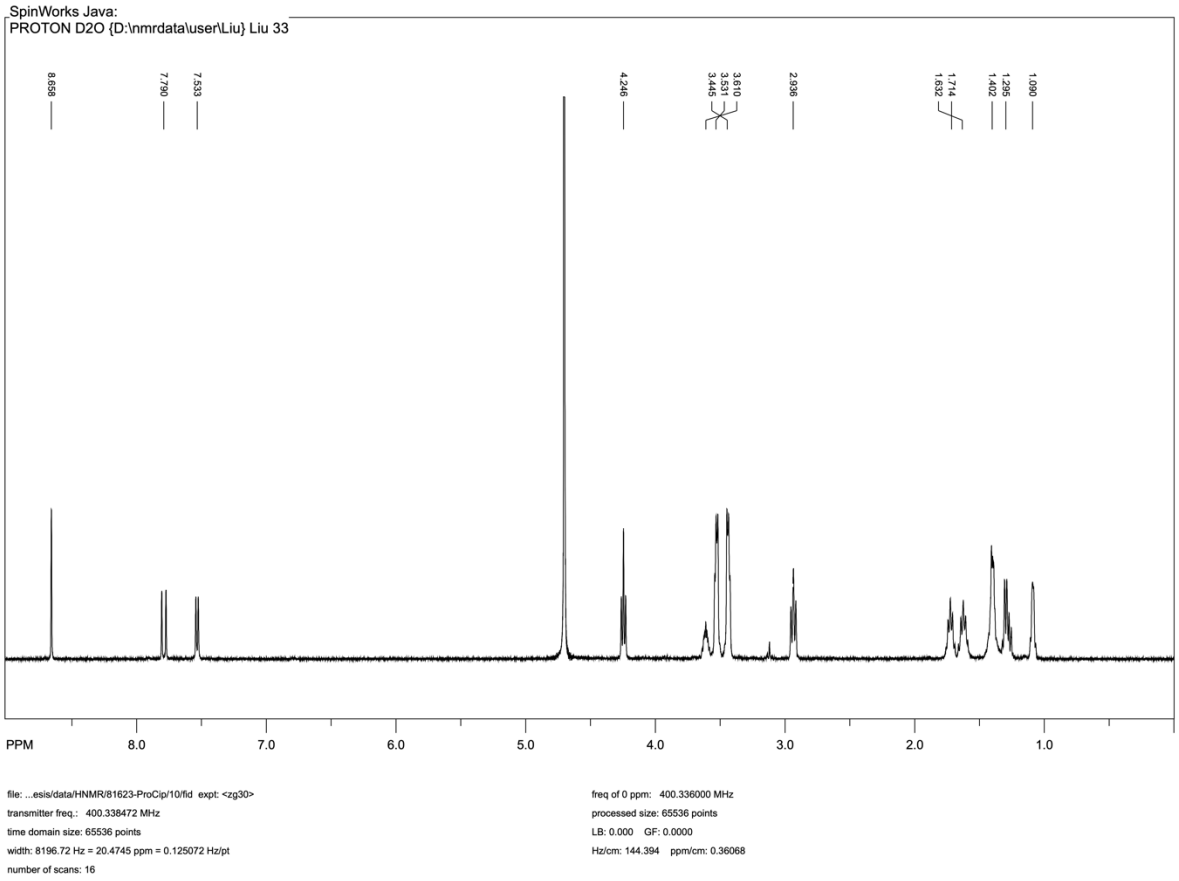

Figure A1. ^{1}H-NMR spectrum of Pro-Cip.

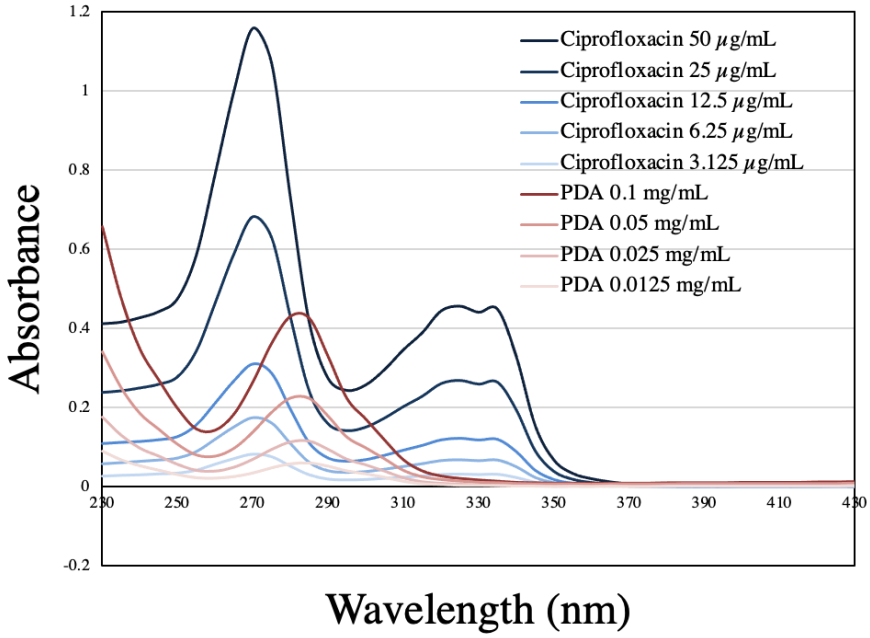

Figure A2. UV-vis absorbance spectra of ciprofloxacin and PDA from 230-430 nm.